

**The Deferral Set Framework:
A Novel Methodology for the Performance Analysis of
Multi-hop Wireless Networks**

A Thesis Presented
by

Yue Fang

to the faculty of
Electrical and Computer Engineering

in Partial Fulfillment of the Requirements
for the Degree of

Doctor of Philosophy

in the field of
Electrical and Computer Engineering

**Northeastern University
Boston, Massachusetts**

December 2005

© Copyright 2005 by Yue Fang
All Rights Reserved

NORTHEASTERN UNIVERSITY
Graduate School of Engineering

Thesis Title: The Deferral Set Framework:
A Novel Methodology for the Performance Analysis of Multi-hop Wireless Networks.
Author: Yue Fang.
Department: Electrical and Computer Engineering.

Approved for Thesis Requirements of the Doctor of Philosophy

_____ Thesis Advisor: Prof.A. Bruce McDonald	_____ Date
_____ Thesis Reader: Prof. Stefano Basagni	_____ Date
_____ Thesis Reader: Prof. Guevara Nobuir	_____ Date
_____ Thesis Reader: Dr. Daqing Gu	_____ Date
_____ Chairman of Department: Prof. Steve McKnight	_____ Date

Graduate School Notified of Acceptance:

_____ Director of the Graduate School	_____ Date
--	---------------

Copy Deposited in Library:

_____ Reference Librarian	_____ Date
------------------------------	---------------

Table of Contents

Table of Contents	4
Abstract	8
Acknowledgments	9
1 Introduction	10
1.1 Motivation	12
1.2 The “Path Coupling” Problem	13
1.3 Philosophy	14
1.4 Contributions of the Proposal	15
1.5 Organization of the Proposal	16
2 Overview of Reconfigurable Wireless Networks	17
2.1 MAC protocol for ad hoc networks	18
2.1.1 Carrier Sense Multiple Access	19
2.1.2 Multiple Access with Collision Avoidance	19
2.1.3 Floor Acquisition Multiple Access	19
2.1.4 IEEE 802.11	20
2.2 Previous Art	24
2.2.1 Theoretical Maximum Throughput of Arbitrary Channel	25
2.2.2 Asymptotic throughput of a single node	25
2.2.3 Saturation throughput of a fully connected ad hoc network	26
2.2.4 Simulation of end-to-end throughput of ad hoc network	27
2.2.5 Throughput and cross-layer interaction	28
2.3 Conclusion	29
3 Deferral Framework Overview	31
3.1 Components of the Framework	31
3.2 Abstract Model	32
3.2.1 Well Established Definitions	32
3.2.2 New concepts	33
3.2.3 Notation and Terminology	37
3.3 Transmission Probability	39
3.4 Node Model	41
3.5 Conclusion	42
4 Channel Capacity Analysis Using Deferral Framework	43
4.1 Methodology	43
4.2 Channel Capacity Analysis	44
4.2.1 Equivalent Competitors	44

4.2.2	Probability of Flow Transmission	53
4.2.3	Detailed Explanation of Node Model	55
4.2.4	Arbitrary Channel Capacity	60
4.2.5	Delay Analysis	64
4.3	Model Validation and Performance Analysis	64
4.3.1	Model Validation	65
4.3.2	Statistical Analysis	67
4.4	Conclusion	69
5	Network Capacity Analysis Using Deferral Framework	73
5.1	Introduction	73
5.2	Network Saturation Capacity (NSC) Analysis	75
5.2.1	Boundary Condition	75
5.2.2	Network Saturation Capacity	82
5.3	Maximum Instantaneous Capacity (MIC) Analysis	83
5.3.1	Maximum Number of Concurrent Active Links	83
5.3.2	The Bottleneck Aggregate Link Set of the Network	88
5.3.3	Discussion	90
5.4	Conclusion	92
6	Routing Algorithm Design using deferral Set Framework — The Dynamic Codeword Routing (DCR)	94
6.1	Introduction	94
6.2	Current Routing Algorithms	96
6.3	“Codeword Routing”— the Cross-layer Routing Design	98
6.4	Dynamic Codeword Routing Algorithm	103
6.5	DCR Implementation and Performance Enhancement	106
6.6	Conclusion	111
7	Conclusion and Future Work	114
7.1	Review of the Thesis	114
7.2	Future Work	114
	Bibliography	115

List of Figures

1.1	possible interference in wireless ad hoc network	14
2.1	“Ad Hoc” Mode of IEEE 802.11	21
2.2	“Infrastructure ” Mode of IEEE 802.11	21
2.3	IEEE 802.11 MAC using RTS/CTS	24
3.1	An example of how to calculate the size of communication set	36
3.2	Markov chain model for a single station’s back-off window size	40
4.1	A typical level-1 interference set	45
4.2	A Typical Level-2 Interference Set	47
4.3	Another Example of Level-2 interference Set	50
4.4	Calculation of Two Hop Neighbors	51
4.5	State transition model for an arbitrary transmission attempt	56
4.6	Transition flow of back-off stage i	61
4.7	Flow transition with corresponding probabilities	63
4.8	How to determine the saturation point	66
4.9	Model Validation: Arbitrary Channel Capacity	67
4.10	Model Validation: Mean Service Time	68
4.11	Statistical Analysis: Channel Capacity of arbitrary link vs. Retry Limit, $m=5$	69
4.12	Statistical Analysis: Channel Capacity of arbitrary link vs. back-off stage m , RL= m	70
4.13	Statistical Analysis: Channel Capacity of arbitrary link with different packet size	70
4.14	Statistical Analysis: MAC Service time of different packet size	71
4.15	Statistical Analysis: Channel Capacity of arbitrary link of different packet size, Analytical vs. Simulation	72
5.1	Network example, $n_{avg} = 3$	74
5.2	Network example, $n_{avg} = 6$	74
5.3	Network example, $n_{avg} = 12$	75
5.4	Illustration of Boundary Condition	76
5.5	Analysis of Boundary Condition	77
5.6	Calculation of “phantom nodes” for communication pair	80
5.7	Number of phantom nodes vs. R/r	82
5.8	Percentage of phantom nodes respect to total number of nodes in the network	82
5.9	Another example of graph transformation	85
5.10	Rules of graph transformation	85
5.11	Flow assignation of Figure-3.1 using the proposed algorithm	87
5.12	Flow assignation of a larger network using the proposed algorithm	88
6.1	Routes obtained by AODV	97
6.2	Alternative Routes for the Communications in Figure-6.1	98

6.3	Performance comparison for different routing assignments	99
6.4	An example of wireless ad hoc network	100
6.5	An example of link cost assignment and DCR algorithm implementation	104
6.6	Another example of link cost assignment and DCR algorithm implementation	105
6.7	Routes selected by AODV, 3 parallel flows	106
6.8	Routes selected by DCR, 3 parallel flows	107
6.9	Comparison of overall throughput using AODV and DCR, 3 parallel flows	108
6.10	Throughput of each of the 3 flows when using AODV, 3 parallel flows	109
6.11	Throughput of each of the 3 flows when using DCR, 3 parallel flows	110
6.12	Routes selected by AODV, 3 cross flows	111
6.13	Routes selected by DCR , 3 cross flows	111
6.14	Comparison of overall throughput using AODV and DCR, 3 cross flows	112
6.15	Throughput of each of the 3 flows when using AODV, 3 cross flows	113
6.16	Throughput of each of the 3 flows when using DCR, 3 cross flows	113

Abstract

Recent years have witnessed increasing interest in reconfigurable wireless networks (ad hoc networks) for military, commercial and sensor network applications. Consequently, theoretical models capable of accurate network characterization have become increasingly important — robust, efficient and scalable network services depend on understanding the capabilities and limitations of these dynamic systems. In this proposal, a novel capacity analysis framework for multi-hop wireless networks is presented. The framework contains novel concept to characterize multi-hop wireless network features as well as novel methodology to analyze the network performance.

The framework studies both channel and network capacity of wireless networks. The novel methodology is based on the following novel concepts: “deferral set” and “equivalent competitor”, which reflect channel contention and routing characterizations of the multi-hop environment. Analysis is conducted by applying above concepts to a medium access specifications based parametric node model based. The mean channel throughput (capacity) and service delay during backlogged periods are studied using the above methodologies and validated by simulations.

Moreover, two semantics for network capacity — “network saturation capacity” (NSC) and “maximum instantaneous capacity” (MIC) are proposed and discussed as well. The effect of node location on capacity is analyzed within the context of “boundary condition” and its impact on evaluation of NSC. On the other hand, MIC metric is intended to characterize the true information capacity of the network as a whole; the optimization problem is shown to be NP-complete and heuristic algorithms to bound the solution from above.

Acknowledgments

I would like to thank my advisor, Professor A. Bruce McDonald, for the advice, support and care that he gave me during my stay at Northeastern. Without his support and care, the journey would have been harder and longer.

My other thanks go to my friends and coworkers Mustafa Ozdemir, Denial Ugarte and Rituparna Ghosh. We had a good time cooperating with each other, I learned a lot of knowledge and received a lot of assistance from them. I wish I could have met them earlier in my research life.

Also I would like to thank the following entities for financial support: The National Science Foundation, Mitsubishi Electronic Laboratories and the College of Engineering and Department of Electrical and Computer Engineering.

Finally, I would express my gratitude and dedicate my Ph.D thesis to my husband Yongjun Fei, who gave up his prospective career in China and came to USA and gave me happy life here in Boston and my family members back home who constantly support me both financially and emotionally. Without the love and care from all of you, I would never make it.

Yue Fang

Boston, USA

Dec 16th, 2003

Chapter 1

Introduction

Recent years have witnessed increasing interest in reconfigurable wireless networks (wireless ad hoc networks). Wireless ad hoc network is a self-organizing network in which static or mobile nodes can communicate with each other without any help of fixed infrastructure. In a wireless ad hoc network, nodes that are not either the source or destination may also participate in the communication by relaying information hop by hop, they may enter or leave the network at any time as well as move freely inside it. Wireless ad hoc networks can be utilized as an important supplement of the existing wired networks in cases like exhibitions or mobile conferences to support unusual high demand for communications or can be implemented independently in military or scientific operations. Compared to the wired counterpart, wireless ad hoc networks face the following (but not limited to) issues that may not be a problem for wired networks such as limited device power, unpredictable variation in channel quality, limited resource, mobility control as well as the stability and scalability issues. Consequently, theoretical models capable of accurate ad hoc network characterization have become increasingly important — robust, efficient and scalable network services depend on understanding the capabilities and limitations of these dynamic systems. For example, fundamental capacity limits of ad hoc networks have theoretical and practical importance. Specifically, understanding performance bounds that are invariant with respect to specific routing or scheduling algorithms becomes necessary to support real-time or other performance bound applications. One of the primary obstacles to finding general results, however, is that ad hoc networks exhibit a distinct interaction between entities of different layers. This must be accounted for in performance analysis and integrated into network design.

In this proposal, we proposed to solve the general problem of channel capacity and network

capacity. Compare to the well-known Gupta and Kumar’s work about capacity limit of wireless network [24], the capacities in this thesis are defined in a more general semantic under a more general environment. efforts are mainly focused on the development of an analytical framework of modelers and analysis of theoretical capacity limitations on multi-hop wireless networks. The methodology used in this thesis is based on a novel framework which evolved from the inherent cross-layer interaction between MAC and routing layer [18] — this leads to the development of the concept and formal characterization of the well defined phenomena referred as “path coupling”.

“Path coupling” refers to a set of inherent characteristics of multi-hop wireless networks that rely on contention based-MAC. The concept is invariant, although the details may be subject to variant in parameters and specific optimizations. The invariant aspects, however, motivated the further investigation to better understand how it impacts the theoretical performance limitations. The goal was to investigate new analytical methods and provide strong simulation based validation that challenge existing embedded beliefs — with the ultimate aim of providing clues for designing better algorithm for network control — MAC, routing, admission control for QoS based on the invariant cross-layer principle first characterized.

The result is a comprehensive and analytical approach based on the novel concept of the *deferral set* — this well defined idea provided the basis of a generalized work — *the deferral framework*.

The framework has wide ranging applications in the domain of ad hoc network analysis. Hence, it has significance as a new meteorological approach. The key contribution of this research are based on the development of accurate models for the theoretical maximum capacity, first of the individual channel and then using the optimization methods to extend the results to the entire network.

The final aspect of the work involves an investigation of practical application of the important concepts that are developed — the focus being on cross-layer routing methods. The novel aspects of works resides in that the “cross-layer control” methodology used in this work, which is based on the understanding of the complex, dynamic inter-related effects and using that knowledge to improve or optimize performance. The results from the work are generalized and can be used to improve nearly any existing routing algorithm — a unique — yet efficient paradigm of cross-layer path coding is presented as an example of practical application of the

work; the result may prove to be even more significant in the area of dynamic topology control including frequency agile transceivers. The detail of this work is beyond the scope of the current research.

Compared to the MANET understanding of “cross-layer control” by looking at the problem as an control interface based on adjusting parameters empirically and experimentally, the approach in this thesis has more theoretical analysis backup thus can provide more insight of the complicate system as researchers pursue the board goals of such as scalability, robustness, large QoS enabled public networks that are much less expensive than the cellular network.

In the rest of this chapter, in subsection-1.1 motivation as well as the move from the specific to general problem are reviewed; in subsection-1.2 the underlying characteristics of the wireless network, which serves as the primary base of the novel framework proposed; in subsection-1.3 the philosophy for the research is summarize and in subsection-1.4 summarized the novelty and contribution of this work. Finally, in subsection-1.5 the organization of the thesis is provided.

1.1 Motivation

Reconfigurable wireless networks are developing very fast recently years both academically and commercially. The high volume and various traffic have demand wireless ad hoc network to provide higher throughput, there is active standardization activities inside IEEE, however, normally, the actual throughput a network can achieve is far more less than the nominal one, which suggests that cross-layer design should be considered in the design of the wireless ad hoc network applications. In order to design efficient routing and upper layer applications, it is necessary to have a comprehensive understanding of how wireless ad hoc networks works and provide an accurate estimation of the capacity performance.

Capacity is an important and fundamental performance metric that serves as the foundation of the design and applications of wireless network. As multi-hop wireless network has become more and more attractive to both researchers and engineers, thus there is a growing interest for complete and accurate multi-hop wireless network capacity analysis . However, compared to the large volume of analysis for channel capacity of single hop wireless network, there has been very little significant achievement in the understanding of multi-hop network capacity [33], [23]. Much has yield pessimistic result [33] or relies impractical assumptions [23]. Thus it is important to have valid theoretical models for multi-hop scenarios and unique applications and

improve the network performance, which is currently unsatisfactory.

In this proposal, the capacity problem has been studied using the methodologies introduced at the beginning of this Chapter. (The details of the methodology will be discussed in the following chapters.) This thesis presents the first complete and fully validated model and capacity analysis reflecting the precise effect of multi-hop wireless network by studying the unique characteristics of wireless communications. The analysis presented here focused on the IEEE 802.11 wireless LAN protocol using the distributed coordination function (DCF) and RTS/CTS handshaking scheme; however the conceptual basis of the theoretical model can be considered as a general model for any contention-based MAC protocol. Hence, it can easily to reflect various proposed optimization and modified MAC protocol such as [2] [30] [20] [14] [41] [17] etc.

1.2 The “Path Coupling” Problem

The cause of several different problems in wireless network is the broadcast nature of its transmission. Unlike the wired counterparts where the channel is exclusive to the communication pair, the transmission medium in wireless networks is shared by a group of nodes, thus all the nodes in the transmission range of the communication pair will hear the transmission and therefore the possible transmissions of those nodes will be affected. Moreover, in multi-hop network, based on the specific medium access control scheme being used, contentions may be extended to a small multi-hop network model consisting nodes that seems to have no direct relation with each other, for example, the hidden terminal and exposed terminal problem.

Due to the different medium access protocol used by the network, those problems may have different appearance, but the intrinsic cause for them are the same, which is summarized by the authors in [18] as “path coupling” phenomenon. In [18] path coupling is defined as the media access contention between nodes distributed along node disjoint paths, it is caused by the broadcast nature of wireless communication and can be served as example of contention of multi-hop network. Figure-1.1 illustrates the main factors of coupling phenomenon caused by the interference among nodes both in single and multi hop network environment. All those problems involves transmission “interference” among different communicating nodes which would not happen in wired network, in other words, the spatial reuse of a single radio channel is the underlying cause of the phenomena and are handled at medium access control (MAC) layer.

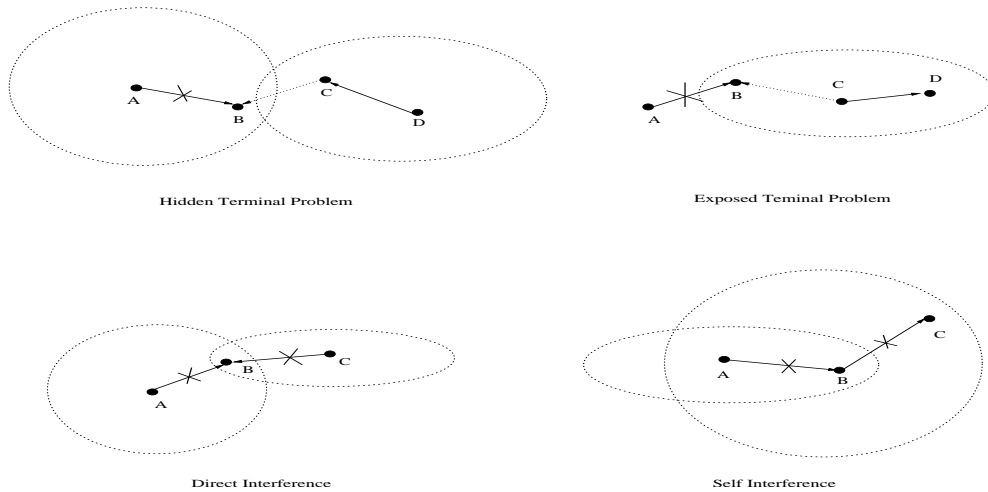


Figure 1.1: possible interference in wireless ad hoc network

Notice that in multi-hop network interference may exist among nodes with no direct spatial reuse relationship.

1.3 Philosophy

The philosophy of this research is elaborated in the following summary:

- There should be a universal model to investigate the capacity of wireless ad hoc network, although different kind of MAC layer specification may be used. In other words, it is the underlying generalities of wireless communication that determine the methods that we used to study them.
- Multi-hop wireless network may have different characteristics from single hop ones. But as discussed before, the intrinsic cause of those characteristics is same, which is the “broadcast” nature of wireless communication. So ultimately it is possible to find out the potential relationship between multi and single hop networks. The objective of this thesis is to find out this relationship and utilize it for capacity analysis of multi-hop wireless network. In this proposal, novel concepts such as “deferral set” and “equivalent competitor” are provided to characterize the potential relationship.
- Besides the reason that no appropriate model which could characterize the unique features of multi-hop is available for researchers when the work of this thesis is done, another reason which contributes to the less amount of successful work in multi-hop capacity

analysis is that the prospective from which the capacity analysis problem is looked at. In [31] classic analysis for single hop wireless network is provided by Kelenrock and Tobagi by studying the behavior of arbitrary channel because all the nodes in the network will share it, however, for multi-hop scenarios, the approach they proposed in [32] which is by transforming the effect of different channel to the channel under interest is not that suitable, especially for some complicated MAC layer protocols whose objective is to prevent different kinds of medium access problem. A more straightforward and easy to understand approach is to study the capacity problem from the node's prospective. Normally, node is the actual existing entity and its behavior will follow the same rule no matter in single or multi-hop scenario, different value of the parameters used by the node prospective approach will reflect the difference between single and multi-hop network.

- Finally, different layers from the OSI 7-layer model should not be treated as independently as they were in the wired network, instead, information from one layer may and should be used by related layer as reference for them to make corresponding decisions. This is the missing property that needs to be considered in the network model. For example, as the communication channel is shared by neighboring stations in the network, the inherent effects of channel contention must be counted in order to achieve reasonable throughput.

1.4 Contributions of the Proposal

This is not a "yet but another" work in the community, the most significant contributions of this work exist in the sense of both challenging previous results as well as establishing objective for network designers — a performance evaluation guide like Shannon capacity law. It present the first general capacity analysis methodology for multi-hop ad hoc networks; the methodology itself has practical application, most directly in the areas of dynamic topological organization, admission control and scheduling algorithms. The results offer accurate and validated characterizations of complex interaction. Hence, they can have immediate impact on routing algorithm design and as cross-layer interface design. Moreover, to our best knowledge, it is the first work that notice and formally address the difference between the normally used channel prospective approach (study the behavior of single channel) and the node prospective approach (study the behavior of single node) of the same problem although some previous work [16] may touch this problem unconsciously. Node prospective has advantage because

no significant modification is needed when extended to multi-hop scenario compared to the widely used channel prospective. In the “deferral framework”, detailed MAC specifications are reflected by specific parametric behaviors that are easily modified. Moreover, as an example of the application of the framework, by addressing the multi-hop scenario the work completes a “family” of related performance studies of the IEEE 802.11 MAC protocol ([5], [9], [19], [44] etc) and provides a more accurate and less conservative estimation of bandwidth capacity.

1.5 Organization of the Proposal

This thesis is divided into 7 chapters. Chapter 2 provide detailed background information about wireless ad hoc network with related media access layer protocol, an extensive discussion of related work of capacity analysis is also provided in Chapter 2. Chapter 3 presented the novel concepts that have been proposed by the author. Chapter-4 and Chapter-5 present the investigation on arbitrary channel and network capacity respectively. Chapter-6 provides another application of the deferral set frame work, the “dynamic codeword routing” algorithm which utilizes the “equivalent competitor” concept to facilitate routing decisions. Chapter-7 summarizes the work in the thesis and discusses the direction of future work.

Chapter 2

Overview of Reconfigurable Wireless Networks

The history of wireless networks started in the 1970's and the interest has been growing ever since. During the last decade and especially at the end, the interest has almost exploded probably because of the fast growing internet. Today we see two kinds of wireless networks but the difference between them is not as obvious as it may seem. The first kind and most used today is wired network built on top of a “wired” network and thus creates a *reliable infrastructure wireless network*. An Example of this kind of network is the cellular-phone networks, and other more recent networks of this kind is wireless networks for offices, cafes etc which usually are called Wireless Local Area Networks (WLAN).

The other kind is as it may seem the orthogonal kind. One where there is no infrastructure at all except the participating wireless nodes. This is called an *infrastructure-less network* or more commonly an *ad hoc* network. The term “ad hoc network” is used to describe the autonomous system of wireless nodes that communicate via a shared medium, with no need of a centralized authority. Some or all nodes within an ad hoc network are expected to be able to route data packets for other nodes in the network who want to reach other nodes beyond their own transmission range.

Ad hoc networks, due to their unique characteristics, has the following advantages, such as they are easy to set up, highly dynamic and resilient so they will be very useful in search and rescue, battlefield operation or scenarios where base stations are unavailable ore unnecessary. On the other hand, the disadvantages are mainly on their limited bandwidth and power supply as well as the security issues.

The remainder of this chapter is organized as following: In section-2.1, different medium

access control protocols used in ad hoc networks are introduced, the merit and shortcoming for each protocol are also discussed; previous performance analysis of wireless ad hoc networks are summarized in section -2.2, those previous work have generate great insight on the performance issue, however, each work has its won limitations. The details can be found in section-2.2. Finally, section-2.3 concludes this chapter.

2.1 MAC protocol for ad hoc networks

Medium Access Control layer (MAC) is a sub-layer of data link layer, the second layer of the seven-layer OSI network architecture [4]. It serves as an intermediate layer to manage the multi-access link , current widely using MAC layer protocols can be classified based on the mechanisms of media access control into the following categories:

- Random access:

Stations in the network will perform carrier sense (maybe collision detection or collision avoidance) and compete against each other for the channel access. The winner gains the channels, and the loser has to back-off and competes again. Medium access is total random and no central scheme is need. Examples for random access MAC protocols are CSMA (Carrier Sense Multiple Access), MACA (Multiple Access with Collision Avoidance)[30], FAMA (Floor Acquisition Multiple Access)[20] and IEEE 802.11 MAC, [6] etc.

- Pre-assigned:

In the system, each station has its own pre-assigned share (time-slots in Time Division Medium Access (TDMA) or code in Code Division Medium Access (CDMA)) of the medium based on the network configuration and topology. Stations can only access the medium at those pre-assigned time-slot or using only the pre-assigned code. Thus there is no collision for the media access.

- Clustered access:

Clustered access is a combination of the first two medium access schemes [3]. The whole network is divided to several small sizes of groups, which is called clusters based on topology or internal relations among stations. Inside the cluster, pre-assigned medium access is performed by the cluster-head. Cluster-head is analogous the base station used

in cellular phone networks, and it is responsible for the coordination of communications intra or inter cluster. Random access will be performed among clusters.

In this section several important MAC layer protocol for wireless ad hoc networks [31], [20],[30], [35], [6] are briefly reviewed here. There are a lot of interesting works on MAC protocol besides the ones discussed here such as, [14], [2], [41],[22], [17], etc. Interested readers can refer to the corresponding literature.

2.1.1 Carrier Sense Multiple Access

The Carrier Sense Multiple Access (CSMA) [31] is one of the most underlying MAC layer protocol in wireless communications. In this protocol, a node senses the channel for ongoing transmission before sending a packet. If the channel is already in use, the node sets a random timer and then waits this period of time before re-attempting the transmission. On the other hand, if the channel is not currently in use, the node starts transmission immediately.

2.1.2 Multiple Access with Collision Avoidance

The Multiple Access with Collision Avoidance (MACA) [30] protocol improves upon CSMA by taking steps towards the avoidance of the hidden terminal problem. The protocol defines Request-To-Send (RTS) and Clear-To-Send (CTS) control packets to announce an upcoming transmission. A node wishing to send a data packet broadcasts a RTS message containing the length of the data frame that will follow. Upon receiving the RTS, the receiver responds by broadcasting a CTS packet that is also contains the length of the upcoming data frame. Any node hear either of these two control packets must be silent long enough for the data packet to be transmitted. In this way, neighboring nodes will not transmit during the data transmission and the number of collision is reduced.

In the event that two nodes send simultaneous RTS frames to the same node, the RTS transmission collide and are lost. If this happens, the node that sent the unsuccessful RTS packets set a random timer utilizing the binary exponential back-off algorithm for the next transmission attempt.

2.1.3 Floor Acquisition Multiple Access

The Floor Acquisition Multiple Access (FAMA) variant discussed here is FAMA-NTR (Non-persistent Transmit Request) [20]. FAMA-NTR builds upon the MACA protocol by adding

non-persistent carrier sensing to the RTS/CTS exchange. Before transmitting a RTS frame, a node first listens to the channel to determine if it is already in use. If the channel is busy, the node calculates a random back-off period to wait before sensing the channel again. The addition of this carrier sense to the control packet exchange aids in the prevention of control packet collisions.

2.1.4 IEEE 802.11

In this proposal, we will concentrate our study on random medium access mechanisms, more precisely, we will focus on IEEE 802.11 MAC layer protocol. The reason why we choose IEEE 802.11 is that it represents a class of access control schemes, even though there are other perhaps “better” protocols, they are just the variation of the widely-used not-easily-to-die IEEE standard. This subsection gives a detail overview of IEEE 802.11 standard. IEEE 802.11 is limited in scope to the Physical (PHY) layer and Medium Access Control (MAC) sub-layer. Initially it is proposed for wireless LAN (WLAN) and became more and more popular as an MAC layer protocol for wireless ad hoc networks for both research and application purpose. The basic topology of an 802.11 network is shown in Figure-2.1. A Basic Service Set (BSS) consists of two or more wireless nodes. Communications can be performed without any help from fixed infrastructure or “central” node. This type of network is referred to as “*ad hoc*” mode. In some instances like Figure-2.2, the BSS contains an Access Point (AP). The main function of AP is to serve as a bridge between wireless and wired LANs. When AP is present, all communications between stations or between a station and a wired network client go through the AP. APs are not mobile, and form part of the wired network infrastructure. A BSS in this configuration is said to be operating in the “*infrastructure*” mode.

- **PHY layer specifications**

We are interested in the MAC layer specifications of IEEE 802.11 standard. This subsection gives a brief summary of PHY layer specification and the following subsection will focus on the MAC layer.

IEEE 802.11 provides three variations of the PHY. These include two (2) RF technologies namely Direct Sequence Spread Spectrum (DSSS) and Frequency Hopping Spread Spectrum (FHSS) and Infra Red (IR). Both RF options are working in the 2.4GHz Industrial, Scientific and Medical (ISM) band, which have worldwide allocations for unlicensed operation.

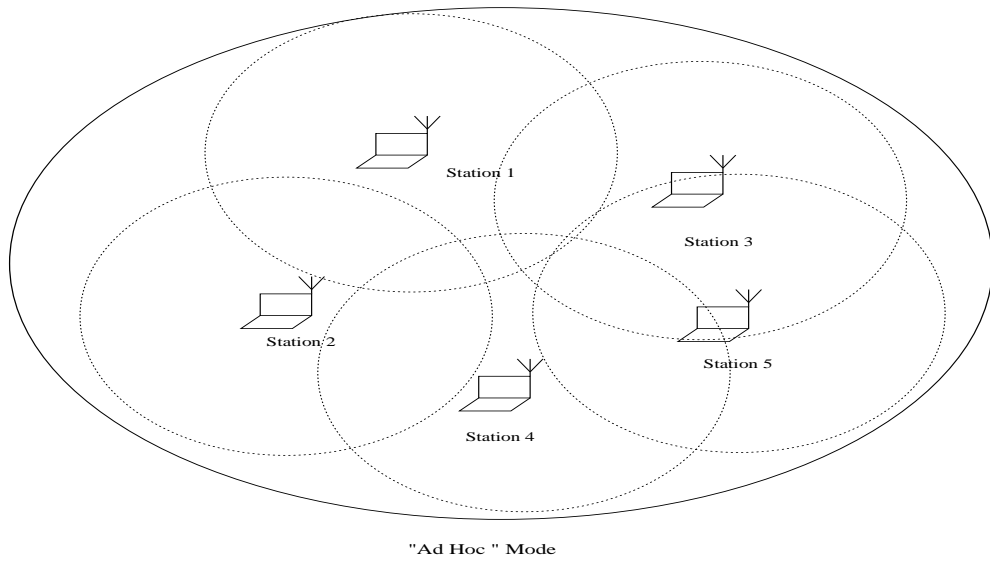


Figure 2.1: "Ad Hoc" Mode of IEEE 802.11

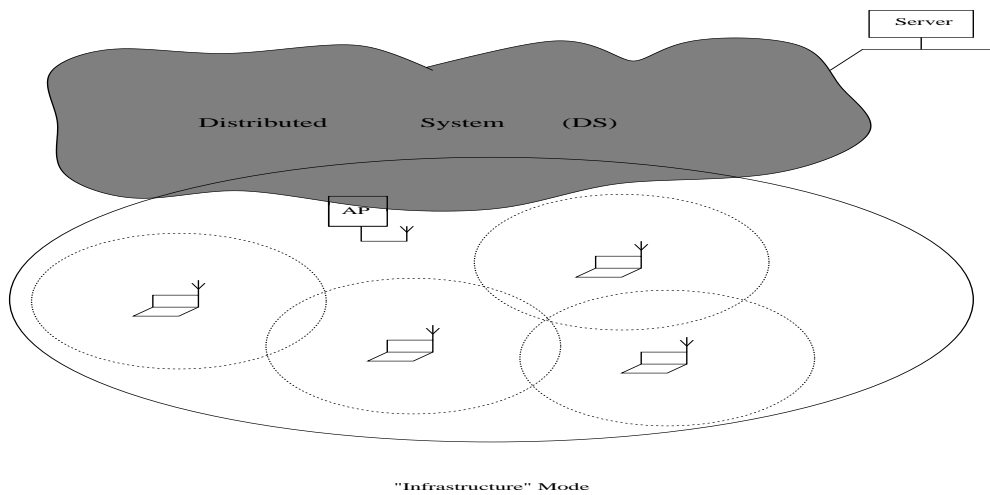


Figure 2.2: "Infrastructure " Mode of IEEE 802.11

Both DSSS and FHSS currently support 1Mbps and 2Mbps data rate. However, 5.5Mbps and 11Mbps data rate is only supported by DSSS. 1Mbps DSSS uses Differential Binary Phase Shift Keying (DBPSK) encoding and 2Mbps DSSS uses Differential Quadrature Phase Shift Keying (DQPSK) encoding. 1Mbps FHSS uses low-level Gaussian Frequency Shift Keying (GFSK) and 2Mbps FHSS uses four-level GFSK encoding .

The IR band is designed for indoor use only and has data rate 1Mbps and 2Mbps. Encoding scheme for 1Mbps IR is 16-pulse position modulation (PPM) and 2Mbps IR uses 4-PPM.

- **Medium Access Control layer**

The Medium Access Control sub-layer is responsible for the channel allocation procedures, protocol data unit (PDU) addressing, frame formatting, error checking and fragmentation and reassembly. IEEE 802.11 supports 3 kinds of frames: management, control and data. MAC sub-layer supports Distributed Coordination Function (DCF) for “ad hoc” mode and Point Coordination Function (PCF) for “infrastructure ” mode. DCF is similar to traditional legacy packet networks supporting best-effort delivery of data. The DCF is designed for asynchronous data transport, where all users with data to transmit have an equality fair chance of accessing the network; while PCF is based on polling that is controlled by AP. The PCF is primarily designed for the transmission of delay-sensitive traffic. DCF is the basic medium access control method for IEEE 802.11 and it is mandatory for all stations, while PCF is an optional extension to DCF and provides a time division multiplicity capability to accommodate time bounded, connection-oriented service. In the scope of this proposal, we are interested in and only DCF is explained in detail. Interested reader can refer to [6] for PCF specifications.

Because a station in wireless network is not able to listen to the channel for collisions while transmitting, so the widely used carrier sensing/collision detection (CSMA/CD) scheme can not be used, instead, carrier sensing/collision avoidance is employed by DCF. In IEEE 802.11, carrier sensing is performed at both the air interface, referred to as *physical carrier sensing*, and at the MAC sub-layer, referred to as *virtual carrier sensing*.

Physical carrier sensing detects the presence of other IEEE 802.11 WLAN users by analyzing all detected packets, and also detects activity in the channel via relative signal strength from other sources. In 802.11, the basic time unit is time-slots, which is $20\mu\text{s}$ for DSSS, $50\mu\text{s}$ for FHSS and $8\mu\text{s}$ for Infra Red. Priority access to the wireless medium is controlled through the use of inter frame space (IFS) intervals between the transmissions of the frames. The IFS

intervals are mandatory periods of idle time on the transmission medium. All the stations in the network listens to the channel, when a station senses the channel is idle, the station waits for a Distributed IFS (DIFS) interval and make sure the channel is still idle, then the station transmit the MAC protocol data unit (MPDU). If the channel is busy, the station should wait until the channel is idle for DIFS, and then set up a back off timer whose value is uniformly choose from $(0, w - 1)$. The value w is called contention window, and depends on the number of transmission attempts for the packet. At the first transmission attempt, w is set to equal a value CW_{min} called minimum contention window. After each unsuccessful transmission attempt, w is doubled, until it reaches its maximum value $CW_{max} = 2^m CW_{min}$, the future failure attempt will not increase w anymore. The back-off scheme is used to prevent multiple stations from seizing the medium immediately after completion of the preceding transmission.

The receiving station calculate the check sum and determines whether the packet was received correctly, if yes, the receiving stations waits for a short IFS (SIFS) interval and transmit a positive acknowledgment frame (ACK) back to the sender. When MPDU packet is transmitted, the duration field of the frame contains the information how long the channel will be utilized to complete the successful transmission after the end of present frame. Other stations hearing the transmission will adjust their network allocation vector based on duration field value, which includes the SIFS interval and the ACK following the MPDU frame.

A source station may perform virtual carrier sensing by sending MPDU duration information in the header of request to send (RTS) and clear to send (CTS) and data frames. RTS and CTS frame is relatively small (20 and 14 bytes respectively) compared to the maximum MPDU packet size (2346 bytes), thus they are used to reserve the channel prior to the transmission of an MPDU and to minimize the amount of bandwidth wasted in case of collision. Prior to transmission a station senses the state of the channel. If the channel is idle for the time interval DIFS ,the station sends RTS to the intended receiver. Upon correct reception of the RTS, the receiving station waits for SIFS interval to reduce the possibility of a collision, and then transmits CTS back to the source station. Upon successful reception of the CTS, the source station is virtually assured that the channel is stable and reserved for successful transmission because all the other stations that can hear either the RTS or the CTS have adjusted their NAV according to the information provided in those packets. The source then waits another SIFS before it is permitted to transmit the DATA frame. If the DATA frame is received correctly,

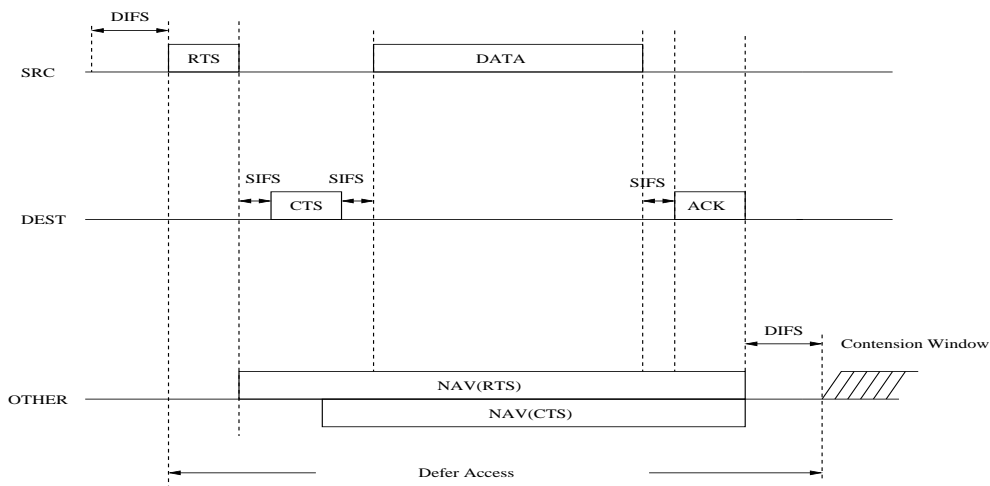


Figure 2.3: IEEE 802.11 MAC using RTS/CTS

the receiving station acknowledges the frame after a SIFS by sending an ACK frame to the source. Figure-2.3 illustrates the transmission of a MPDU using the RTS/CTS scheme.

Stations can choose never use RTS/CTS, always use RTS/CTS and only use RTS/CTS when the packet size exceed some specific threshold depending on the traffic load the available bandwidth. Large MPDUs can be fragmented to increase transmission reliability. When an MPDU is fragmented, all fragments are transmitted sequentially. The channel will not be released until the complete MPDU has been transmitted successfully. If RTS/CTS is used, only the first fragment is sent using the handshake mechanism. The duration value of RTS and CTS only account for the transmission of the first fragment through the receipt of its ACK. Stations in the BSS thereafter maintain their NAV by extracting the duration information from all subsequent fragments. If an ACK is not received for a previously transmitted fragment, the source station halts the transmission and re-contends for the channel.

2.2 Previous Art

A number of analysis have appeared in the literature in recent years that studies the throughput of ad hoc networks using IEEE 802.11 at the MAC-layer. The existing analysis are either based on simulation [7], [33] or by means of analytical models using a simplified back-off assumption [24],[5],[19]. The majority of theoretical work has focused on throughput analysis that assumes a fully connected ad hoc network, namely, all nodes are within a single hop of all other nodes. The existing work provides important insight, however, robust theoretical throughput

analysis is needed that characterizes multiple-hop performance.

2.2.1 Theoretical Maximum Throughput of Arbitrary Channel

In [28], Jun and Peddabachagari Calculate the theoretical MAC layer throughput of different 802.11 protocol specifications under ideal condition by considering the effect of the overhead of data transmission. It is the nominal value of the protocol but has nothing to do with real traffic etc. Their result provides an unrealistic performance upper bound that would never be achieved in real life thus can just serve as a rough estimation of the channel capacity and more thorough investigation need to be done for the capacity study.

2.2.2 Asymptotic throughput of a single node

In [24], Gupta and Kumar present asymptotic analysis for the maximum theoretical throughput for a fixed ad hoc network that can be obtained by an individual node based on the following assumptions: the network consists of n uniformly distributed fixed nodes; each node is capable of transmission a fixed data rate of W bits-per-second (bps) using a fixed range; traffic patterns are random with uniformly distributed destinations. Their main result shows that throughput per source-destination pair decreases as the number of nodes per-unit-area increases. Specifically, the report that the asymptotic throughput for each node is given by: $\Theta(W/\sqrt{n \log n})$ bps. Moreover, they claim that given optimal circumstances according to the following criterion: each node is optimally placed in a disk of unit area; traffic patters (routes) are optimally assigned; and, the transmission range of each node is optimally selected, then the maximum throughput improves on the order of $\sqrt{\log n}$ to: $\Theta(W/\sqrt{n})$ bps.

A significant shortcoming of the model from [24], however, stems from its lack of parametric network characterization. Although the results illustrate multi-hop performance bounds they are derived from highly abstract models. As such, they lack practical insight that can be applied to design more effective networks. Moreover, the results promote an overly pessimistic vision, specifically, by failing to account for the benefits of temporal and spatial diversity, coupled with the non-parametric approach a pre-maturely negative tone emerged in the research community. Other the other hand, Grosslauser and Tse examine the effects of random independent mobility to achieve multi-user diversity in [23]. Their main result shows that mobility provides natural route diversity that increases the effective capacity per source-destination pair such that it remains constant as the number of nodes per unit area increases. Although the specific results

of Grosslauser and Tse allow for infinite delay and adopts idealized random mobility patterns to minimize the long-term average path length, the analysis is significant in that it demonstrates the potential for exploiting diversity. Further the analysis in [1], wherein, a mixed set of mobile and fixed nodes is arranged a subject to random uniform traffic patterns among the static nodes. Bansal and Liu show verify that mobility increases throughput and can do so with a bounded delay. Specifically, they show that the optimal asymptotic throughput for each node is given by: $\Theta(W(m/n))$, where m is the number of mobile nodes and n is the number of fixed nodes. Similarly, Perevelov and Blum exploit both multi-user diversity and multi-path diversity to investigate delay limited capacity in [36].

2.2.3 Saturation throughput of a fully connected ad hoc network

The analysis presented by in [5] [25] develops an elegant and accurate analytical model for computing the throughput of IEEE 802.11 DCF under single-hop saturation conditions. In the derivation the following assumptions are made: there are a finite number of nodes; the network is fully connected, hence, all transmissions are synchronized into fixed slots, the channel is “ideal” in the sense that its characteristics remain fixed; all nodes are operating under continuous backlog conditions—i.e., every node always has a frame ready to transmit; and, in a manner similar to the well known analysis of the ultimate instability of the Aloha protocol, it is assumed that the probability of a collision during the transmission of any frame is independent and stationary. Specifically, with probability p any frame in transmission will experience a collision. It is a valid approximation under saturation conditions, wherein average response is being assessed. This is true because all nodes are subject to statistically equivalent conditions over time. This assumption allows a two-dimensional DTMC (Markov-Chain) formulation for the back-off procedure at each node. The solution to the DTMC leads to the stationary probability τ that a node transmits in randomly chosen time slot.

Equation (7) in [5] expresses the probability τ as a function of the fixed collision probability p and the size of the smallest and largest possible contention windows: $W = CW_{min}$ and $CW_{max} = 2mCW_{min}$ where m is the maximum number of retransmission attempts. Note that IEEE 802.11 DCF adopts an exponential back-off scheme for collision handling in which the back-off time is slotted. The slot time, σ , is set equal to the time required for any node to detect a transmission from its neighbors. At each frame transmission, the back-off timer is randomly selected from a uniform distribution over the range $(0;w)$ where w is the contention window. The

contention window size varies from CW_{min} and is doubled following each collision until it reaches CW_{max} . The probability τ is derived by noting that a node will transmit when the back-off time is zero regardless of the stage. Thus, it can be computed by taking the sum of the transition probabilities from all stages into back-off stage zero. The remainder of Bianchi's analysis considers the detailed events that occur in a given time-slot, thus, completing the derivation of saturation throughput as a function of the stationary probability τ . One question that arises is selection of the parameter p . Bianchi applies the independence assumption and ergodicity to relate p and τ —clearly for a collision to occur there must be at least two transmissions during a randomly chosen time slot, which leads to Equation (9) of [5].

Equations (7) and (9) in [5] form a nonlinear system in two unknowns. Numerical techniques can be used to find feasible solutions. By inverting τ and expressing it as a functional of p it is shown to be continuous and monotonically increasing over the feasible range $p \in (0, 1)$. This is sufficient to prove that there is a unique solution. The question remains, however, as to the sensitivity of the results to the choice of p and indeed to the more abstract meaning of p . Since the network mode adopted in [5] assumed fixed nodes it would seem feasible to tie to value of p somehow to factors that are influence by node mobility. This point is beyond the scope of the thesis therefore will not be discussed here anymore.

2.2.4 Simulation of end-to-end throughput of ad hoc network

[33] studies the interaction between the 802.11 MAC and packet forwarding via simulation. The main results both validate and refute the Gupta-Kumar capacity limitation, namely that network capacity is highly dependent on network size, traffic patterns, and local radio interactions. The later point references the localized effects of MAC and physical layers that are exacerbated when the network becomes very dense. Many of the earlier results assumed a fixed network size and increased the number of nodes. Clearly this results in greater contention at the MAC-layer. Given the ability to engage power control and directional antennas it seems likely that future ad hoc networks will be able to benefit from more optimal topology control. For the study in [33] the authors simulated various controlled scenarios to assess network throughput. In one experiment traffic routing was constrained to follow a chain of (interfering) nodes along horizontal or vertical paths in a regular lattice network. In another experiment they selected cross traffic in the lattice to increase the interference, and finally they studied the effects of random traffic patterns. As expected, the end-to-end throughput decreased with

the size of the network. However, the results also demonstrated that certain traffic patterns were significantly more scalable than others. Thus, the authors argued that the locality of the traffic represents the key factor reflecting network capacity and scalability. It is interesting to note that deeper examination of the body of related literature reveals two irrefutable trends: (1) Given the worst possible scenario wherein there is little or no locality of reference and spatial contention increases with the number of nodes system capacity will go approach zero; this situation is analogous to congestion collapse. The interesting question is whether or not there is an invariant that can characterize the point of collapse with respect to the relevant network parameters. (2) The Gupta-Kumar capacity limitation is not a fundamental limit — capacity can be increased as a natural side effect of inherently induced diversity, for example, node mobility, route diversity and non-uniform traffic patterns; furthermore control techniques can be engaged to further exploit particular aspects of diversity to increase capacity and bound delay. Examples of these techniques include multiple-path and dispersity based routing [36] or the addition of fixed nodes [1] into a mobile network. It would also seem feasible to add nodes with deterministic or highly predictable mobility patterns to capture both advantages simultaneously.

2.2.5 Throughput and cross-layer interaction

The central theme of [18] focused on cross-layer approach to understanding and improving power efficiency and throughput based on the abstract notion of “path-coupling”. The authors introduced the term “path-coupling” to more concretely demonstrate the cross-layer interaction between MAC and routing. As such, they were the first to fully and succinctly characterize this phenomena in a well-define manner. This path coupling phenomena is caused by the broadcast nature of the wireless communications “link”, wherein, multiple nodes contend for access to a single frequency channel or code sequence (in the case of CDMA). The authors address performance implications for a wireless ad hoc network routing algorithm that relies on any of the class of contention based MAC-layer protocols. Given these circumstances traffic routed along link and node disjoint paths may be subject to transmission delays and packet loss due to contention with a neighbor for the channel or competition from hidden terminals. Results suggest that the effects of path-coupling can seriously degrade network performance. As such, the cross-layer implications are clear: The MAC-layer should be able to measure the “degree of coupling” and report it to the routing-layer. Knowledge of traffic flows and path coupling

could provide the criteria for route selection that reduces energy consumption and increases throughput to acceptable levels. In the related works [7] Crow et al did not address the hidden terminal problem, while in [5] discussed previously the hidden terminal problem is considered, but the work is limited to single-hop systems. Recently, discouraging performance results for several ad hoc routing protocols were reported in [37] that has helped to draw attention to the issue of cross-layer interaction and network performance. An analysis of the effects of different MAC-layer protocols on specific ad hoc network routing algorithms was presented in [15], however, it is concerned that this approach is prone to bias and interaction with respect to the routing algorithm; furthermore, the authors did not make any attempt to explicitly characterize the interaction nor its theoretical impact on energy efficiency or throughput. The first paper to directly address the issue of 802.11 feasibility for ad hoc networks is [45]; however, the results are based on TCP performance over DSR, hence, they are unable to provide a clear distinction between the effects. The work by Li discussed earlier [33] reports very interesting results that agree in principle with the results reported by [18]. However, the authors conclude that this result is the key factor affecting the ultimate feasibility of ad hoc networking. They fail to suggest the possibility of MAC-aware routing, cross-layer optimizations or alternative access control strategies.

The work in [18] considers the problem of using a contention based MAC layer protocol (802.11) in ad hoc networks. Unlike previous research in this area [18] approaches the problem as a cross-layer interaction that results in a virtual coupling of network-layer paths. Both analytical and simulation results were developed and show the precise mechanism for the problem. The results agree in principle with previous work, however, the perspective taken is one of isolating the MAC-layer effects to understand them, and then utilize that understanding in future work to control the cross-layer interaction by developing routing metrics and cross-layer optimization methodologies that account for this important yet little studied problem. The first principle of the proposed admission control framework builds on these concepts.

2.3 Conclusion

In this chapter, background knowledge related reconfigurable wireless networks (RWN) is discussed. Medium access control protocols for wireless ad hoc networks are reviewed and the

summary of the previous work on performance analysis of wireless ad hoc networks are presented. Among previous work, some of them did not consider multi-hop wireless environment, others, although multi-hop wireless network is studied, is based on highly abstract model and lack of parametric network characterization. Moreover, cross-layer interaction is not considered in both research hence is not able to discuss the possible benefit and disadvantage introduced by cross-layer interaction and temporal and spatial diversity.

In the next chapter, a novel deferral framework to characterize the nature of wireless networks more accurately is introduced and this framework will be used to facilitate performance analysis of multi-hop wireless ad hoc networks. In this framework, the behavior of wireless node is characterized in detail by a node behavior model through which the cross-layer interaction and temporal and spatial diversity can be accounted. Hence, the proposed framework addressed the shortcomings of the previous performance models and is able to provide accurate capacity analysis of multi-hop wireless networks.

Chapter 3

Deferral Framework Overview

As discussed in Chapter 1, a deferral framework is proposed to study the capacity bounds and other invariant performance characteristics which are crucial elements required for the development of future ad hoc network (ANS) systems designed to support real-time and other performance-bound applications. In this chapter, the overview of the deferral framework is presented. First the components of the framework are enumerated, then, each component of the framework is studied respectively.

3.1 Components of the Framework

The objective of the deferral framework is to provide an universal methodology and a comprehensive model to facilitate capacity analysis. It consists the following components.

1. An appropriate abstract model that can characterize the inherent cross-layer interactions in multi-hop wireless environment.
2. An algorithm to calculate the probability of transmission of each single node in the network, usually the algorithm is based on multi-dimensional Markov chain model.
3. Node behavior model containing information from 1 and 2 to serves as the direct workspace for capacity analysis.

Different types of wireless networks can be characterized by the framework through modifications of specific parametric behaviors and re-evaluation of the associated probabilities. Hence, the framework is an extensible, flexible, parametric framework that is emerging as a powerful tool for ad hoc network and design. In the rest of this chapter, each component of the framework is discussed respectively; in the next two chapters, two applications of the framework

are presented, namely, the channel and network capacity analysis of multi-hop wireless ad hoc networks based on arbitrary routing and scheduling coupled with the characteristics of IEEE 802.11 DCF [6] with RTS/CTS exchange.

3.2 Abstract Model

In this section important concepts are introduced. Among those concepts, some are already well established, and were presented in subsection-3.2.1 for the completeness and consistency; others are introduced by the authors in subsection-3.2.2 in order to appropriately characterize the inherent cross-layer interaction in multi-hop wireless networks. Moreover, Definition-3.2.1 to definition-3.2.4 are the basic definitions suitable to all kinds wireless network, while the rest of the definitions will only be needed in multi-hop network analysis and are specifically proposed based on the observation that when IEEE 802.11 four way-handshake DCF is employed, all the nodes that are in two hops away from the communicating pair have to defer their access to the channel even though in fact they won't content for the same channel which is being used given no specific scheduling scheme is present. For other MAC specifications, similar definitions can be made in the same fashion.

3.2.1 Well Established Definitions

Definition 3.2.1. Link

(x, y) from node x to node y is defined as a wireless communications channel over which nodes x and y are able to reliably exchange frames without relaying through intermediate nodes. The parameters that affect the availability of a link at a given time include, but are not necessarily limited to, distance, topography, transmission power and frequency, transmit and receive antenna gain, receiver sensitivity, modulation and coding schemes, SNR and a given threshold probability of received symbol error; the set of communications parameters are expressed together in the variable length vector: \bar{p} . The indicator variable $l(x, y, t, \bar{p})$ reflects the link status between nodes x and y at time t. If link (x, y) is available, then $l(x, y, t, \bar{p}) = 1$; otherwise link (x, y) is considered unavailable with $l(x, y, t, \bar{p}) = 0$.

Definition 3.2.2. Communications

A pair of nodes {x, y} with an available link (x, y) are defined as being Communications Active if nodes x and y are engaged in the exchange of a frame (in either direction); otherwise they are defined as being Communications Inactive. The indicator variable $c(x, y, t)$ reflects the

communications status between nodes x and y at time t . If $\{x, y\}$ are Communications Active, then $c(x, y, t) = 1$; otherwise $c(x, y, t) = 0$.

Definition 3.2.3. Neighbor Set

$N_x(t)$ of node x at time t is defined as the set of nodes, each of which share an available link with node x at time t . If $V(t)$ is the set of nodes in the network at time t , the Neighbor Set of x is given by the following expression:

$$N_x(t) = \{y | \forall y \in V(t), l(x, y, t, \bar{p}) = 1\}$$

Definition 3.2.4. The Incident-Link Set

$E_x(t)$ of node x at time t is defined as the set of links incident with x and each node in its Neighbor Set. The set is specified by the following expression:

$$E_x(t) = \{(x, k) | \forall k \in N_x(t)\}$$

Property 3.2.1. Definition 3.2.3 and Definition 3.2.4 may also be used collectively with respect to sets of nodes, namely, given a set of node $S = \{x_1, x_2, \dots\}$ at time t , $\cup N_{x_i}(t) = N_S(t)$ and $\cup E_{x_i}(t) = E_S(t)$. The following relationships follow directly:

$$\begin{aligned} N_{\{N_x(t)\}}(t) \cup N_{\{N_y(t)\}}(t) &= N_{\{N_x(t) \cup N_y(t)\}} \\ E_{\{N_x(t)\}}(t) \cup E_{\{N_y(t)\}}(t) &= E_{\{N_x(t) \cup N_y(t)\}} \end{aligned}$$

3.2.2 New concepts

Graph-theoretic models have dominated the development of routing algorithms and related research associated with wireless ad hoc networks. Definitions in the subsection-3.2.1 are drawn based those graph-theoretic models. In general, however, a traditional graph model is not able to reflect the broadcast nature of node transmission and the contention based media access generally assumed. Moreover, the presence of hidden and exposed terminal further complicates the graph-based modeling of these systems. It would not be unreasonable to argue that the design of algorithms based on an obviously flawed model is unlikely to result in the most efficient algorithms. Unfortunately the community has been left without a better model to choose from and an enormous body of work is based on the incorrect assumption that a “link” in an ad hoc network can be modeled as an edge — uni-directional or bi-directional. The truce interactions, however, are far more complex and the notion of “link” itself is an abstraction drawn from a broadcast channel.

In this subsection, novel concepts “deferral set” and “equivalent competitor” are introduced. They characterize the interacting and competition phenomena of multi-hop wireless networks. They provide a virtual transformation of the traditional graph model that enables the analysis of ad hoc networks by focusing on a well-defined sub-group of nodes associated with a pair of actively communicating nodes. Each of the following definition is defined with respect to *communication active pair* $\{x, y\}$ at time t : namely, $y \in N_x(t)$ and $c(x, y, t) = 1$.

As indicated above, the “deferral set” concept is based on the characteristics of IEEE 802.11 DCF RTS/CTS scheme, however, the phenomena is inherent to contention based medium access control due to the broadcast transmission paradigm. To understand the concept consider the following: Given an active transmission between a pair of adjacent nodes *all direct neighbors* of either or both nodes (source or destination of active transmission) must defer any transmissions. Furthermore, any transmissions from any two hop away neighbor (a node adjacent to a direct neighbor that is not itself a direct neighbor of either node) that are destined to a direct neighbor must also be deferred. These rules are used to avoid collisions. Hence, it can be observed that all “links” that are less than or equal to two hops from the currently active link must be idle for the duration of the transmission. Based on this observation, the level I and II interference as well as deferral set are defined. These concepts provide a snapshot of the network at an arbitrary time. In addition to providing a basis for the network modeling it can be used to facilitate better routing decisions, control dynamic clustering and improve traffic scheduling.

Definition 3.2.5. Level-1 Interference Node Set

$I_{Node}^1(x, y, t)$ of the communication active pair $\{x, y\}$ at time t is defined as the set of nodes

$$I_{Node}^1(x, y, t) = \{k | \forall k \in \{N_x(t) \cup N_y(t)\}, k \neq x, y\}$$

The degree of the level-1 interference node set can also be represented by $I_{Node}^1(x, y, t)$, it is defined as the number of nodes in level-1 interference node set.

Definition 3.2.6. Level-1 Interference Link Set

$I_{Link}^1(x, y, t)$ of the communication active pair $\{x, y\}$ at time t is defined as the set of links

$$I_{Link}^1(x, y, t) = \{(j, k) | \forall (j, k) \in \{E_x(t) \cup E_y(t)\}, (j, k) \neq (x, y)\}$$

The degree of the level-1 interference link set can also be represented by $I_{Link}^1(x, y, t)$, it is defined as the number of links in level-1 interference link set.

Definition 3.2.7. Level-2 Interference Node Set

$I_{Node}^2(x, y, t)$ of the communication active pair $\{x, y\}$ at time t is defined as the set of nodes

$$I_{Node}^2(x, y, t) = \{k | \forall k \in N_{N_x(t) \cup N_y(t)} - \{N_x(t) \cup N_y(t)\}\}$$

The degree of the level-2 interference node set can also be represented by $I_{Node}^2(x, y, t)$, it is defined as the number of nodes in level-2 interference node set.

Definition 3.2.8. Level-2 Interference Link Set

$I_{Link}^2(x, y, t)$ of the communication active pair $\{x, y\}$ at time t is defined as the set of links

$$I_{Link}^2(x, y, t) = \{(j, k) | \forall (j, k) \in E_{N_x(t) \cup N_y(t)} - \{E_x(t) \cup E_y(t)\}\}$$

The degree of the level-2 interference link set can also be represented by $I_{Link}^2(x, y, t)$, it is defined as the number of links in level-2 interference link set.

Definition 3.2.9. Deferral Node Set

$D_{Node}(x, y, t)$ of the communication active pair $\{x, y\}$ at time t is defined as the set of nodes $\{k | \forall k \in \{N_{N_x(t) \cup N_y(t)} \cup N_x(t) \cup N_y(t)\}, k \neq x, y\}$.

$$D_{Node}(x, y, t) = \{I_{Node}^1(x, y, t) \cup I_{Node}^2(x, y, t)\}$$

The degree of the deferral node set can also be represented by $D_{Node}(x, y, t)$, it is defined as the number of nodes in the deferral node set.

Definition 3.2.10. Deferral Link Set

$D_{Link}(x, y, t)$ of the communication active pair $\{x, y\}$ at time t is defined as the set of links $\{(j, k) | \forall (j, k) \in \{E_{N_x(t) \cup N_y(t)} \cup E_x(t) \cup E_y(t)\}, (j, k) \neq (x, y)\}$.

$$D_{Link}(x, y, t) = \{I_{Link}^1(x, y, t) \cup I_{Link}^2(x, y, t)\}$$

The degree of the deferral link set can also be represented by $D_{Link}(x, y, t)$, it is defined as the number of links in the deferral link set.

Notice that level-2 interference set and deferral set may overlap. Therefore, attention should be paid to avoid counting the same link or node twice in different level-2 interference set and deferral set, for this link or node have already been deferred by one communication can not be deferred again by another *simultaneous* communication. Such as in Figure-3.1, hollow nodes represent nodes that are currently involved with ongoing communication, solid nodes are one hop neighbors, while shadowed nodes are two hop neighbors. One-hop link is solid and the

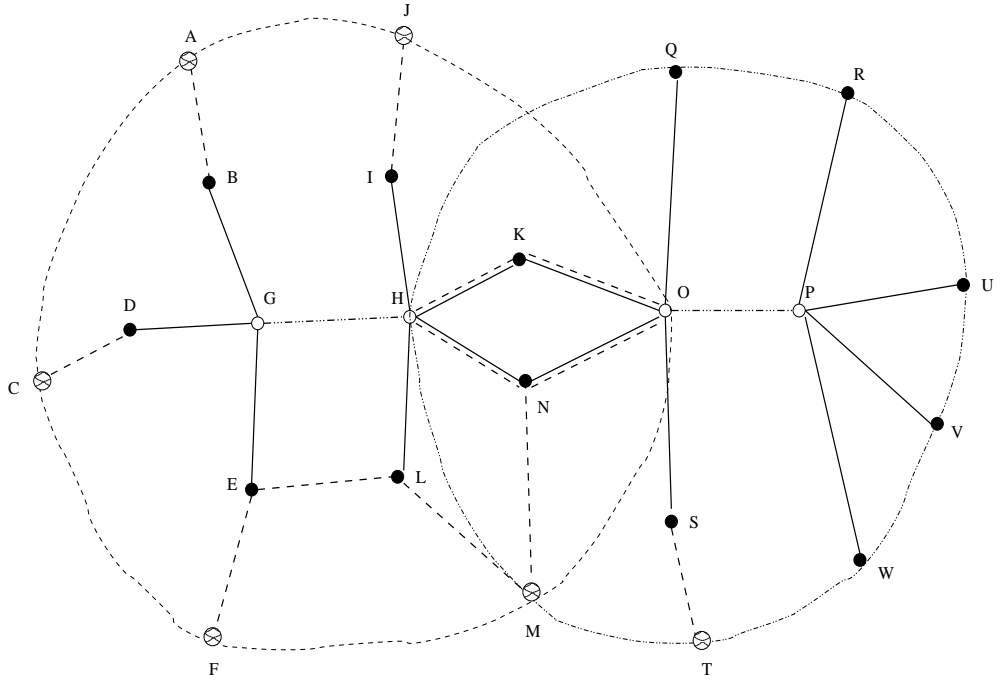


Figure 3.1: An example of how to calculate the size of communication set

two hop link is dashed. Nodes (links) may have different roles in different level-II interference set. For example, node H is one of the communication nodes in $C(G,H,t)$ while it is also the two hops neighbor in $C(O,P,t)$; link HK is the one hop link in $C(G,H,t)$ and two hops link in $C(O,P,t)$. Links between one solid and one hollow nodes or two hollow nodes must be deactivated while links between two shadowed nodes (not show in Figure-3.1) can be used for simultaneous transmission.

If $D_{Link}(O, P, t)$ is calculated first, link OK, ON, HK, HN and MN are counted, so we have:

$$D_{Link}(O, P, t) = 12$$

Then for $D_{Link}(G, H, t)$, link OK, ON, HK, HN and MN should not be counted, thus we got :

$$D_{Link}(G, H, t) = 11$$

Lemma-3.2.1 summarizes the channel access rule of the links in the network.

Lemma 3.2.1. *Assume that $c(x,y) = 1$ over a certain time interval Δt . During the entire interval Δt every node $k \in D_{Node}(x,y)$ must defer its channel access on any link $(j,k) \in$*

$D_{Link}(x, y)$ over the entire interval: Formally, when $c(x, y) = 1$ during Δt :

$$c(m, n) = 0 \quad \forall m, n \in \{N_x \cup N_y\} \quad (3.2.1)$$

$$c(m, k) = 0 \quad \forall m \in \{N_x \cup N_y\}, \forall k \in N_m - \{N_x \cup N_y\} \quad (3.2.2)$$

Lemma-3.2.1 provides the fundamental building block for performance analysis. Put simply the lemma states that when two arbitrary nodes x and y are engaged in the exchange of data have captured the channel, no direct neighbor of either nodes may transmit to any other one hop neighbor of either node. (3.2.1), and no two hop neighbor of either node may transmit to or receive from any one-hop neighbor of either node. (3.2.2).

The difficulty of characterizing effective interference caused by multi-hop contention effects is that only a specific transmission configuration for two hop away neighbors can cause potential interference. Hence, the concept of the “equivalent competitor” is introduced. As noted before — **any communication originated from the nodes in level-I interference node set will definitely affect current communication, while only the communication originated from nodes in level-II interference node set toward nodes in level-I interference node set will affect the current communication**, the actual competition from a single two hop neighbor is represented by the value of “equivalent two hop competitors”, which must less than or equal to unity. The sum of direct neighbors and the “equivalent two hop competitors” is defined as “equivalent competitor”.

Definition 3.2.11. Equivalent Competitor

Eq_{com}(x, y, t) of the communication active pair {x, y} at time t is defined as actual “competition” generated by the whole deferral node set in terms of the effect of “competition” generated by direct neighbor of the communication active pair .

The actual “competition” the current communication experienced characterized by “equivalent competitor” is not as serious as the degree of “deferral node set” suggested, actually it is a weighted value of the degree of “deferral node set”.

Based on these new concepts a wireless ad hoc network can be interpreted as a set of concurrent deferral sets. In each deferral set there can be one-and-only-on active transmission. The scope of contention is characterized by the “equivalent competitors”.

3.2.3 Notation and Terminology

In this subsection the notations and variables used through the thesis are listed. Table-3.1

lists notations of the new concepts introduced in the thesis and their related variables, while table-3.2 lists the notations of the intrinsic network or protocol parameter. Note that the variables in those Tables are not always independent to each other and their relations will be discussed in the rest of the thesis when necessary.

Notations	Meaning
x	node x expressed by its id
$l(x, y, t, \bar{p})$	indicator variable of link status between node x and y at time t .
$c(x, y, t)$	communication between node x and y at time t
$N_x(t)$	node x 's neighbor set at time t
$E_x(t)$	node x 's incident-link set at time t
$I_{Node}^1(x, y, t)$	level-1 interference node set of the communication active pair (x,y) at time t
$I_{Link}^1(x, y, t)$	level-1 interference Link set of the communication active pair (x,y) at time t
$I_{Node}^2(x, y, t)$	level-2 interference node set of the communication active pair (x,y) at time t
$I_{Link}^2(x, y, t)$	level-2 interference Link set of the communication active pair (x,y) at time t
$D_{Node}(x, y, t)$	Deferral node set of the communication active pair (x,y) at time t
$D_{Link}(x, y, t)$	Deferral link set of the communication active pair (x,y) at time t
$N'(x, y, t)$	Number of equivalent competitor of the communication active pair (x,y) at time t
$Area_1(x, y, t)$	area covered by level-1 interference set at time t
$Num_{I1}(t)$	number of non-overlapping level-1 interference set at time t
$Area_D(x, y, t)$	area covered by deferral set at time t
$Num_D(t)$	number of possible deferral set at time t

Table 3.1: Deferral Set Framework Variables

Notations	Meaning
L	The radius of network
N	Number of nodes in the network
n_{avg}	Average number of neighbors of each node
ρ	Node density of the network
N_l	Number of links in the network
ρ_l	Link density of the network
W	CW_{min}
m	maximum back-off stage, $CW_{max} = 2^m W$
δ	propagation delay
H	packet header, $H = PHY_{hdr} + MAC_{hdr}$
r	transmission range

Table 3.2: System Parameters

3.3 Transmission Probability

In section-3.2 the abstract model of wireless ad hoc networks is discussed, this section studies the probability of transmission of an arbitrary node in the network given back-logged load. The probability of transmission is closely tied to the back-off algorithm the MAC layer protocol utilized. One example of probability of transmission investigation below uses a two-dimensional Markov chain model presented in [5]. The probability of transmission in this thesis is obtained by similar approach provided in [5] coupled with the “equivalent competitor” that characterizes the multi-hop environment.

As discussed in Chapter-2, IEEE 802.11 DCF adopts an exponential back-off scheme when collision happens. Back-off time is slotted and stations are allowed to transmit at the beginning of the time slot. The slot time, σ , is set equal to the time needed for any station to detect the transmission from its neighbors. At each packet transmission, the back-off timer is random uniformly chosen from range $(0, w-1)$. Where w is called contention window, contention window size starts with the minimum value CW_{min} , and will double at each failure of transmission/retransmission until it reach a maximum value CW_{max} , the relation between CW_{max} and CW_{min} is $CW_{max} = 2^m CW_{min}$, where m is back-off stage.

[5] proposed a Markov chain model and it was modified by [25] for a single station’s back-off window size that is shown in Figure-3.2.

The combination of random variables back-off stage $s(t)$ which corresponding to current contention window size and back-off counter $b(t)$ which corresponding to the slots to be wait before the station can try to transmit again is modeled by a discrete-time Markov chain under the approximation that at each transmission attempt, each packet collides with constant and independent probability p regardless of the number of retransmission. Use the same notation as [5]¹, the Markov chain can be expressed as following:

$$\begin{cases} P\{i, k|i, k+1\} = 1 & k \in (0, W_i - 2), i \in (0, m) \\ P\{0, k|i, 0\} = (1-p)/W_0 & k \in (0, W_0 - 1), i \in (0, m) \\ P\{i, k|i-1, 0\} = p/W_i & k \in (0, W_i - 1), i \in (1, m) \\ P\{m, k|m, 0\} = p/W_m & k \in (0, W_m - 1) \end{cases}$$

where p is the probability of that the packet being sent ends up with collisions with other packets and let $b_{i,k}$ be the stationary distribution of the Markov chain, then

$$\frac{b_{i-1,0} = pb_{i-1,0}, \quad 0 < i \leq m}{^1 P\{i_1, k_1|i_0, k_0\} = P\{s(t+1) = i_1, b(t+1) = k_1, |s(t) = i_0, b(t) = k_0\}}$$

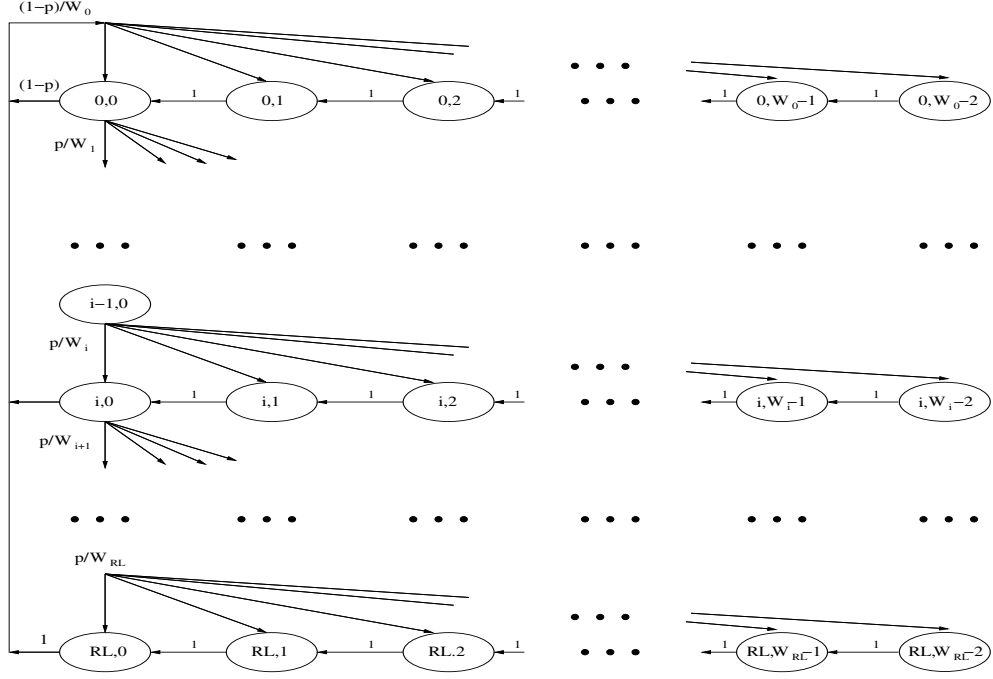


Figure 3.2: Markov chain model for a single station's back-off window size

and since the chain is regular, so for each $k \in (0, W_i - 1)$,

$$b_{i,k} = \frac{W_i - k}{W_i} \begin{cases} (1-p) \sum_{j=0}^{m-1} b_{j,0} + b_{m,0} & i = 0 \\ pb_{i-1,0} & 0 < i \leq m \end{cases}$$

and given that fact that sum of all the probabilities in each state is 1, and the probability of a node to start a new transmission is just the sum of the probability that the node in state $b_{i,0}, i = 0, \dots, m$,

$$1 = \sum_{i=0}^m \sum_{k=0}^{W_i-1} b_{i,k} = \sum_{i=0}^m b_{i,0} \sum_{k=0}^{W_i-1} \frac{W_i - k}{W_i} = \sum_{i=0}^m b_{i,0} \frac{W_i + 1}{2}$$

$$\tau = \sum_{i=0}^m b_{i,0} = \frac{1 - p^{m+1}}{1 - p} b_{0,0} \quad (3.3.1)$$

In [25] $b_{0,0}$ is derived as:

$$b_{0,0} = \begin{cases} \frac{2(1-2p)(1-p)}{W(1-(2p)^{RL+1})(1-p) + (1-2p)(1-p^{RL+1})} & RL \leq m \\ \frac{(1-p)}{+W2^m p^{m+1}(1-2p)(1-p^{RL-m})} & RL > m \end{cases}$$

In the stationary state, a station transmit a packet with probability τ , thus we have

$$p = 1 - (1 - \tau)^n$$

p is the probability that any transmitted frame will result in a collision. The Markov assumption results initially from the one-hop assumption. Synchronization is easily achieved between adjacent nodes under back-logged conditions, because in this case a the node always has packet to transmit, apparently each node will be either in back-off state or in transmit/receive state, fully connected network guaranteed that the vision of the network seen from every node are same. In other words, time is divided into a sequence of non-overlapping slots, Φ ², which represents the elapsed time between two successful transmissions. In principle multi-hop wireless synchronization is a non-trivial problem, hence, it is less reasonable to assume multi-hop Φ level synchronization. Without loss of generalization, however, slot-level (α) synchronization is assumed under continuous back-logged conditions; the capacity limit of a channel is reached when all the nodes are continuously busy. The synchronization assumption is justified by observing that each node is either in the back-off, transmission or receiving state. Hence, all adjacent nodes retain Φ level synchronization and nodes that are ≥ 2 hops away are synchronized via α through any intermediate nodes. Thus (3.3.1) can also be used in back-logged multi-hop scenario without any modification. Notice here in (3.3.1), the probability of retransmission is already counted, which has no difference with “first transmission” in terms of information exchange.

3.4 Node Model

In this proposal, “deferral set” and “equivalent competitor” facilitate the capacity analysis in a unique way: From the perspective of the node. This diverges from the more traditional approach of taking the channel oriented perspective [31], [32]. The node oriented approach is more natural and provide s a straight-forward and extensible analytical methodology. A key insight is that a node reacts to contention in the same way regardless of whether it originated from a neighbor or multiple hops away. Thus, in concert with the novel concepts introduced in the thesis — the node perspective reduces the complexity of multi-hop analysis, thus it facilitates theoretical results for arbitrary network configurations.

² Φ (variable) refers to time interval between two consecutive back-off time counter decreased, which is different from the slot time σ which is constant

The node behavior model is a finite state machine that characterized the node's behavior by the probabilities of the transmission from different "states" of the nodes. Chapter-4 provides an example of the node behavior model. Same as the probability of transmission, the node behavior model is also tightly related to the specific MAC layer protocol the node employs, again, in the proposal, IEEE 802.11 Distributed Coordination Function (DCF) with RTS/CTS scheme is the underlying medium access control protocol, hence the node behavior model is built based on those specifications.

3.5 Conclusion

This chapter presents an overview of the deferral framework, the three components of the framework are introduced, namely, for the abstract model to characterize the multi-hop wireless environment — a deferral set for an ongoing communication is proposed, the deferral set included all the nodes and links that should not be active simultaneously with the ongoing communication; there are some algorithms available to calculate the transmission probability for an arbitrary node, in the context of the proposal, the algorithm is based on [5]'s two-dimension markov chain model and an novel concept "equivalent competitor" is proposed to account for the multi-hop environment. The third, and the last component is the node behavior model—a finite state machine that characterize the node's behavior.

In the following two chapters, two applications of the deferral framework are presented for capacity analysis in multi-hop wireless ad hoc network, namely, the channel and network capacity analysis of multi-hop wireless ad hoc networks.

Chapter 4

Channel Capacity Analysis Using Deferral Framework

Chapter-3 presents the overview of the deferral framework, in this chapter one application of the deferral framework — the fundamental capacity limit of an ad hoc network channel (or node) under multi-hop conditions is presented. Node and channel capacity reflect of the maximum capability of data exchange per unit time for an arbitrary node of channel. The result is invariant with respect to routing, scheduling or any other network control — the only constraint is the contention due to wireless access control. It is assumed that traffic at a given node may have originated at that node or be in transmit with that node acting as a router. Hence, the result is an inherent limit.

4.1 Methodology

Based on the deferral framework proposed in Chapter 3, in this section a novel methodology is developed for arbitrary channel capacity analysis. This proposed methodology utilize a novel approach — integrate deferral set concept and the algorithm for transmission probability to obtain the probability of a node in multi-hop wireless network to transmit at arbitrary time, then this information is used in the node behavior model to obtain the channel capacity. This novel methodology can be summarized as the following steps:

1. Based on the specific MAC layer protocol, build the appropriate deferral set model and calculated the fundamental parameters that will determine the performance of such as “degree of deferral set”, “equivalent competitor”, etc .

2. Calculate the probability of transmission p and the new transmission attempt probability τ of an individual node according to the network configuration. Unique multi-hop characteristics — “equivalent competitors s ” and “deferral sets” are applied to modify the two dimensional continuous time Markov chain (CTMC) [5] [25] proposed to model back-off stage occupancy probabilities in earlier single-hop analyses. The values of p and τ are functions of the number of “equivalent competitors” N , in a deferral set, which is dependent on the node density, effective transmission range and traffic distribution.
3. Given p , τ , create the parametric node behavior state transition model based on the underlying MAC layer protocol and the probability of successful transmission, retransmission, failure can be derived respectively given the state transition model. Again in this proposal, node transition model is built based on IEEE 802.11 DCF.
4. From results derived from step 3, channel (or node) capacity and network capacity can be derived using appropriate method. In this Chapter arbitrary channel capacity is studied and next Chapter discusses the network capacity analysis.

4.2 Channel Capacity Analysis

This section builds on the methodology described in the previous section and presents a detailed example of the “deferral framework”. Also the channel capacity analysis introduced here is served as the basis for network capacity analysis.

4.2.1 Equivalent Competitors

In order to obtain the equivalent competitor, the network is studied geometrically to calculate area covered by level-1 and level-2 interference set and therefore — the deferral set. Given the areas and the node density of network, number of one hop neighbors, two hop neighbors and corresponding equivalent competitors can be derived.

Given a wireless ad hoc network, without loss of generality, it is assumed that nodes are uniformly distributed in the network, thus, statistically each node is expected to have the same number of neighbor. The network will be characterized by either N and n_{avg} or N and ρ .

$$\rho = \frac{n_{avg} + 1}{\pi r^2}$$

Next, given the N and n_{avg} , the radius of the topology L and number of links in the network N_l are

$$\begin{aligned}\frac{\pi r^2}{n_{avg} + 1} &= \frac{\pi L^2}{N} \\ L &= \sqrt{\frac{N}{n_{avg} + 1}} \cdot r \\ N_l &= \frac{N \cdot n_{avg}}{2}\end{aligned}$$

Other important parameters includes the average area covered the level-1 and level-2 interference set ($\overline{Area_1(x, y, t)}$ and $\overline{Area_2(x, y, t)}$) and the expected degree of level-1 and level-2 interference node set $E[I_{Node}^1(x, y, t)]$ and $E[I_{Node}^2(x, y, t)]$. The values of those parameters are derived as follows:

- Area covered level-1 Interference set - $Area_1(x, y, t)$

A typical level-1 interference set is shown in Figure-4.1

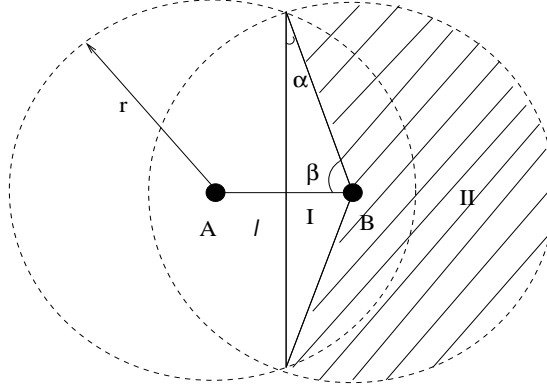


Figure 4.1: A typical level-1 interference set

As shown in Figure-4.1, the area cover by level-1 interference set, given the Euclidean distance between the two communicating nodes A and B is l can be calculated as:

$$\begin{aligned}Area_1(l) &= 2 \times (\text{Area of part I} + \text{Area of part II}) \\ \alpha &= \sin^{-1}\left(\frac{l}{2r}\right) = \sin^{-1}\left(\frac{l}{2r}\right)\end{aligned}$$

$$\begin{aligned}
\text{Area of part I} &= \frac{1}{2} \times \frac{l}{2} \times (2\sqrt{r^2 - \frac{l^2}{2}}) \\
&= \frac{l}{4} \sqrt{4r^2 - l^2} \\
\text{Area of part II} &= \pi r^2 \times \frac{\pi + 2\alpha}{2\pi} \\
&= \frac{(\pi + 2\alpha)r^2}{2} \\
\text{Area}_1(l) &= (\pi + 2\alpha)r^2 + \frac{l}{2} \sqrt{4r^2 - l^2}
\end{aligned}$$

Under assumption that nodes are uniformly distributed in the network, the Euclidean distance between the communicating pair can be regarded as uniformly distributed between (0,r) and expectation of the area of level-I interference set will be:

$$\begin{aligned}
\overline{\text{Area}_1} &= \int_0^r f(l) \text{Area}_1(l) dl \\
&= \int_0^r \frac{1}{r} ((\pi + 2\alpha)r^2 + \frac{l}{2} \sqrt{4r^2 - l^2}) dl \\
&= \pi r^2 + 2r \int_0^r \sin^{-1} \frac{l}{2r} dl + \frac{1}{4r} \int_0^r \sqrt{4r^2 - l^2} dl^2 \\
&= \pi r^2 + 4r^2 \left(\frac{l}{2r} \sin^{-1} \left(\frac{l}{2r} \right) + \sqrt{1 - \left(\frac{l}{2r} \right)^2} \right) \Big|_0^r + \frac{1}{4r} \cdot \frac{2}{3} (4r^2 - l^2)^{\frac{3}{2}} \Big|_0^r \\
&= \pi r^2 + 0.47r^2 + 0.512r^2 \\
&= (\pi + 0.98)r^2
\end{aligned} \tag{4.2.1}$$

- Expected degree of level-1 interference node set — $E[I_{Node}^1(x, y, t)]$

Given the nodes are uniformly distributed in the topology and the average area covered by level-1 interference set, it is obvious that

$$\begin{aligned}
E[I_{Node}^1(x, y, t)] &= \rho \cdot \overline{\text{Area}_I} \\
&= \rho(\pi + 0.98)r^2 \\
&= \frac{(n_{avg} + 1)(\pi + 0.98)}{2\pi}
\end{aligned} \tag{4.2.2}$$

- Probability of a node being two hop neighbor - *Pr2 hop*

set up an x,y space, the coordinates of the nodes A, B, D are:

$$A(-\frac{l}{2}, 0), B(\frac{l}{2}, 0), D(D_x, D_y)$$

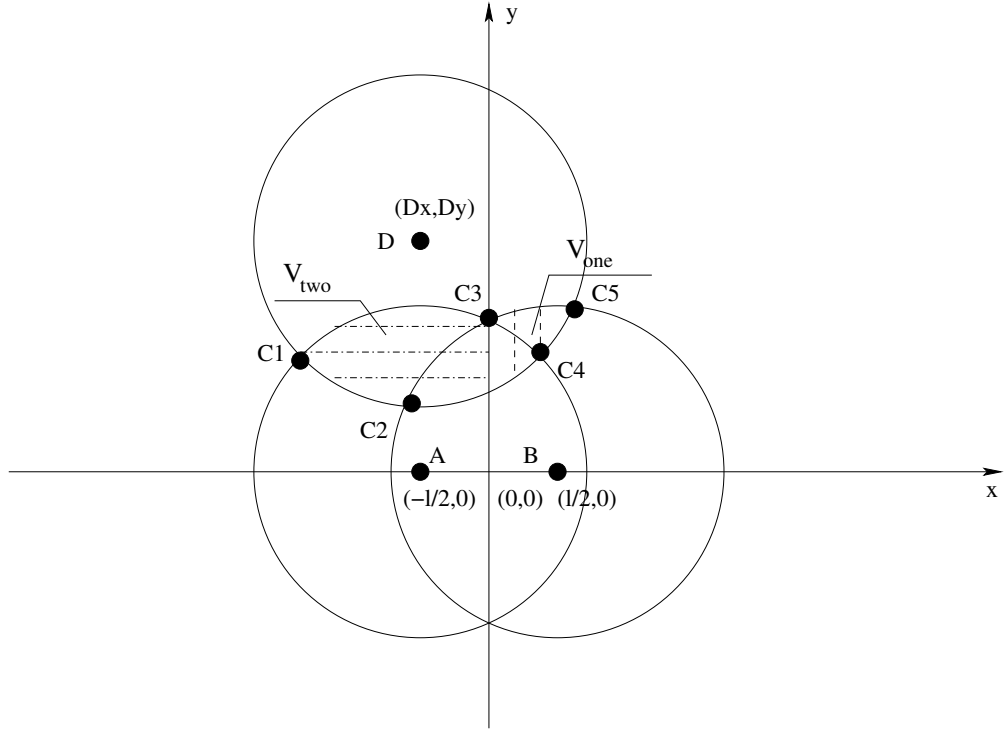


Figure 4.2: A Typical Level-2 Interference Set

Step 1: Finding the coordinates of the intersection nodes:

node C1, C4:

$$\begin{cases} (x - D_x)^2 + (y - D_y)^2 = (x + \frac{l}{2})^2 + y^2 \\ (x + \frac{l}{2})^2 + y^2 = r^2 \end{cases}$$

$$\begin{cases} (l + 2D_x)x + 2D_y y = D_x^2 + D_y^2 - \frac{l^2}{4} \\ y = \frac{D_x^2 + D_y^2 - \frac{l^2}{4} - (l + 2D_x)x}{2D_y} \end{cases}$$

$$\begin{cases} x^2 + lx + \frac{((D_x^2 + D_y^2 - \frac{l^2}{4}) - (l + 2D_x)x)^2}{4D_y^2} = r^2 - \frac{l^2}{4} \\ (4D_x^2 + 4D_x l + l^2 + 4D_y^2)x^2 + (4D_y^2 l - 2(l + 2D_x)(D_x^2 + D_y^2 - \frac{l^2}{4}))x \\ + (D_x^2 + D_y^2 - \frac{l^2}{4})^2 + l^2 D_y^2 - 4D_y^2 r^2 \end{cases}$$

let

$$\begin{cases} A_1 = 4D_x^2 + 4D_x l + 4D_y^2 + l^2 \\ A_2 = 4D_y^2 l - 2(l + 2D_x)(D_x^2 + D_y^2 - \frac{l^2}{4}) \\ A_3 = (D_x^2 + D_y^2 - \frac{l^2}{4})^2 + l^2 D_y^2 - 4D_y^2 r^2 \end{cases}$$

then

$$\begin{cases} x_{1,2} = \frac{-A_2 \pm \sqrt{A_2^2 - 4A_1A_3}}{2A_1} \\ y_{1,2} = \frac{D_x^2 + D_y^2 - \frac{l^2}{4} - (l+2D_x)x}{2D_y} \end{cases}$$

$$\begin{cases} C1(x) = \frac{-A_2 - \sqrt{A_2^2 - 4A_1A_3}}{2A_1} \\ C1(y) = \frac{D_x^2 + D_y^2 - \frac{l^2}{4} - (2D_x+l)C1(x)}{2D_y} \\ C4(x) = \frac{-A_2 + \sqrt{A_2^2 - 4A_1A_3}}{2A_1} \\ C4(y) = \frac{D_x^2 + D_y^2 - \frac{l^2}{4} - (2D_x+l)C4(x)}{2D_y} \end{cases} \quad (4.2.3)$$

node C2, C5

$$\begin{cases} (x - D_x)^2 + (y - D_y)^2 = (x - \frac{l}{2})^2 + y^2 \\ (x - \frac{l}{2})^2 + y^2 = r^2 \end{cases}$$

$$\begin{cases} (2D_x - l)x + 2D_y y = D_x^2 + D_y^2 - \frac{l^2}{4} \\ y = \frac{D_x^2 + D_y^2 - \frac{l^2}{4} - (2D_x - l)x}{2D_y} \end{cases}$$

$$\begin{cases} x^2 - lx + \frac{((D_x^2 + D_y^2 - \frac{l^2}{4}) - (2D_x - l)x)^2}{4D_y^2} = r^2 - \frac{l^2}{4} \\ (4D_x^2 - 4D_x l + l^2 + 4D_y^2)x^2 + (-4D_y^2 l - 2(2D_x - l)(D_x^2 + D_y^2 - \frac{l^2}{4}))x \\ + (D_x^2 + D_y^2 - \frac{l^2}{4})^2 + l^2 D_y^2 - 4D_y^2 r^2 = 0 \end{cases}$$

let

$$\begin{cases} B_1 = 4D_x^2 - 4D_x l + 4D_y^2 + l^2 \\ B_2 = -4D_y^2 l - 2(2D_x - l)(D_x^2 + D_y^2 - \frac{l^2}{4}) \\ B_3 = (D_x^2 + D_y^2 - \frac{l^2}{4})^2 + l^2 D_y^2 - 4D_y^2 r^2 \end{cases}$$

then

$$\begin{cases} x_{1,2} = \frac{-B_2 \pm \sqrt{B_2^2 - 4B_1B_3}}{2B_1} \\ y_{1,2} = \frac{D_x^2 + D_y^2 - \frac{l^2}{4} - (2D_x - l)x}{2D_y} \end{cases}$$

$$\begin{cases} C2(x) = \frac{-B_2 - \sqrt{B_2^2 - 4B_1B_3}}{2B_1} \\ C2(y) = \frac{D_x^2 + D_y^2 - \frac{l^2}{4} - (2D_x - l)C2(x)}{2D_y} \\ C5(x) = \frac{-B_2 + \sqrt{B_2^2 - 4B_1B_3}}{2B_1} \\ C5(y) = \frac{D_x^2 + D_y^2 - \frac{l^2}{4} - (2D_x - l)C5(x)}{2D_y} \end{cases}$$

node C3:

C3's coordinates will be $(0, \sqrt{r^2 - \frac{l^2}{4}})$.

Step 2: Integration

region V can be partitioned to 2 disjoint parts, $V_{one}(l)$ and $V_{two}(l)$. Note here the integral limitations of variable y are based on the assumption that node D resides in the 1st and 2nd quadrant, because of symmetry, if a node D resides in the 3rd or 4th quadrant, we can easily transformed the problem to a 1st or 2nd quadrant position by taking the symmetry regarding to y axis.

$$V_{one}(l) = \int_{C3(x)}^{C5(x)} \int_{D_y - \sqrt{r^2 - (x - D_x)^2}}^{\sqrt{r^2 - (x - \frac{l}{2})^2}} dy dx$$

$$V_{two}(l) = \int_{C1(x)}^{C3(x)} \int_{D_y - \sqrt{r^2 - (x - D_x)^2}}^{\sqrt{r^2 - (x + \frac{l}{2})^2}} dy dx$$

thus

$$\begin{aligned} V_1(l) &= \int_{C3(x)}^{C5(x)} \int_{D_y - \sqrt{r^2 - (x - D_x)^2}}^{\sqrt{r^2 - (x - \frac{l}{2})^2}} dx dy + \int_{C1(x)}^{C3(x)} \int_{D_y - \sqrt{r^2 - (x - D_x)^2}}^{\sqrt{r^2 - (x + \frac{l}{2})^2}} dy dx \\ &= \int_{C3(x)}^{C5(x)} \sqrt{r^2 - (x - \frac{l}{2})^2} - D_y + \sqrt{r^2 - (x - D_x)^2} dx \\ &\quad + \int_{C1(x)}^{C3(x)} \sqrt{r^2 - (x + \frac{l}{2})^2} - D_y + \sqrt{r^2 - (x - D_x)^2} dx \\ &= \int_{C3(x)}^{C5(x)} \sqrt{-x^2 + lx + (r^2 - \frac{l^2}{4})} dx + \int_{C1(x)}^{C3(x)} \sqrt{-x^2 - lx + (r^2 - \frac{l^2}{4})} dx \\ &\quad + \int_{C1(x)}^{C5(x)} \sqrt{-x^2 + 2D_x x + (r^2 - D_x^2)} dx - D_y(C5(x) - C1(x)) \end{aligned} \quad (4.2.4)$$

There is a closed form integration for $\int \sqrt{ax^2 + bx + c} dx$

$$\begin{aligned} &\int \sqrt{ax^2 + bx + c} dx \\ &= \frac{2ax + b}{4a} \sqrt{ax^2 + bx + c} - \frac{b^2 - 4ac}{8a} \int \frac{1}{\sqrt{ax^2 + bx + c}} dx \\ &\quad \int \frac{1}{\sqrt{ax^2 + bx + c}} dx \\ &= \frac{1}{\sqrt{a}} \ln(2ax + b + 2\sqrt{a}\sqrt{ax^2 + bx + c}) \quad \text{when } a > 0 \\ &= \frac{1}{\sqrt{-a}} \arcsin\left(\frac{-2ax - b}{\sqrt{b^2 - 4ac}}\right) \quad \text{when } a < 0, b^2 - 4ac > 0 \end{aligned}$$

In some cases which depends on the value of D_x , D_y , the interception may have a different shape, such as shown in Figure-4.3. Clearly, in those cases, there are just two interception

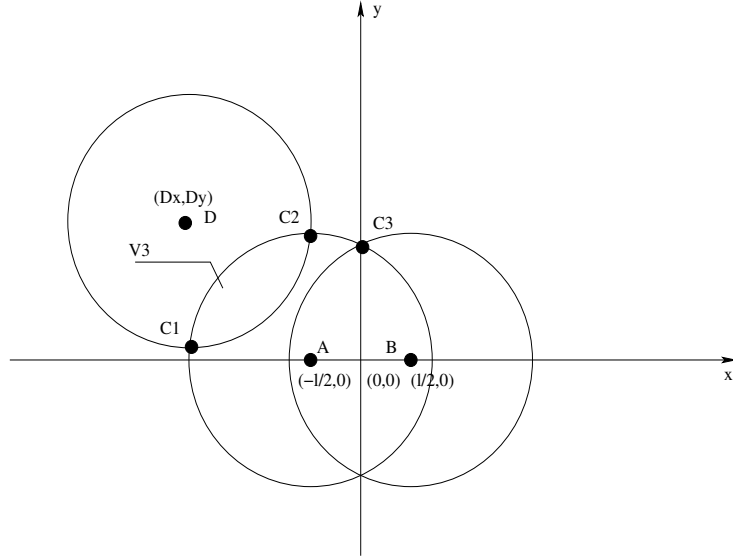


Figure 4.3: Another Example of Level-2 interference Set

points C1 and C2. Thus the integration becomes:

$$\begin{aligned}
 V_2(l) &= \int_{C1(x)}^{C2(x)} \int_{D_y - \sqrt{r^2 - (x - D_x)^2}}^{\sqrt{r^2 - (x + \frac{l}{2})^2}} dy dx \\
 &= \int_{C1(x)}^{C2(x)} \sqrt{-x^2 - lx + (r^2 - \frac{l^2}{4})} - D_y + \sqrt{-x^2 + 2D_x x + (r^2 - D_x^2)} dx
 \end{aligned} \tag{4.2.5}$$

or, if node D resides in the first quadrant,

$$\begin{aligned}
 V_3(l) &= \int_{C1(x)}^{C2(x)} \int_{D_y - \sqrt{r^2 - (x - D_x)^2}}^{\sqrt{r^2 - (x - \frac{l}{2})^2}} dy dx \\
 &= \int_{C1(x)}^{C2(x)} \sqrt{-x^2 + lx + (r^2 - \frac{l^2}{4})} - D_y + \sqrt{-x^2 + 2D_x x + (r^2 - D_x^2)} dx
 \end{aligned} \tag{4.2.6}$$

To summarize, given a node D in position (D_x, D_y) , first check if the transmission range of node D has interception with the transmission range of node A and B, if it intercepts with both nodes, use equation-(4.2.4) to calculate the area of interception. Otherwise (e.g. there is no solution either for C1 and C4 or C2 and C5), use either equation-(4.2.5) or (4.2.6).

Step 3: the probability of at least 1 node in the region

The probability of at least 1 node in region V can be calculated as:

$$Pr_2 \text{ hop} = \min(\rho V(l), 1)$$

- Expected degree of level-2 interference set - $E[I_{Node}^2(x, y, t)]$

Notice that a node lies in the area covered by deferral set doesn't mean that node will always be the two hop neighbors of the communicating pair, and it is clear that the probability that node D is two hop neighbor of node A or B equals the probability that there is at least 1 node in intercept region of node D and node A,B 's transmission range. So the expectation of two hop neighbors should be calculated by the following step:

The conditional probability of a node being two hop neighbor of the communicating pair given the location of the node is:

$$Pr(\text{node D being two hop neighbors of communicating pair (A,B)} | (D_x, D_y))$$

Then the expectation of the number of two hop neighbors can be calculated by integrating the probability of two hop neighbor over the shaded area (region II) in Figure-4.4.

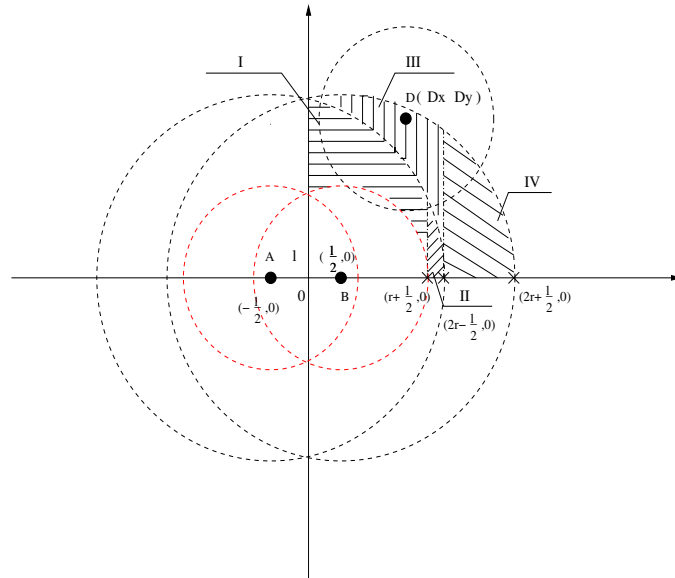


Figure 4.4: Calculation of Two Hop Neighbors

Given the nodes are uniformly distributed in the network, which in turn means they are also uniformly distributed in the shaded area, so the integrations in different quadrant are symmetry, therefore we only need to calculate the integration of the first quadrant. Let's call the probability $Pr(\text{D being two hop neighbors of (A,B)})$ to be $Pr_{2 \text{ hop}}$, from Figure-4.4 the integral region is divided to 4 parts because of different integral limitations:

$$\begin{aligned}
& E(I_{Node}^2)(l) \\
&= 4E(\text{two hop neighbors in 1st quadrant})(l) \\
&= 4 \int \int_{\text{shaded region in 1st quadrant}} \min(\rho V(l), 1) \rho dD_x dD_y \\
&= 4\rho \underbrace{\left(\int_0^{r+\frac{l}{2}} \int_{\sqrt{r^2-(x-\frac{l}{2})^2}}^{\sqrt{4r^2-(x+\frac{l}{2})^2}} \min(\rho V_1(l), 1) dD_y dD_x \right)}_I \\
&\quad + \underbrace{\left(\int_{r+\frac{l}{2}}^{2r-\frac{l}{2}} \int_0^{\sqrt{4r^2-(x+\frac{l}{2})^2}} \min(\rho V_1(l), 1) dD_y dD_x \right)}_{II} \\
&\quad + \underbrace{\left(\int_0^{2r-\frac{l}{2}} \int_{\sqrt{4r^2-(x-\frac{l}{2})^2}}^{\sqrt{4r^2-(x+\frac{l}{2})^2}} \min(\rho V_3(l), 1) dD_y dD_x \right)}_{III} \\
&\quad + \underbrace{\left(\int_{2r-\frac{l}{2}}^{2r+\frac{l}{2}} \int_0^{\sqrt{4r^2-(x-\frac{l}{2})^2}} \min(\rho V_3(l), 1) dD_y dD_x \right)}_{IV} \tag{4.2.7}
\end{aligned}$$

In equation-4.2.7, $V(l)$ can be the result from equation-(4.2.4), (4.2.5) or (4.2.6), respectively $V_1(l)$, $V_2(l)$ and $V_3(l)$ which are also functions of D_x and D_y

The last variable is the Euclidean distance l between the communicating pairs A and B, which is uniformly distributed between $(0, r)$, thus given the node density of the network, by taking the integral, the expect number of two hop neighbors in deferral set is:

$$\begin{aligned}
E(I_{Node}^2) &= \int_0^r f(l) E(I_{Node}^2)(l) dl \\
&= \int_0^r \frac{1}{r} E(I_{Node}^2)(l) dl \tag{4.2.8}
\end{aligned}$$

- Equivalent two hop neighbor and Equivalent Competitors

Above the number of two hop nodes for a given communication pair is studied, and the ongoing communication will affect the data communication for those nodes, however, notice that *not all* the transmission along those two hop nodes will affect the active communication. In fact, only when those two hop neighbors try to communicate the direct neighbor of either of the communication pair, the current active communication will be affected, thus, it's necessary to get the number of the “equivalent two hop neighbors” which reflects the actual interference caused by nodes in the deferral set in terms of direct neighbor. For example, if a two hop

neighbor has m neighbors which is also the neighbor of the communication pair, then the value of “equivalent two hop neighbor” is $\frac{m}{n_{avg}}$. So the expectation of the “equivalent two hop neighbor” can be calculated by:

$$\begin{aligned}
& E(\text{equivalent two hop neighbor})(l) \\
&= 4E(\text{equivalent two hop neighbor in 1st quadrant})(l) \\
&= 4 \int \int_{\text{shaded region in 1st quadrant}} \min(\rho V(l), 1) \frac{\rho V(l)}{n_{avg}} \rho dD_x dD_y \\
&= 4 \frac{\rho^2}{n_{avg}} \left(\int_0^{r+\frac{1}{2}} \int_0^{\sqrt{4r^2-(x+\frac{1}{2})^2}} \min(\rho V_1(l), 1) V_1(l) dD_x dD_y \right. \\
&\quad + \int_{r+\frac{1}{2}}^{2r-\frac{1}{2}} \int_0^{\sqrt{4r^2-(x+\frac{1}{2})^2}} \min(\rho V_1(l), 1) V_1(l) dD_x dD_y \\
&\quad + \int_0^{2r-\frac{1}{2}} \int_{\sqrt{4r^2-(x+\frac{1}{2})^2}}^{\sqrt{4r^2-(x-\frac{1}{2})^2}} \min(\rho V_3(l), 1) V_3(l) dD_x dD_y \\
&\quad \left. + \int_{2r-\frac{1}{2}}^{2r+\frac{1}{2}} \int_0^{\sqrt{4r^2-(x-\frac{1}{2})^2}} \min(\rho V_3(l), 1) V_3(l) dD_x dD_y \right) \tag{4.2.9}
\end{aligned}$$

and

$$\begin{aligned}
E(N_{eq_2}) &= E(\text{equivalent two hop neighbor}) \\
&= \int_0^r f(l) E(\text{equivalent two hop neighbor})(l) dl \\
&= \int_0^r \frac{1}{r} E(\text{equivalent two hop neighbor})(l) dl \tag{4.2.10}
\end{aligned}$$

It is difficult to have the closed form expression for (4.2.7), (4.2.8), (4.2.9) and (4.2.10), however, numerical method can be used to calculate the expected number of two hops neighbors in level-II interference set, a simple matlab program can do this task.

Table-4.1 shows the expectation of two hop neighbor and “equivalent two hop neighbors” with different network configuration (ρ).

Finally, the equivalent competitor of a specific node will be the sum of the one hop neighbors and the equivalent two hop neighbors of the node.

4.2.2 Probability of Flow Transmission

As shown in Chapter-3, the probability τ of a station to transmit RTS packet in a random selected slot is derived under the Markov chain back-off window model:

n_{avg}	$E(N_{eq2})$	n_{avg}	$E(N_{eq2})$	n_{avg}	N_{2hop}	n_{avg}	N_{2hop}
3	1.713267	4	2.64172	3	7.10	4	9.998876
5	3.175967	6	3.701267	5	12.99494	6	16.061809
7	4.22086	8	4.73649	7	19.183077	8	22.347319
9	5.249029	10	5.759578	9	25.544785	10	28.772907
11	6.268337	12	6.775844	11	32.024762	12	35.298698
13	7.282298	14	7.787837	13	38.591657	14	41.90065
15	8.292658	16	8.796717	15	45.224458	16	48.559346
17	9.300342	18	9.803449	17	51.907474	18	55.265388
19	10.306113	20	10.808521	19	58.632178	20	62.009697

Table 4.1: $E(N_{eq2})$ for different node density

$$\tau = \sum_{i=0}^{RL} b_{i,0} = \frac{1 - p^{RL+1}}{1 - p} b_{0,0}$$

where

$$b_{0,0} = \begin{cases} \frac{2(1-2p)(1-p)}{W(1-(2p)^{RL+1})(1-p) + (1-2p)(1-p^{RL+1})} & RL \leq m \\ \frac{2(1-2p)}{W(1-(2p)^{m+1})(1-p) + (1-2p)(1-p^{RL+1})} & \\ \frac{(1-p)}{+W2^m p^{m+1}(1-2p)(1-p^{RL-m})} & RL > m \end{cases}$$

Same as in Chapter-3, p is the conditional collision probability and W is the minimum back-off window size, $W = CW_{min}$.

In general, these probabilities depend on the conditional collision probability p , which is still unknown. Notice that the probability that a transmitted packet encounters a collision is the probability that there is more than one node tries to access the channel at the same time. The reason for collision may be that the direct neighbor of the node also trying to send RTS or they try to send CTS as the reply which two hop neighbor sent before, let

$$N' = n_{avg} + \frac{E(N_{eq2})(x, y, t)}{2}$$

we have:

$$p = 1 - (1 - \tau)^{N'} \quad (4.2.11)$$

Like equation (7) and (9) from [5], equations (3.3.1) and (4.2.11) represent a nonlinear system in the two unknowns τ and p , which can be solved using numerical techniques. It is easy to prove that this system has a unique solution. In fact, inverting (4.2.11), then:

$$\tau(p) = 1 - (1 - p)^{\frac{1}{N'}}$$

This is a continuous and monotone increasing function in the range $p \in (0, 1)$, that starts from $\tau(0) = 0$ and grows up to $\tau(1) = 1$. Equation $\tau(p)$ defined by (3.3.1) is also continuous in the range $p \in (0, 1)$. [5]

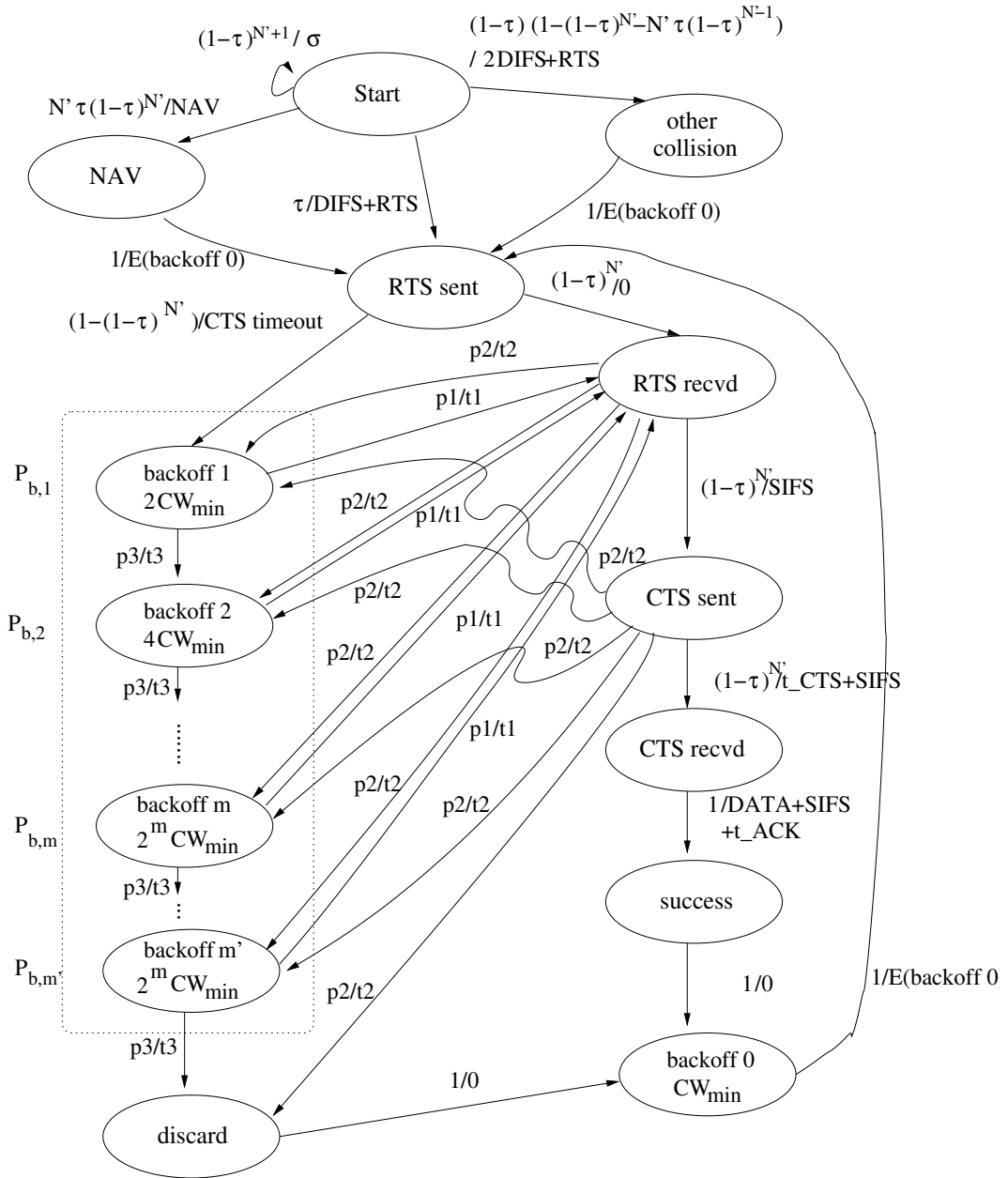
Having the probability that a station trying to access channel with RTS packet, now in order to find the channel capacity, we should, find out the probability of successful packet exchange and the mean time needed for a packet to get transmitted. In order to find those parameters, an accurate mode behavior model is needed, in subsection-4.2.3 such a model is given for 802.11 DCF.

4.2.3 Detailed Explanation of Node Model

In this subsection a parametric node behavior model is presented. Coupled with probabilities p and τ obtained above, the probability that a packet can be transmitted successfully is derived, and consequently the channel (or node) capacity of the back-logged multi-hop wireless ad hoc network can be obtained.

Figure-4.5 depicts the finite state model with the associated transition probabilities for an individual node based on IEEE 802.11 DCF with RTS/CTS [6] under saturation conditions. The following clarifies the notation in the figure: each transition is marked with an expression of the form “x/y”, where x is the transition probability and y is the expected time in the current state prior to the associated transition. Additional notation includes N , which is the number of “equivalent competitors”, τ , which is the probability that node will attempt to transmit during an arbitrary slot time and $p_{b,i}$, which is the probability that a node remains in back-off stage i . The states include the following: during state “NAV” a node is deferring its own transmission and ceases to count-down its back-off timer while a transmission is active; the “other collision” state is entered when the node cannot retrieve sufficient information following a collision. each back-off stage is identified together with its exponentially increasing window size. The remaining states are straight forward. Observe that each node is back-logged, hence, as depicted in the figure, following each service completion (successful or not) the node enters back-off stage 0 followed by transmission of its RTS message immediately. This is intended to increase fairness under loaded conditions.

Focusing on Figure-4.5 notes the following behavior: following initialization each node may access the channel immediately or defer access due to an active transmission or collision. If the node defers access first it transmits with probability 1 after a random back-off. The transmitted



$$\text{Let } p1/t1 = (1-\tau)^{N'}/DIFS+t_{RTS}$$

$$p2/t2 = (1-(1-\tau)^{N'})/CTS \text{ timeout}$$

$$p3/t3 = (1-(1-\tau)^{N'})/DIFS+t_{RTS}+CTS \text{ timeout}$$

Figure 4.5: State transition model for an arbitrary transmission attempt

packet may experience multiple collisions resulting in multiple back-off stages until the packet is successfully transmitted or discarded if retry limit (RL) is reached. Next the possible transitions

are scrutinized.

From Figure-4.5, after initialization, at an arbitrary time slot σ , the node under interest, say, node A, may be in one of the following four possible states.

- **“NAV”**: Node A enters “NAV” state when one and only one of node A’s neighbor access the channel, thus node A set its NAV and wait for channel contention again with probability $p_a = N'\tau(1 - \tau)^{N'}$
- **“Others Collision”**: Node A enters this state when more than one of node A’s neighbor try to access channel and collision happened, node A will wait for channel be idle again to contend for the channel with probability $p_b = (1 - \tau)(1 - (1 - \tau)^{N'} - N'\tau(1 - \tau)^{N'-1})$
- **“Reenter”**: Node will stay at the same state “start” when nobody tries to access channel at this slot with probability $p_c = (1 - \tau)^{N'+1}$
- **“RTS sent”**: Node A will enter “RTS sent” state when it send out RTS packet no matter the action of other nodes with probability $p = \tau$

Given that node A sends out RTS packet, it is not guaranteed that the data exchange will be successful. The expected CTS packet may not arrive either due to RTS collision at receiver, say, node B side or the receiver has a long NAV which makes the CTS can not be generated and transmitted at the given time or even CTS packet has been transmitted, it may not be successfully received by node A. The following shows all the possible states that node A may be in after RTS packet has been sent.

- **“RTS sent”** :
 - The RTS sent by node A may be successfully received by its destination, say, node B with probability $p_d = \tau(1 - \tau)^{N'}$, go to “RTS recvd” state;
 - The RTS sent by node A may be not received by node B due to collision with probability $p_e = 1 - (1 - \tau)^{N'}$, go to “back-off” state according to the previous transmission attempts;
- **“RTS recvd”** :
 - After receive RTS, if none of node B’s competitor transmits, node B will sent CTS, the probability for such event to happen is $p_f = \tau(1 - \tau)^{N'}$, then node A go to “CTS sent” state

- Otherwise, node B can not send CTS with probability $p_g = 1 - (1 - \tau)^{N'}$, after CTS timeout, node A will go to “back-off” state according to the previous transmission attempts;
- **“CTS sent”** :
 - The CTS packet will be received by node A with probability $p_h = \tau(1 - \tau)^{N'}$, thus go to “CTS recvd” state
 - On the other hand, the CTS packet will not received by node A with probability $p_i = 1 - (1 - \tau)^{N'}$, then node A will go to “back-off” state according to the previous transmission attempts.
- **“CTS recvd”** : According to the assumptions made in this paper, in this case data exchange will be successful with probability $p_j = 1$ then node A will go to the “success” state.
- **“success”**: Since the node works under saturation condition, so node will directly enter back-off state with back-off window size CW_{min} and go to “RTS sent” state according to the MAC algorithm.
- **“back-off”**: node A will leave “back-off” state and enter “RTS sent” state directly when the back-off timer reaches zero under saturation condition.

- Study of back-off State

As defined in the IEEE 802.11 protocol, the back-off procedure shall be invoked by a node to transfer a frame when find the medium busy at either transmitter or receiver side. All back-offs slots occur following a DIFS period that the medium is determined to be idle for the duration of the DIFS period. A node performing the back-off procedure shall use the carrier-sense mechanism to determine whether there is activity during each back-off slot. If no medium activity is detected for the duration of a particular back-off slot, then the back-off procedure shall decrement its back-off time by σ . If the medium is determined to be busy at any time during a back-off slot, then the back-off procedure is suspended, that is, the back-off timer shall not decrement for that slot. The medium shall be determined to be idle for the period of DIFS before the back-off procedure is allowed to resume. Transmission shall commence whenever the back-off timer reaches zero.

The transmission started right after the back-off timer reaches zero, thus it is impossible for a node to enter NAV state after leaving back-off state, thus the transmission attempt will end up to back-off with the same probability $p_{backoff} = (1 - (1 - \tau)^{N'})$ and be successful with probability $1 - p_{backoff} = (1 - \tau)^{N'}$ no matter how many back-off stage it has been experienced before.

If the transmission attempt failed Retry Limit times, the packet will then be discarded and back-off window will be reset for the transmission attempt for next packet. So in the worst case, a packet will experience at most Retry Limit back-off state before being discarded. Because the back-off window size doubles each time for consecutive transmission attempt failures until it reaches the maximum back-off window size, so the average time needed to back-off will differ. Next the mean time a node stays at back-off stage n is studied. ($CW(n) = CW_{min}2^{n-1}$)

The node shall adjust its NAV even though it is in back-off state, following table shows the possible occasions when a node is in back-off state.

Probability	Time Elapsed	Explanation
$p_1 = (1 - \tau)^{N'}$	σ	No direct neighbor is involved in packet exchange
$p_2 = N'\tau(1 - \tau)^{N'-1}$	\overline{NAV}	one direct neighbor involves in packet exchange
$p_3 = 1 - p_1 - p_2$	EIFS+RTS	Collision happens

Table 4.2: Possible occasions for a node in back-off state

Combine p_2 and p_3 in Table-4.2 to be p'_2 , the mean time $E(n)$ that a node stay in back-off state n is:

$$\begin{aligned}
p'_2 &= 1 - p_1 = p_2 + p_3 \\
\overline{T}_{no\ decr} &= (p_2NAV + p_3(EIFS + RTS))/(p_2 + p_3) \\
T_{decr} &= \sigma \\
E(n) &= \sum_{i=0}^{\infty} C_{i+CW(n)/2-1}^i p_1^{CW(n)/2} (1 - p_1)^i \left(\frac{CW(n)}{2} \sigma + i\overline{T}_{no\ decrease} \right)
\end{aligned} \tag{4.2.12}$$

Where $\overline{T}_{no\ decr}$ and T_{decr} represents the mean time needed between two back to back decrease attempts when the attempt fails and succeeds respectively and $NAV=DIFS+RTS+CTS+E[P]+ACK+3SIFS$. In (4.2.12) $\frac{CW(n)}{2}$ is used because for each back-off stage, since the back-off window size is chosen to be random uniformly distributed from $[0, CW(n)]$, the mean value is $\frac{CW(n)}{2}$.

4.2.4 Arbitrary Channel Capacity

In multi hop wireless ad hoc network, for a specific pair of nodes, there is a mean time that a packet will stay at the head of outgoing queue, after that, the packet will either be transmitted successfully ($P_{success}$) or discard due to multiple transmission attempt failures. Throughput for the communication between them is defined as:

$$\begin{aligned}
 S &= \frac{\text{E}(\text{data exchanged during transmission attempt})}{\text{E}(\text{time needed to complete the transmission attempt})} \\
 &= \frac{\text{E}(\text{data exchanged during transmission attempt})}{P_{success}\overline{T}_{success} + P_{fail}\overline{T}_{fail}} \quad (4.2.13)
 \end{aligned}$$

From Fig-4.5, probability that data exchange is in i_{th} ($i=0,1,\dots$, Retry Limit) $p_{b,i}$ and in turn the probabilities of successful and failure data exchange are:

$$\begin{aligned}
 p_{b,0} &= (1 - (1 - \tau)^{N'}) + (1 - \tau)^{N'}(1 - (1 - \tau)^{N'}) + (1 - \tau)^{2N'}(1 - (1 - \tau)^{N'}) \\
 &= (1 - (1 - \tau)^{3N'}) \\
 p_{b,1} &= p_{b,0}(1 - (1 - \tau)^{N'}) + p_{b,0}\tau(1 - \tau)^{N'}(1 - (1 - \tau)^{N'}) \\
 &\quad + p_{b,0}\tau(1 - \tau)^{2N'}(1 - (1 - \tau)^{N'}) \\
 &= p_{b,0}(1 - (1 - \tau)^{3N'}) \\
 &\cdot \\
 &\cdot \\
 &\cdot \\
 p_{b,i} &= p_{b,i-1}(1 - (1 - \tau)^{N'}) + p_{b,i-1}\tau(1 - \tau)^{N'}(1 - (1 - \tau)^{N'}) \\
 &\quad + p_{b,i-1}\tau(1 - \tau)^{2N'}(1 - (1 - \tau)^{N'}) \\
 &= p_{b,i-1}(1 - (1 - \tau)^{3N'}) \\
 &= (1 - (1 - \tau)^{3N'})^{i+1} \quad (i = 0, \dots, RL)
 \end{aligned}$$

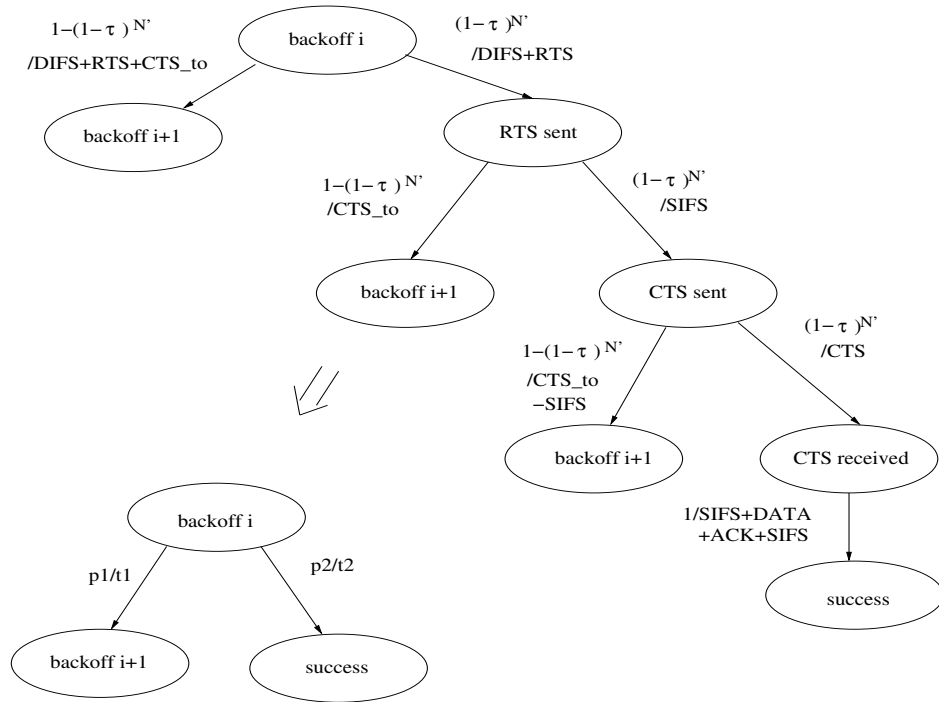
Thus from Figure-4.5 the probability that a packet can be successfully transmitted or failed

are:

$$\begin{aligned}
P_{success} &= (1 - \tau)^{3N'} + p_{b,0}(1 - \tau)^{3N'} + p_{b,1}(1 - \tau)^{3N'} + \dots + p_{b,RL}(1 - \tau)^{3N'} \\
&= (1 - \tau)^{3N'} \sum_{i=0}^{RL} (1 - (1 - \tau)^{3N'})^i \\
&= 1 - (1 - (1 - \tau)^{3N'})^{RL+2}
\end{aligned} \tag{4.2.14}$$

$$\begin{aligned}
P_{fail} &= p_{b,RL}(1 - (1 - \tau)^{3N'}) \\
&= (1 - (1 - \tau)^{3N'})^{RL+2}
\end{aligned} \tag{4.2.15}$$

Next the $\bar{T}_{success}$ and \bar{T}_{fail} — average time needed for a packet to be successfully transmitted or dropped are derived. Study the i_{th} back-off stage, the possible transitions are shown in Figure-4.6.



$$\begin{aligned}
p1 &= 1 - (1 - \tau)^{N'} + (1 - \tau)^{N'}(1 - (1 - \tau)^{N'}) + (1 - \tau)^{2N'}(1 - (1 - \tau)^{N'}) \\
&= 1 - (1 - \tau)^{3N'} \\
t1 &= ((1 - (1 - \tau)^{N'}) (DIFS+RTS+CTS_{to}) + (1 - \tau)^{N'}(1 - (1 - \tau)^{N'}) (DIFS+RTS+CTS_{to}) \\
&\quad + (1 - \tau)^{2N'}(1 - (1 - \tau)^{N'}) (DIFS+RTS+CTS_{to})) / 1 - (1 - \tau)^{3N'} \\
&= (DIFS+RTS+CTS_{to}) \\
p2 &= (1 - \tau)^{3N'} \\
t2 &= DIFS+RTS+3SIFS+CTS+DATA+ACK
\end{aligned}$$

Figure 4.6: Transition flow of back-off stage i

Figure-4.6 illustrates that for a transmission attempt in back-off stage i ($i = 0, 1, \dots, RL-1$),

the probability it moves to next back-off stage (i+1) or complete the transmission successfully are, note that Figure-4.6 hold for the state transition from RTS sent to back-off stage 0 too :

$$\begin{cases} p_1 = 1 - (1 - \tau)^{3N'} \\ p_2 = (1 - \tau)^{3N'} \end{cases}$$

Let $T_{CTS_{t_o}} = DIFS + SIFS + CTS_{t_o}$, then the time needed respectively is:

$$\begin{cases} t_1 = T_{CTS_{t_o}} \\ t_2 = NAV \end{cases}$$

Based on above analysis, the state transition diagram (Figure-4.5 can be transformed to Figure-4.7. At each back-off stage, the transmission attempt may be successful, otherwise it moves to next back-off stage until retry limit is reached and the packet will be dropped.

Before the entering the transmit state, the node may experience some intermediate state, the time elapsed in those states can be calculated as:

$$\begin{aligned} t_{intermediate} = & \frac{(1 - \tau)^{N'+1}\sigma + (1 - \tau)(1 - (1 - \tau)^{N'} - N'\tau(1 - \tau)^{N'-1})(2DIFS + RTS)}{(1 - \tau)^{N'+1} + (1 - \tau)(1 - (1 - \tau)^{N'} - N'\tau(1 - \tau)^{N'-1})} \\ & + \frac{N'\tau(1 - \tau)^{N'}NAV}{+N'\tau(1 - \tau)^{N'}} \end{aligned} \quad (4.2.16)$$

So $\bar{T}_{success}$ and \bar{T}_{fail} can be expressed as:

$$\begin{aligned} \bar{T}_{success} \cdot P_{success} = & (1 - \tau)^{3N'}(\tau NAV + (1 - \tau)(t_{intermediate} + NAV)) \\ & + (1 - \tau)^{3N'}(1 - (1 - \tau)^{3N'})(T_{CTS_{t_o}} + E[0] + NAV + (1 - \tau)t_{intermediate}) \\ & + (1 - \tau)^{3N'}(1 - (1 - \tau)^{3N'})^2(T_{CTS_{t_o}} + E[0] \\ & + T_{CTS_{t_o}} + E[1] + NAV + (1 - \tau)t_{intermediate}) \\ & + \dots \\ & + (1 - \tau)^{3N'}(1 - (1 - \tau)^{3N'})^{m+1} \left(\sum_{i=0}^m E[i] \right. \\ & \left. + (m + 1)T_{CTS_{t_o}} + NAV + (1 - \tau)t_{intermediate} \right) \\ & + (1 - \tau)^{3N'}(1 - (1 - \tau)^{3N'})^{m+2} \left(\sum_{i=0}^m E[i] + E[m] \right. \\ & \left. + (m + 2)T_{CTS_{t_o}} + NAV + (1 - \tau)t_{intermediate} \right) \\ & + \dots \\ & + (1 - \tau)^{3N'}(1 - (1 - \tau)^{3N'})^{RL+1} \left(\sum_{i=0}^m E[i] \right. \\ & \left. + (RL - m)E[m] + (RL + 1)T_{CTS_{t_o}} + NAV + (1 - \tau)t_{intermediate} \right) \end{aligned} \quad (4.2.17)$$

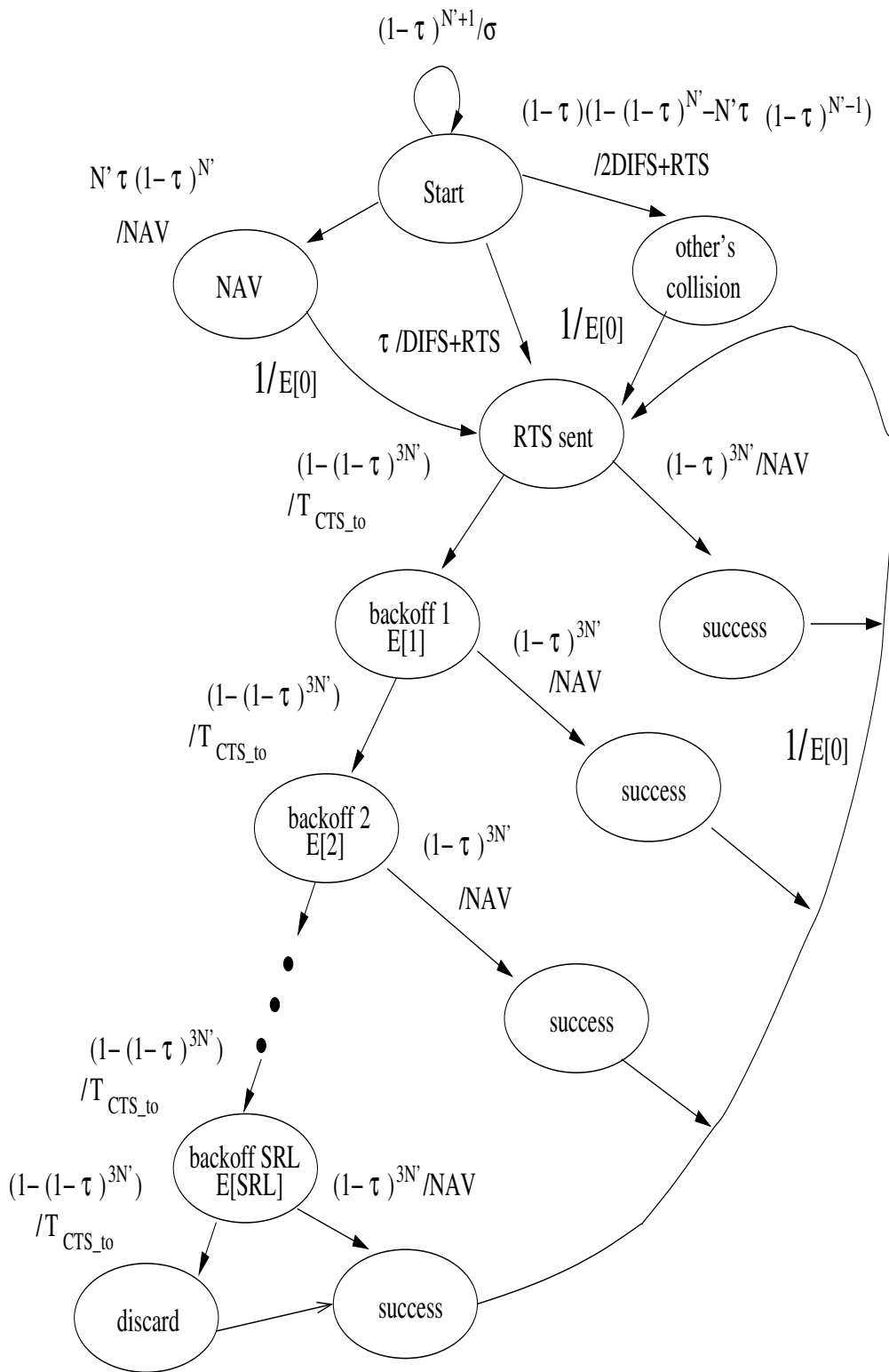


Figure 4.7: Flow transition with corresponding probabilities

$$\begin{aligned}\bar{T}_{fail} \cdot P_{fail} &= (1 - \tau)^{3N'} (1 - (1 - \tau)^{3N'})^{RL+2} \left(\sum_{i=0}^m E[i] + (RL - m)E[m] \right) \\ &\quad + (RL + 2)T_{CTS_{to}} + (1 - \tau)t_{intermediate}\end{aligned}\quad (4.2.18)$$

Revisit (4.2.13) here

$$\begin{aligned}S &= \frac{\text{E(data exchanged during transmission attempt)}}{\text{E(time needed to complete the transmission attempt)}} \\ &= \frac{\text{E(data exchanged during transmission attempt)}}{P_{success}\bar{T}_{success} + P_{fail}\bar{T}_{fail}}\end{aligned}\quad (4.2.19)$$

Put (4.2.14) (4.2.17) (4.2.18) and in (4.2.19), the node capacity is derived. Since a link reflects a bi-directional association between two nodes and assuming that traffic is uniformly distributed such that a node transmits to any of its neighbors with equal probability, the maximum “link” capacity S_{link} is given by the following:

$$S_{link} = \frac{S \cdot 2}{n_{avg}}$$

4.2.5 Delay Analysis

In this subsection the mean service delay each packet experienced is studied. Under the back-logged assumption, the mean service time for the packet is the from the second the packet becomes the head of queue until it got successful received by the intended destination or in other words, the MAC service delay. Using the state transition model provided in Figure-4.5 and Figure-4.7 and notice that only the successful transmission is measured, so the mean service delay can be obtained easily by

$$\begin{aligned}\text{Mean Service Time} &= \bar{T}_{success} \\ &= \frac{P_{success}\bar{T}_{success}}{P_{success}}\end{aligned}\quad (4.2.20)$$

4.3 Model Validation and Performance Analysis

This subsection presents selected results from discrete event simulation experiments and analysis used to validate the analytical result from section-4.2 and in next subsection, more simulation results are presented for statistical analysis.

4.3.1 Model Validation

Network simulator (*ns2*) is used in our simulation. The system parameter for analysis and simulation are the default value used by *ns2*. In all cases statistically significant analysis has failed to shown and difference between simulation and the analytical models. The following identifies the important assumptions and Table-4.3 identifies the main system parameters and their values as used in the experiments.

- The topology considered in the simulation consists of a finite number of nodes that are uniformly distributed in a circular space with radius L .
- All packets have the same length and the RTS/CTS scheme is mandatory.
- The effect of propagation delay is insignificant with respect to frame transmission time and media access delay; hence, it is negligible in the analysis. This is a very realistic assumption for transmission ranges $\leq 250m$.
- Only a single ad hoc network consisting of one BS is considered. Hence, it is assumed there are no interfering BASS—the DHSS spreading sequence is unique.
- The channel is idle, in other words, collisions caused by simultaneous transmission are assumed to be the most significant cause of packet corruption.
- Node mobility is assumed negligible with respect to frame transmission time. Hence, transmissions always complete before a mobile receiver moves out of range.

Parameters	Value	Parameters	Value
CW_{min}	32	DIFS	$50 \mu s$
CW_{max}	1024	SIFTS	$10 \mu s$
m	5	rate	1Mb/s
σ	$20 \mu s$	RTS	44 bytes
H	6 bytes	CTS	38 bytes
r	250 m	ACK	38 bytes

Table 4.3: System parameter values.

The first step in validation is to select a random deferral set from the network and finds the saturation point. This is determined using an iterative approach combined with graphical interpretations. Increasing the traffic loads are injected to the deferral set until saturation point

is reached. Figure-4.8 shows the procedure for a deferral set with $n_{avg} = 3$ and packet size of 512 bytes. The figure represents the average of several simulation runs. It can be seen that saturation is reached at a load about 10 packets/second. T

The comparison between the analytical and simulation result is shown in Figure-4.9. Each simulation point represents the average of 15 independent runs —95% confidence intervals are shown on the plot. Table-4.4 shows complete details from the corresponding date of Figure-4.9.

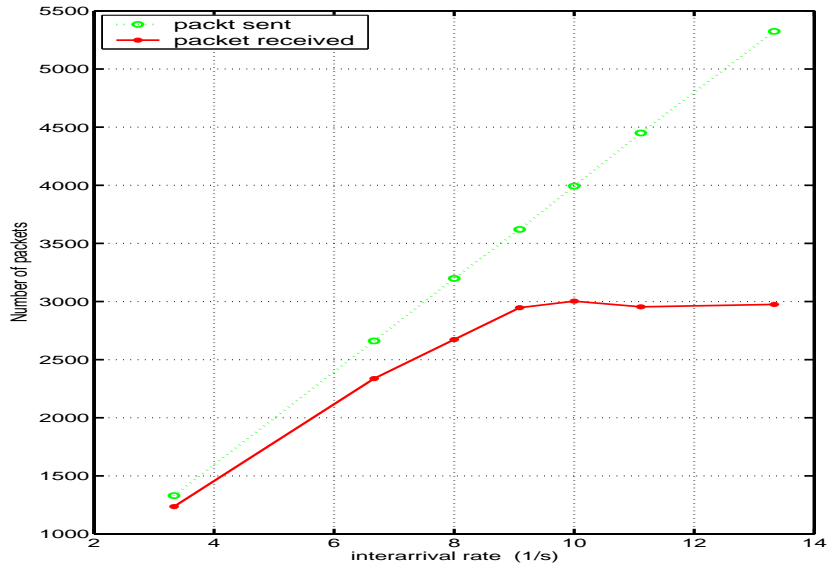


Figure 4.8: How to determine the saturation point

n_{avg}	Analytical	Simulation	95% CI (h)	95% CI (l)
3	0.025221	0.024781	0.0280	0.0215
4	0.012222	0.010850	0.0131	0.0086
6	0.004346	0.004977	0.0057	0.0042
8	0.002130	0.002860	0.0036	0.0021
11	0.001012	0.001327	0.0016	0.0010
12	0.000834	0.001034	0.0013	0.0008
15	0.000519	0.000619	0.0007	0.0005
18	0.000360	0.000363	0.0005	0.0003

Table 4.4: Analytical and Simulation Result of Arbitrary Channel Capacity (Mb/s)

Figure-4.9 compares the maximum (saturation) link throughput versus the average number of neighbors when the traffic is uniformly distributed and packet length is fixed. Hence, moving from left to right these results reflect arbitrary link within sparse to dense networks. Clearly the

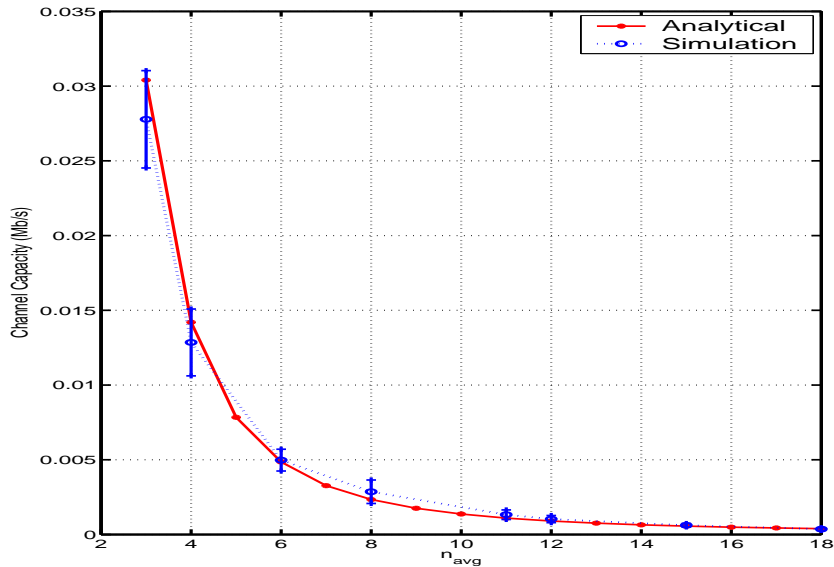


Figure 4.9: Model Validation: Arbitrary Channel Capacity

more two-hop neighbors that are encountered the larger the number of equivalent competitors a node must contend with for scarce transmission bandwidth. This explains the rapid non-linear drop in capacity as the number of neighbors increases.

Figure-4.10 validates the result for delay. The component of delay of interest is the mean MAC service delay. This measures the delay from the time a packet starts service to the completion of its transmission. For efficiency in the simulation this time was taken as the time between two consecutive ACKs from a specific node. Intuitively the inter-arrival times in the simulation should equal the service time under saturation conditions. Comparison of the simulation result of mean service time and the corresponding inter-arrival times valid this hypothesis.

4.3.2 Statistical Analysis

Figure-4.11 illustrates the channel capacity versus different value of Retry Limit (RL) given fixed back-off stage value m . The plot shows that larger values of RL degrade channel capacity. The explanation is that spending more time attempting to service a given packet reduces the transmission opportunities for newly arriving or lesser delayed packets. The rate of degradation decreases after the RL exceeds back-off stage m . This is because the window size no longer

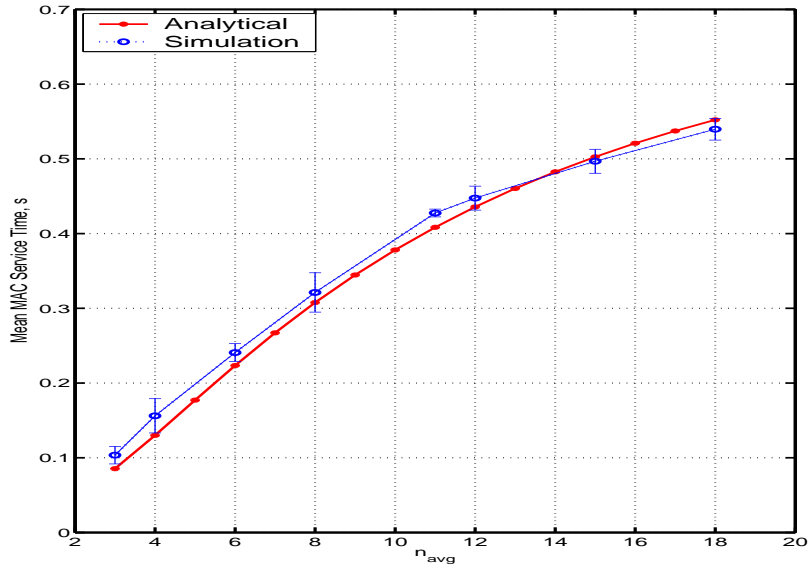


Figure 4.10: Model Validation: Mean Service Time

increases, thus , restoring a degree of fairness into the competition as more nodes will contend using the same back-off window size. In contrast, Figure-4.12 shows that increasing the value of back-off stage m for a fixed value of RL improves the channel capacity. Larger back-off window size induces more randomness into packet transmission, hence, decreasing the probability of collision and increasing channel capacity. These results suggest that retry limit RL is a more sensitive parameter than the back-off stage, particularly when it is smaller than m .

n_{avg}	Size	Analytical	Simulation	CI (h)	CI(l)
3	64	0.007742	0.007851	0.0090	0.0067
4	256	0.009092	0.008684	0.0106	0.0068
18	512	0.000360	0.000363	0.0005	0.0003
6	1024	0.005014	0.005740	0.0066	0.0049
8	1600	0.002632	0.003371	0.0045	0.0022
12	2324	0.001073	0.001483	0.0020	0.0010

Table 4.5: Saturation Throughput of different packet size, Analytical vs. Simulation with 95% Confidence Interval (Mb/s)

Figure-4.13 and Figure-4.14 depicts analytical result of arbitrary channel capacity and mean service delay with different packet size and simulation results in Figure-4.15 validates the analysis. a close look at Figure-4.13 and 4.14 it can be seen that increase in channel capacity

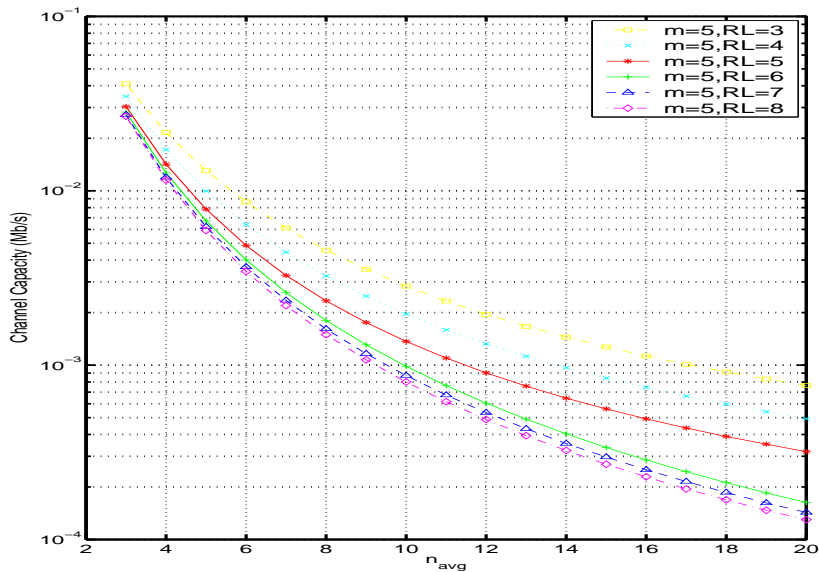


Figure 4.11: Statistical Analysis: Channel Capacity of arbitrary link vs. Retry Limit, $m=5$

decreases to half each time as the packet size doubles. The mean service delay also has the same property.

Moreover, scrutinize the trend of delay increase in Figure-4.14 it could be seen that when after the rapid growth at the lower end of the n_{avg} (under 20), the delay tends to increase with a constant rate up to some n_{avg} , (i.e. 80) then the rate starts to increase, which implies that there is a stable region for the network, after that, the mean delay will grow with higher rate which makes the network difficult to maintain stable and acceptable performance. (In reality, it is quite possible that those stable points are much lower than the one found here.)

4.4 Conclusion

In this chapter, the channel (or node) capacity analysis of multi-hop wireless ad hoc networks is discussed as an application example of the deferral framework. Next chapter will discuss another application, the network capacity analysis of multi-hop wireless ad hoc networks.

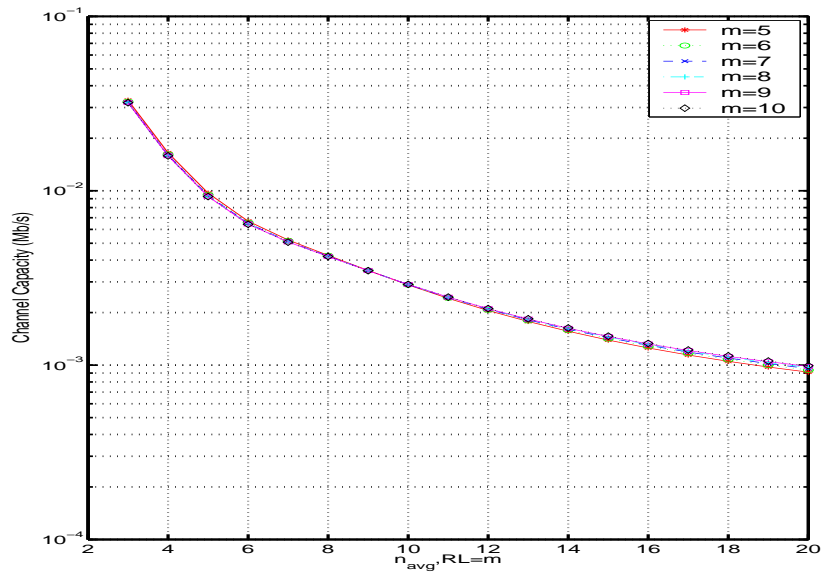


Figure 4.12: Statistical Analysis: Channel Capacity of arbitrary link vs. back-off stage m , $RL=m$

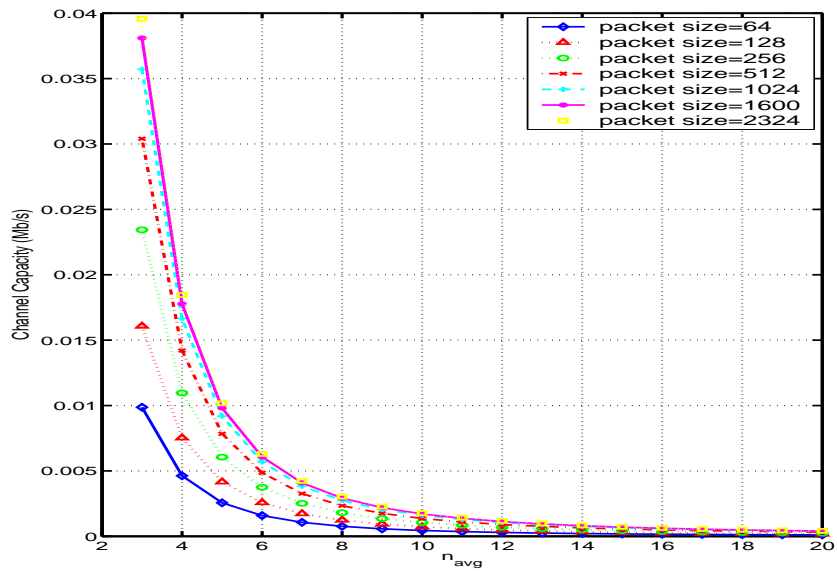


Figure 4.13: Statistical Analysis: Channel Capacity of arbitrary link with different packet size

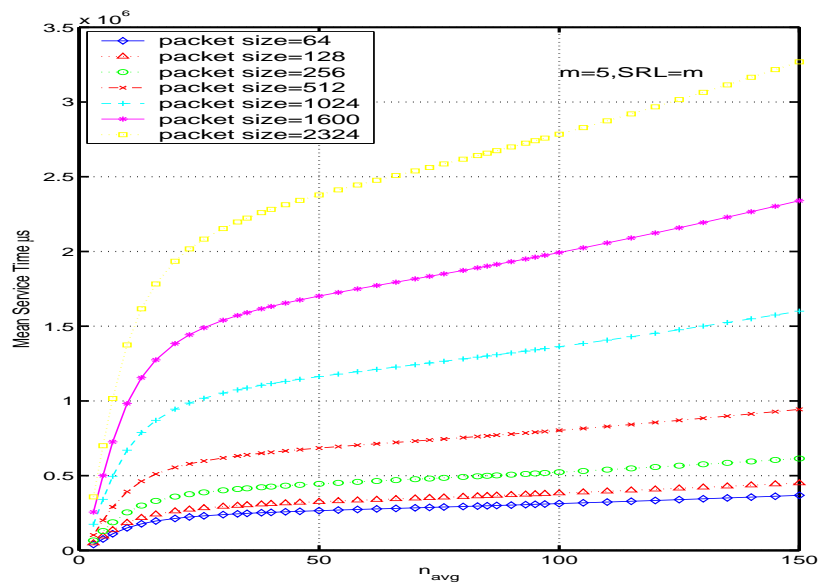


Figure 4.14: Statistical Analysis: MAC Service time of different packet size

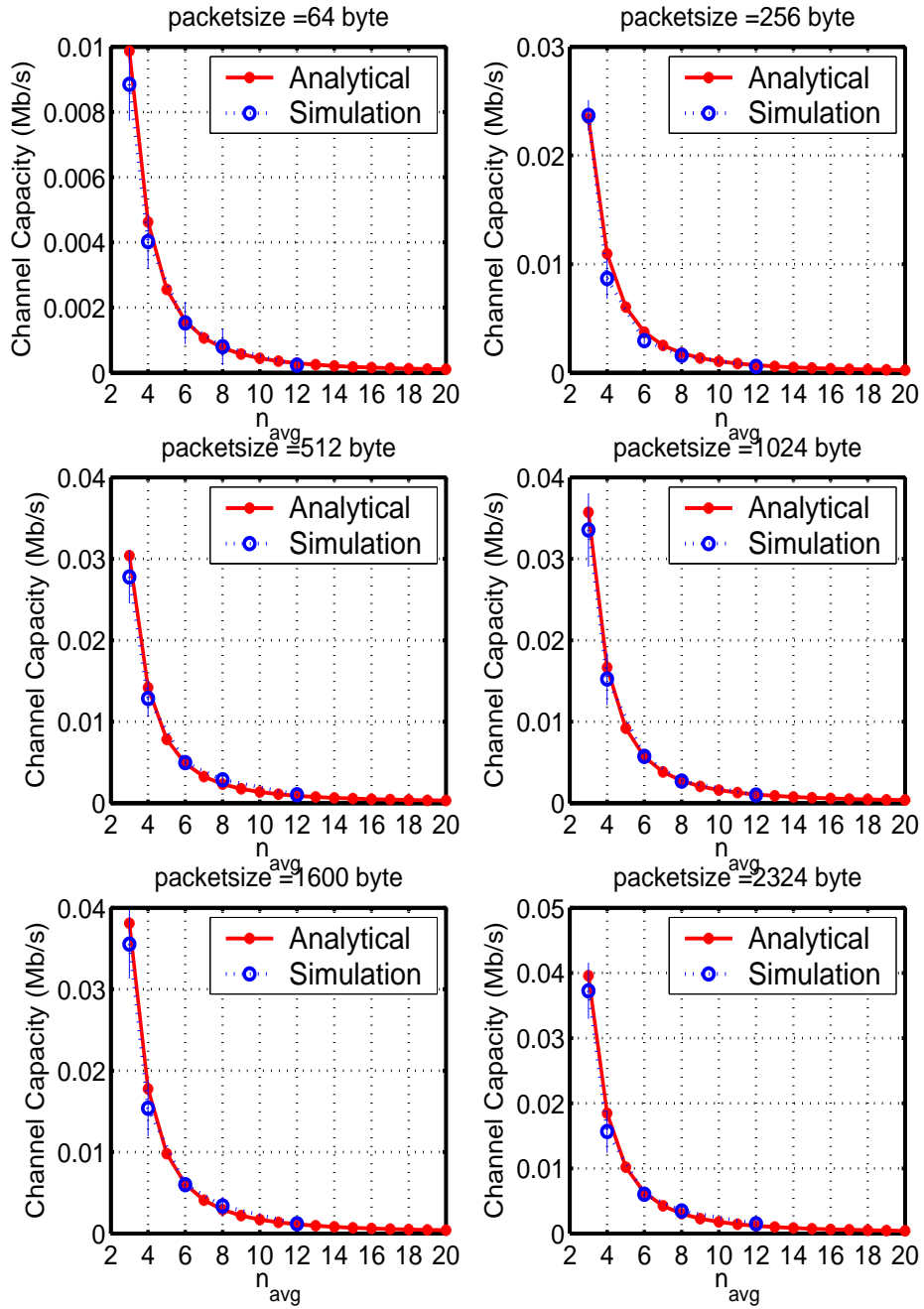


Figure 4.15: Statistical Analysis: Channel Capacity of arbitrary link of different packet size, Analytical vs. Simulation

Chapter 5

Network Capacity Analysis Using Deferral Framework

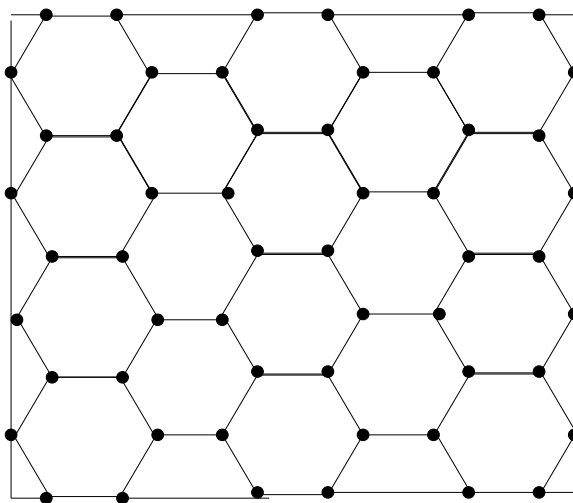
In Chapter-4 the capacity of arbitrary channel in the network is studied. However, in order to evaluate the performance of a network, the network capacity is also needed. In this chapter we investigate the network capacity issue. Specifically, a comprehensive investigation focusing on two related approaches on the problem of ad hoc network capacity is presented.

5.1 Introduction

One of the difficulties encountered is the obtuse nature of the *network capacity* problem itself. In contrast to *channel capacity* the definition of network capacity lacks a universal semantic. The ambiguity, however, is used to advantage, namely, by engaging in multiple interpretations more insight is provided. In the context of this proposal, network capacity is interpreted in two ways. namely, as (1) “maximum instantaneous capacity” (MIC) and (2) “network saturation capacity” (NSC). The MIC is the maximum amount of data flow in the network at any instant given ideal routing and scheduling; whereas the NSC is the sum of the capacity of all the channels in the network assuming that nodes and traffic are uniformly distributed independent of routing and scheduling algorithms. Both metrics are important for performance analysis, the first is an upper bound, whereas, the second reflects an achievable flow rate under back-logged conditions.

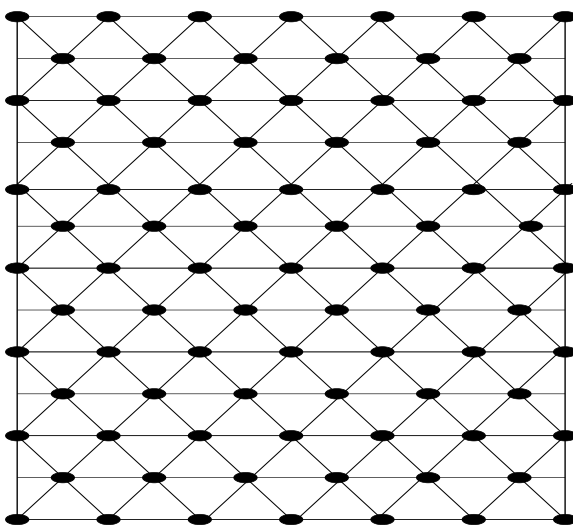
Because the network capacity are affected by a lot of factors, in order to focus on those factors which are deterministic and reduce the effect of randomness as much as possible, the networks topology in this thesis are created by repeating the specific pattern, some of the examples are shown in the Figure-5.1 to Figure-5.3. In those figures, solid line indicates that

two nodes are in each other's transmission range therefore can communicate with each other directly.



n_avg=3

Figure 5.1: Network example, $n_{avg} = 3$



n_avg=6

Figure 5.2: Network example, $n_{avg} = 6$

By scrutinizing Figure-5.1 to Figure-5.3, nodes that are at the boundary of network have less neighbors than the nodes in the center of the network, this phenomenon is defined as “boundary condition” and will be studied in detail in the following section.

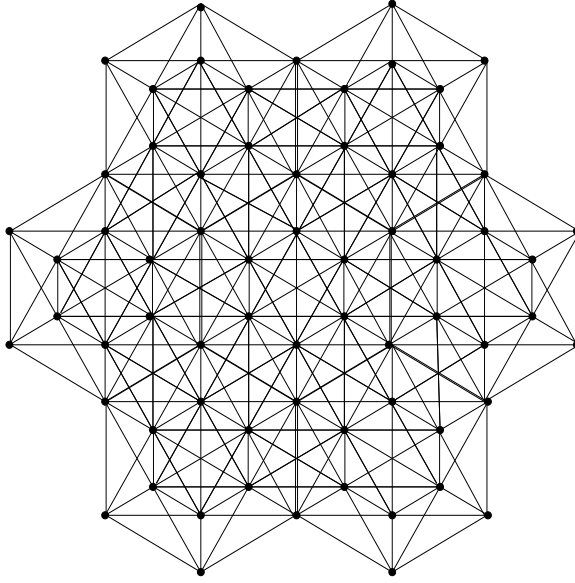


Figure 5.3: Network example, $n_{avg} = 12$

5.2 Network Saturation Capacity (NSC) Analysis

5.2.1 Boundary Condition

Without deeper inspection one may mistakenly assume that given a wireless network with uniformly distributed nodes, all the “links” will have same capacity, thus the network saturation capacity is the product of the channel capacity and the number of links in the network. Unfortunately, it is not this simple. Node location, for example, has a direct impact on network capacity. In order to estimation network capacity with sufficient precision it is necessary to study the relation between the capacity and node location; one difficulty arises due to the “boundary conditions”.

Table-5.1 several examples of NSC. The table compares simulation results with the $S_{link} \times N_l$ (both S_{link} and N_l are obtained in Chapter-4) formulation. The error increases with increasing node density near the boundary (for a fixed network radius). The reason is that the nodes close to the boundary of the network have fewer neighbors, hence, less channel contention. Consequently, in general, links close to the boundary have greater available capacity than those in the center of the network. The following definition is required to formalize the problem.

Definition 5.2.1. Boundary Zone

Let X be a random variable that measures the distance from a node $i \in G$ to the network boundary. Assume without loss of generality that transmission is omni-directional and the

n_{avg}	Num	$N_l \times S_{channel}$	Simulation
3	49	1.75	1.779
4	64	1.56	1.636
6	81	1.06	1.52
8	81	0.957	1.17
11	75	0.417	0.86
12	81	0.405	0.82
18	60	0.194	0.337

Table 5.1: Comparison between simulation result and direct product of network saturation capacity (NSC)

fixed value r is the an accurate estimation of the nominal transmission rage given an ergodic, homogeneous network. The boundary zone is defined as the doughnut shaped region occupied by all nodes $i \in G | X_i < 2r$

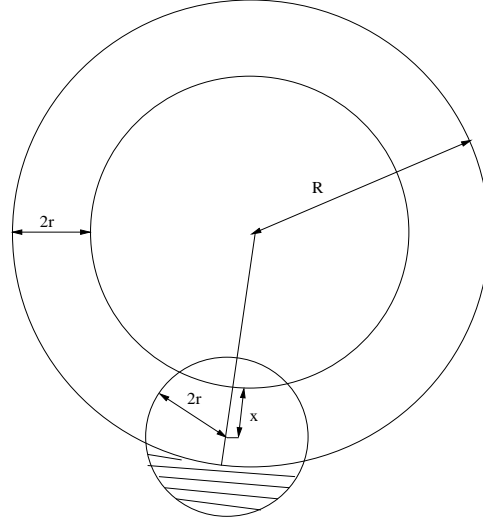


Figure 5.4: Illustration of Boundary Condition

An example of “boundary zone” is illustrated in Figure-5.4. Without loss of generality a circular boundary is assumed for the geometric analysis. The boundary condition quantifies the overestimation of access contention within the boundary zone. A more detail depiction of “boundary zone” is shown in Figure-5.5. The arc at the lower part of the figure is the network boundary, while the dashed circle represents the “deferral set” zone of node O_2 . Observe, however, that for nodes in the boundary zone the physical area covered by the actual deferral set must exclude the shaded area — $Area_{IV}$, the “phantom zone”, which lies outside the network, hence, contains no active nodes. To find the conditions for which the error is negligible assume that the area is occupied by “phantom nodes” that do not produce traffic and participate in data

$$\begin{aligned}
y &= |2r \cos \beta| = 2r |\cos \alpha| \\
&= \frac{|8r^2 + x^2 - 4Rr - 4rx + 2Rx|}{2(R - 2r + x)} \\
&= \begin{cases} \frac{-8r^2 - x^2 + 4Rr + 4rx - 2Rx}{2(R - 2r + x)}, & 0 < x < 2r + \sqrt{R^2 - 4r^2} - R \\ \frac{8r^2 + x^2 - 4Rr - 4rx + 2Rx}{2(R - 2r + x)}, & 2r + \sqrt{R^2 - 4r^2} - R < x < 2r \end{cases}
\end{aligned} \tag{5.2.5}$$

$$\begin{aligned}
z &= 2r - x - y \\
&= 2r - x - \frac{|8r^2 + x^2 - 4Rr - 4rx + 2Rx|}{2(R - 2r + x)} \\
&= \begin{cases} \frac{4rx - x^2}{2(R - 2r + x)}, & 0 < x < 2r + \sqrt{R^2 - 4r^2} - R \\ \frac{-16r^2 - 3x^2 + 8Rr + 12rx - 4Rx}{2(R - 2r + x)}, & 2r + \sqrt{R^2 - 4r^2} - R < x < 2r \end{cases}
\end{aligned} \tag{5.2.6}$$

$$\begin{aligned}
Area_I &= \pi(2r)^2 \frac{2\alpha}{2\pi} = 4r^2 \alpha \\
&= 4r^2 \arccos \frac{8r^2 + x^2 - 4Rr - 4rx + 2Rx}{4r(R - 2r + x)}
\end{aligned} \tag{5.2.7}$$

$$\begin{aligned}
Area_{II} &= \frac{1}{2}(2 \cdot 2r \sin \beta)(2r \cos \beta) \\
&= 4r^2 \sin \beta \cos \beta = 2r^2 \sin(2\beta) \\
&= 2r^2 |\sin(2\alpha)| = 4r^2 \sin \alpha |\cos \alpha|
\end{aligned}$$

$$\begin{aligned}
&\text{let } A = \sqrt{(x^2 + 2Rx)(4r - x)(2R - 4r + x)} \\
&= \begin{cases} \frac{A(-8r^2 - x^2 + 4Rr + 4rx - 2Rx)}{4(R - 2r + x)^2}, & 0 < x < 2r + \sqrt{R^2 - 4r^2} - R \\ \frac{A(8r^2 + x^2 - 4Rr - 4rx + 2Rx)}{4(R - 2r + x)^2}, & 2r + \sqrt{R^2 - 4r^2} - R < x < 2r \end{cases}
\end{aligned} \tag{5.2.8}$$

$$\begin{aligned}
Area_{III} &= \text{Area of fan} - \text{Area of triangle} \\
&= \pi R^2 \frac{2\gamma}{2\pi} - \frac{1}{2} 2 \cdot 2r \sin \beta (R - z) \\
&= \gamma R^2 - 2r \sin \beta (R - z) \\
&= \arcsin \frac{\sqrt{(x^2 + 2Rx)(4r - x)(2R - 4r + x)}}{2R(R - 2r + x)} \cdot R^2 - \\
&\quad \begin{cases} \frac{A(2R^2 - 4Rr + 2Rx - 4rx + x^2)}{4(R - 2r + x)^2}, & 0 < x < 2r + \sqrt{R^2 - 4r^2} - R \\ \frac{A(2R^2 - 12Rr + 6Rx + 16r^2 + 3x^2 - 12rx)}{4(R - 2r + x)^2}, & 2r + \sqrt{R^2 - 4r^2} - R < x < 2r \end{cases}
\end{aligned} \tag{5.2.9}$$

$$\begin{aligned}
Area_{IV} &= Area_{phantom} = \pi(2r)^2 - Area_I - Area_{II} - Area_{III} \\
&= 4\pi r^2 - 4r^2\alpha - 2r^2|\sin(2\alpha)| - \gamma R^2 - 2r \sin \beta(R - z) \\
&= 4\pi r^2 - 4r^2 \arccos \frac{8r^2 + x^2 - 4Rr - 4rx + 2Rx}{4r(R - 2r + x)} \\
&\quad - R^2 \arcsin \frac{\sqrt{(x^2 + 2Rx)(4r - x)(2R - 4r + x)}}{2R(R - 2r + x)} \\
&\quad + \begin{cases} \frac{A(R^2 - 4Rr + 2Rx - 4rx + x^2 + 4r^2)}{2(R - 2r + x)^2}, & 0 < x < 2r + \sqrt{R^2 - 4r^2} - R \\ \frac{A(4r^2 + x^2 - 4Rr - 4rx + 4Rx + R^2)}{2(R - 2r + x)^2}, & 2r + \sqrt{R^2 - 4r^2} - R < x < 2r \end{cases}
\end{aligned} \tag{5.2.10}$$

So the average number of “phantom node” can be calculated by integration:

$$\begin{aligned}
\bar{N}_{phantom} &= \int_0^{2r} \frac{1}{2r} \rho Area_{IV} dx \\
&= 4\pi r^2 \rho - 2r \rho \int_0^{2r} \arccos \frac{8r^2 + x^2 - 4Rr - 4rx + 2Rx}{4r(R - 2r + x)} dx \\
&\quad - \frac{R^2 \rho}{2r} \int_0^{2r} \arcsin \frac{\sqrt{(x^2 + 2Rx)(4r - x)(2R - 4r + x)}}{2R(R - 2r + x)} dx \\
&\quad + \frac{\rho}{2r} \int_0^{2r + \sqrt{R^2 - 4r^2} - R} \frac{\sqrt{(x^2 + 2Rx)(4r - x)(2R - 4r + x)}}{2(x + R - 2r)^2} \\
&\quad \frac{(x^2 + (2R - 4r)x + R^2 - 4Rr + 4r^2)}{dx} \\
&\quad + \frac{\rho}{2r} \int_{2r + \sqrt{R^2 - 4r^2} - R}^{2r} \frac{\sqrt{(x^2 + 2Rx)(4r - x)(2R - 4r + x)}}{2(x + R - 2r)^2} \\
&\quad \frac{(x^2 - 4rx + 4Rx + R^2 + 4r^2 - 4Rr)}{dx}
\end{aligned} \tag{5.2.11}$$

Notice the $\bar{N}_{phantom}$ above are derived for only one node, however, a communication need two nodes, so the actual $\bar{N}_{phantom}$ will be counted for both nodes too. The following shows how to modify the calculation.

Figure-5.6 illustrates the boundary condition with respect to a pair of actively communicating nodes (A,B). The “phantom zone” is the union of $Area_{IV}$ with the parameterized triangular region bounded by C_1 , C_2 and C_3 , which is the portion of the zone covered by only one of the nodes (referred as “Moditest” in the equations). Construct an x, y coordinate system with the x axis tangent to the network boundary and the y axis perpendicular to the axis at the x coordinate of the node closest to the network boundary (node B in the figure). The coordinates of C_1 , C_2 and C_3 can be obtained geometrically:

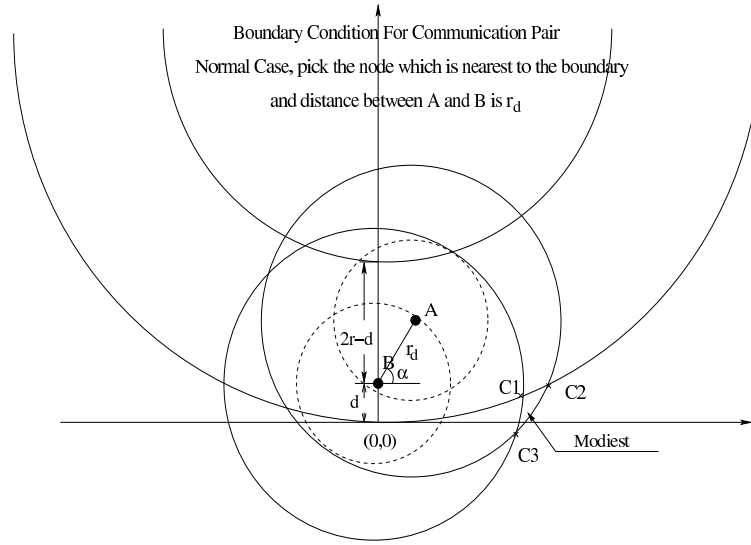


Figure 5.6: Calculation of “phantom nodes” for communication pair

- coordinates of C1

$$\begin{cases} x^2 + (y - d)^2 = 4r^2 \\ x^2 + (y - R)^2 = R^2 \end{cases}$$

$$\begin{cases} C1_y = \frac{4r^2 - d^2}{2(R - d)} \\ C1_x = \frac{\sqrt{(4r^2 - d^2)(4R^2 - 4Rd - 4r^2 + d^2)}}{2(R - d)} \end{cases} \quad (5.2.12)$$

- coordinates of C2

$$\begin{cases} (x - r_d \cos \alpha)^2 + (y - (d + r_d \sin \alpha))^2 = 4r^2 \\ x^2 + (y - R)^2 = R^2 \end{cases} \quad (5.2.13)$$

(5.2.13) can be transformed to quadratic equation with respect to y with the form $ay^2 + by + c = 0$, where

$$\begin{cases} a = 4(R - d - r_d \sin \alpha)^2 + 4r_d^2 \cos^2 \alpha \\ b = -4(R - d - r_d \sin \alpha)(4r^2 - r_d^2 - d^2 - 2dr_d \sin \alpha) - 8Rr_d^2 \cos^2 \alpha \\ c = (4r^2 - r_d^2 - d^2 - 2dr_d \sin \alpha)^2 \end{cases} \quad (5.2.14)$$

and the relationship between x and y are

$$x = \frac{2(R - d - r_d \sin \alpha)y - (4r^2 - r_d^2 - d^2 - 2dr_d \sin \alpha)}{2r_d \cos \alpha}$$

From (5.2.13) (5.2.14) the coordinates of C2 can be obtained.

- coordinates of C3

$$\begin{cases} (x - r_d \cos \alpha)^2 + (y - (d + r_d \sin \alpha))^2 = 4r^2 \\ x^2 + (y - d)^2 = 4r^2 \end{cases} \quad (5.2.15)$$

(5.2.15) can be transformed to quadratic equation with respect to y with the form $ay^2 + by + c = 0$, where

$$\begin{cases} a = 4r_d^2 \\ b = -(4r_d^3 \sin \alpha + 8r_d^2 d) \\ c = r_d^4 + 4dr_d^3 \sin \alpha + 4d^2 r_d^2 - 16r^2 r_d^2 \cos^2 \alpha \end{cases} \quad (5.2.16)$$

and the relationship between x and y are

$$x = \frac{2dr_d \sin \alpha + r_d^2 - 2r_d \sin \alpha y}{2r_d \cos \alpha}$$

From (5.2.15) (5.2.16) the coordinates of C3 can be obtained.

- revision of $\bar{N}_{phantom}$

The modification of $Area_{phantom}$ and $\bar{N}_{phantom}$ will be:

$$\begin{aligned} Area_{phantom}(d, \alpha, r_d) = & \int_{C3(x)}^{C1(x)} \int_{d+r_d \sin \alpha - \sqrt{4r^2 - (x-r_d \cos \alpha)^2}}^{d - \sqrt{4r^2 - x^2}} dy dx + \\ & \int_{C1(x)}^{C2(x)} \int_{d+r_d \sin \alpha - \sqrt{4r^2 - (x-r_d \cos \alpha)^2}}^{R - \sqrt{R^2 - x^2}} dy dx \end{aligned} \quad (5.2.17)$$

$$\bar{N}_{phantom} = \rho \left(\int_0^{2r} \frac{1}{2r} (Area_{IV}(d) + \left(\int_0^\pi \frac{1}{\pi} d\alpha \int_0^r \frac{1}{r} Moditest(d, \alpha, r_d) dr_d \right)) dd \right) \quad (5.2.18)$$

The limits of integration reflect the coordinate system and are chosen with respect to the location of the node closest to the boundary. Thus the other node must be closer to the center. α varies from 0 to π to cover all positions of node A in this region; the distance r_d between node A and B is varied from 0 to r reflecting the uniform distribution of nodes.

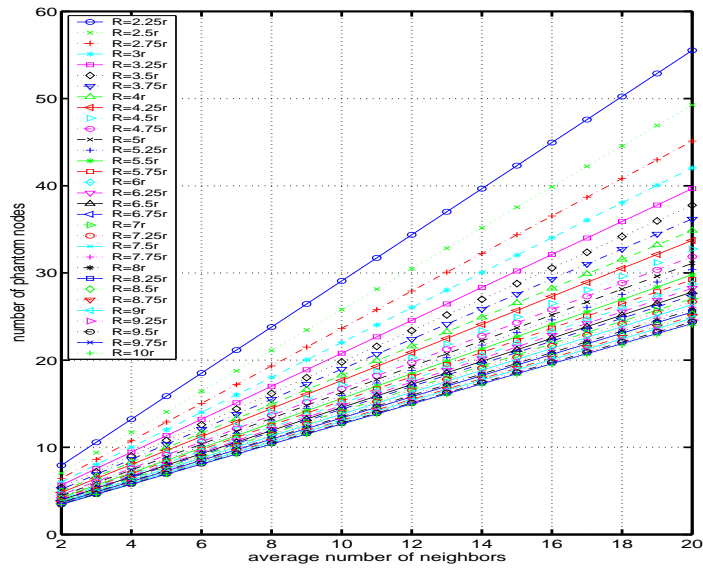


Figure 5.7: Number of phantom nodes vs. R/r

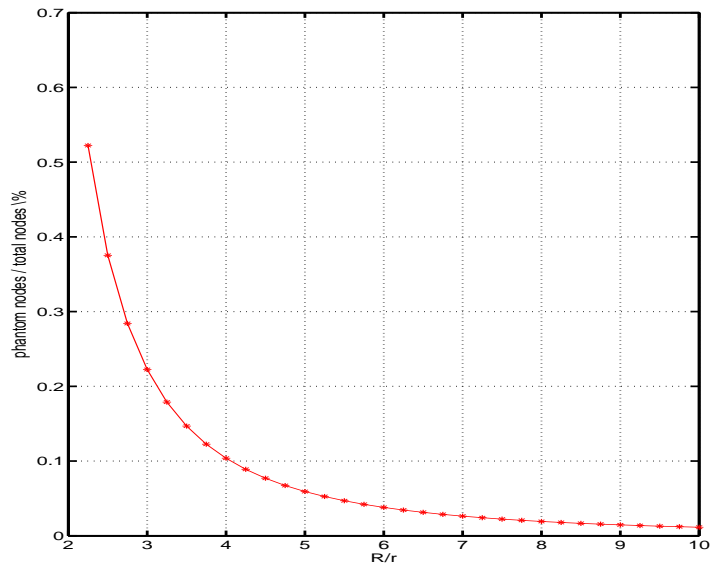


Figure 5.8: Percentage of phantom nodes respect to total number of nodes in the network

5.2.2 Network Saturation Capacity

Numerical analysis depicted in Figure-5.7 and Figure-5.8 shows that only when the network

diameter (R) is greater than 10 times of the nominal transmission range (r), the effect of “boundary condition” is less than 1%. This can be regarded as “negligible”, thus, the NSC can be approximated by the product of S_{link} and N_l . The analysis illustrates how the location of the nodes affects channel capacity, and in turn the NSC. Hence, for moderate to large size networks the boundary effect can be ignored without affecting the accuracy of the NSC.

There are additional parameters that may affect network capacity. The most important of these include: spatial and temporal variation of the distribution of nodes, traffic characteristics, the wireless channel and node mobility. A significant advantage of the present model is that the analysis of these factors is facilitated through probabilistic interpretation of the “equivalent competitor” of the deferral framework and enumeration of the effects of the dynamic of the aforementioned parameters.

However, current available simulators (OPNET, ns2, etc) are not capable to produce valid simulation result for networks that contain several hundred of nodes, thus the above claim is left un-validated. In the future, the relationship between the percentage of boundary nodes and the NSC should be studied and the possible functions depicts those relationships are expected when appropriate simulation environment becomes available.

5.3 Maximum Instantaneous Capacity (MIC) Analysis

The analysis of MIC reflects the bottleneck achievable throughput between *any set of sources and destinations*. Given ideal transmission scheduling it represents a lower-bound on maximum simultaneous flows between *all* node pairs — given the “ideal scenario” every link must either be transmitting, receiving or in deferral due to the “coupling” effect. Thus, there are fixed number of links that may be activated simultaneously. The idea is to find a sequence of simultaneously active links that cover the connected network; at each step the number of active links is maximized — the minimum size set represents the desired bottleneck. The shortest covering sequence minimizes the delay as well. The MIC is approximated in two steps. First find the maximum concurrent active links, second, find the bottleneck of the concurrent active links — the capacity in this case is MIC.

5.3.1 Maximum Number of Concurrent Active Links

The first step in solving for MIC is finding the maximum feasible number of concurrent active links. After showing that this problem is NP complete, a sub optimal solution is found

using a greedy algorithm.

- NP-completeness

Given a graph $G(V,E)$ and the definition of deferral link set $D_{Link}(i,j)$ provided in Chapter-3 associated with link (i,j) , consider the following definitions, which are required for the problem formulation:

Definition 5.3.1. Aggregate Deferral Link Set

An aggregate deferral link set, D_n , is defined as a set of deferral link sets associates with a set of simultaneously active links (i,j) . The size of D_n , is equal to the number of deferral link sets in D_n and is denoted $S(D_n)$

Definition 5.3.2. Deferral Partition

Given network $G(V,E)$, an aggregate deferral link set is defined as a deferral partition of G : $D_n = DP_n(G(V,E))$, if and only if it includes all the edges (links) in G

$$\bigcup_{(i,j)} D_{Link}(i,j) = E(G)$$

Problem Formulation

Given: $G(V,E)$

Maximize: $S(D_n)$

Over: all $n|D_n = DP_n(G(V,E))$

Such that:

$$\forall D_{Link}(i,j) \in D, \text{ and } \forall D_{Link}(m,n) \in D_i \neq D_{Link}(i,j), (i,j) \ni D_{Link}(m,n).$$

The problem can be reduced in polynomial time to the maximum independent set problem from graph theory¹, which has been shown to be NP-Complete [27] [43]. Thus, the problem of finding the maximum number of simultaneously active links in a network is equivalent to finding the maximum number of independent sets in the transformed graph $G'(V',E')$. The rules for transforming $G(V,E)$ to $G'(V',E')$ are given as follows:

- $\forall e \in E$, create a corresponding node n' in graph G' such that $\bigcup n' = V'$,
- $\forall e \in E$, let $E_2(e) = \{e_2|e_2 \text{ is less than or equal to two hops away from } e\}$, create a corresponding link e' connects nodes generated by e and every $e_2 \in E_2(e)$ such that $\bigcup e' = E'$

¹An independent set is the largest subset of vertices of V such that no pairs of vertices defines an edge of E for a given graph $G(V,E)$. Refer [27], [43] for formal definition of maximum independent set.

Figure-5.9 illustrates the rules of graph transformation while Figure-5.10 is another example. In Figure-5.10, the one of the possible maximum independent set of graph G' — node(1,2), node(5,7) is also one of the possible maximum aggregate link sets of graph G .

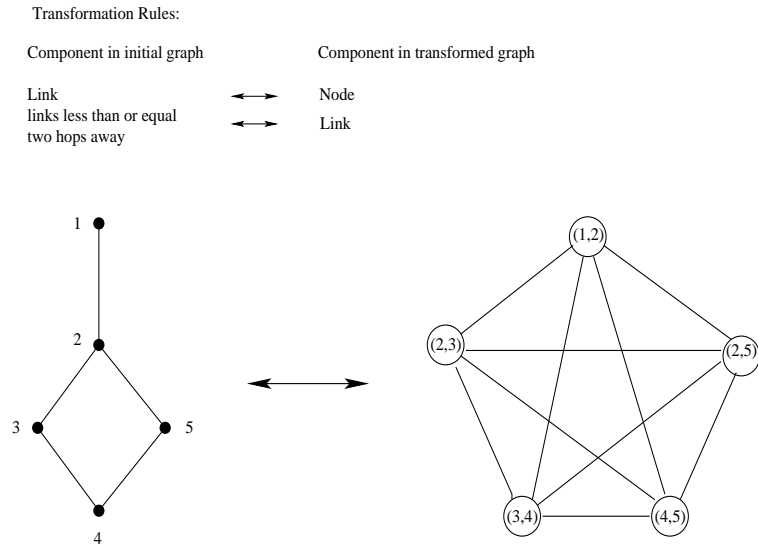


Figure 5.9: Another example of graph transformation

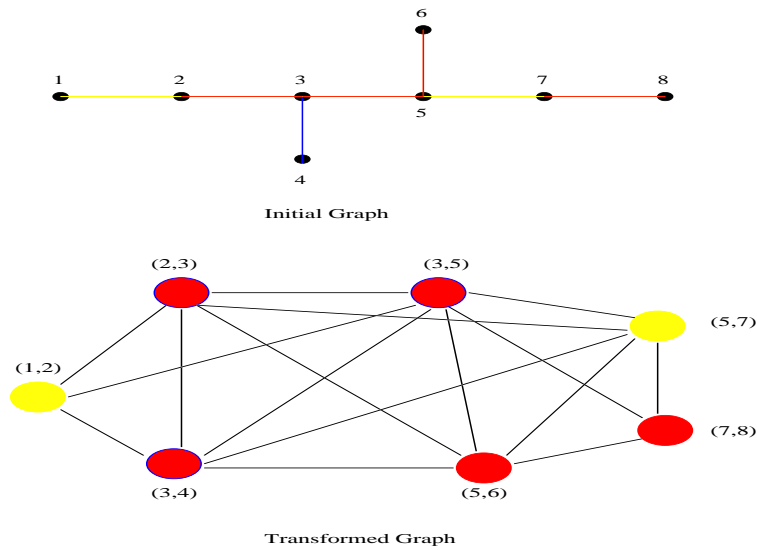


Figure 5.10: Rules of graph transformation

Several algorithms for finding the maximum independent set of a random graph can be found in [39], [29] etc. As stated in [39], the maximum independent set of same graph will be different if the algorithm start from different edge. This property can be utilized to find out the bottleneck of network by calculating the maximum independent set for all the links in the

network, as shown in subsection-5.3.2. The details of those algorithms are beyond the scope of the thesis and not discussed here.

- The Greedy Algorithm

Heuristic algorithms exist that are efficient and capable of finding optimal solutions to the maximum independent set problem under a well-defined set of conditions. Sufficiently interesting results, however, are attainable for the present capacity problem using a simple iterative greedy algorithm as follows:

Algorithm 5.3.1. Greedy Algorithm to Find the Maximum Concurrent Active Link

- **Step 1:** A unique deferral set is associated with each adjacent pair of nodes. A given deferral set is “feasible” if and only if the pair of nodes are not otherwise deferred. List all the feasible deferral sets in ascending order by the number of links in each set.
- **Step 2:** Pick the first deferral set in the list, the corresponding link is assumed to be active since its link deferral set has the fewest links. Hence, transmission or flow on the link causes the minimum possible access contention.
- **Step 3:** Update the set of feasible deferral sets: Sets associated with link within two hops of any active link must be removed from the feasible set because flow on these links will interfere with already active transmissions.
- **Step 4:** Update the size of remaining feasible deferral sets: Care must be taken not to double count any links. Any link that has already been deferred by an active transmission must be removed from any other deferral sets. This can be put in a more straightforward way: During the calculation, links that are not feasible should not be counted.
- **Step 5:** If more than one deferral set has the same size, the tie is broken by activating the link incident to the pair of nodes with the strongest and most stable signal, or alternatively, the minimum LOS (line-of-sight) distance.
- **Step 6:** Repeat steps 1-5 until the set of feasible deferral sets is empty.

An example of the results from execution of Algorithm-5.3.1 is depicted in Figure-5.11. Based on the execution of the algorithm there will be 5 simultaneously active links in the network. At any instant when all 5 links are active *all remaining links in the network* must

defer any attempt to access the transmission medium. Recall that in Figure-3.1, only two links can be active at same time.

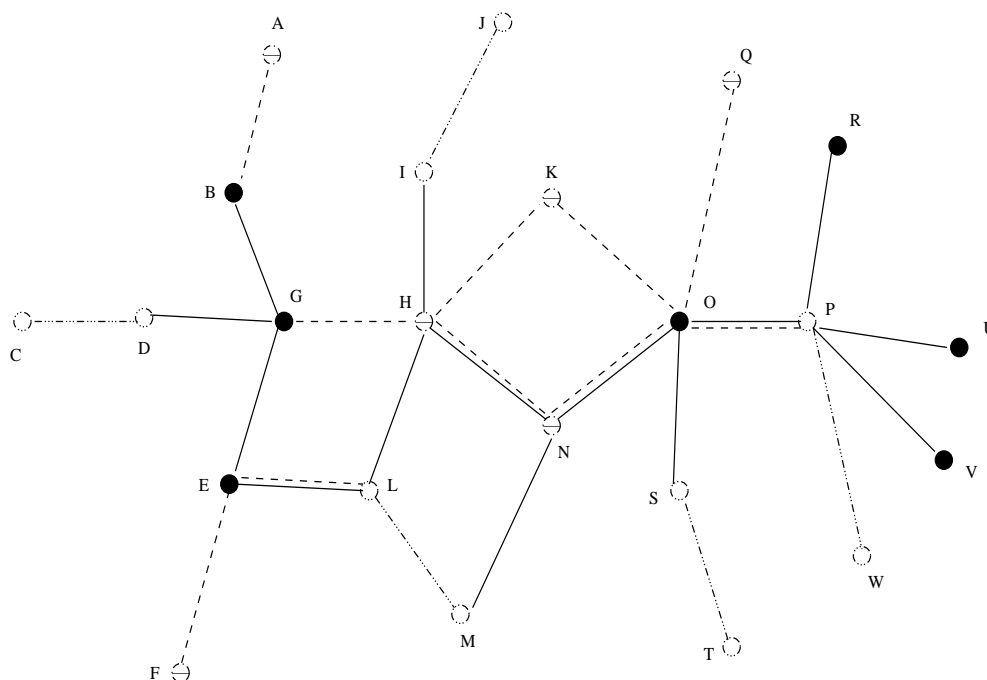


Figure 5.11: Flow assignment of Figure-3.1 using the proposed algorithm

Figure-5.12 depicts the ideal load assignment of a medium size ad hoc network where solid links represents active link, while dashed and darkened links are the one-hop and two-hop away links respectively. Numerical examples of the maximum number of simultaneously active links (l_{max}) for different configurations based on algorithm-5.3.1 are given in Table-5.2.

N	n_{avg}	l_{max}
432	3	118
530	4	119
732	6	139
952	8	163

Table 5.2: Number of simultaneously active links l_{max} using greedy algorithm

- The Random Link Selection Algorithm

A non-deterministic algorithm for estimating l_{max} uses random selection: The algorithm is initialized by placing all the links on the feasible list. At each iteration a link is randomly selected from the feasible list and all the links in its link deferral set are removed from the feasible list. The algorithm iterates until the list is empty.

N	n_{avg}	mean	std	ci (95%)
432	3	99	2.7806	1.1125
530	4	87	2.4815	0.9928
732	6	108	1.8173	0.7271
952	8	115	1.7425	0.6971
1312	12	118	3.5834	1.4437

Table 5.3: Number of concurrent links using random selection

that reflects the maximum instantaneous flow. However, in discussing the motivation for this analysis the desired metric was to reflect the *bottleneck* flow with respect to an arbitrary set of communicating nodes. Hence, MIC must represent the maximum lower bound for the flow of data among arbitrary entities in the network. The optimal solution requires multiple iterations of the independent set problem, hence, it is NP-complete. The following algorithm consists of a polynomial bounded number of iterations of the greedy algorithm.

Algorithm 5.3.2. Algorithm to find out Bottleneck

- **Step 1:** Repeat a modified version of algorithm-5.3.1 for each link; use the corresponding link to select the initial deferral set and construct a candidate set.
- **Step 2:** Sort the list according to the number of simultaneous activate links.
- **Step 3:** Select the largest aggregate deferral set from the candidate list . If all the active links are in the covered link list remove it from the candidate list.
- **Step 4:** Repeat Step-3 until a set is selected with at least one link not in the covered list set.
- **Step 5:** Move the set from the candidate list to the selected list and add any new links to the covered link set.
- **Step 6:** Repeat 2-5 until all the links are in the covered link set.

At each iteration the algorithm selects the aggregate deferral set from the candidate list that maximizes the number of simultaneously active link so long as it contains at least one active link that has not previously been covered. Thus, the algorithm terminates and provides reachability between all nodes in the connected network. The final iteration represents the bottleneck. Due to the uniformity of the network and the application of the sub-optimal greedy algorithm the

upper and lower bounds do not differ significantly. Table-5.4 shows the simulation result of algorithm-5.3.1 and 5.3.2

N	n_{avg}	Round	bottleneck for MIC
432	3	116	111
530	4	241	110
732	6	591	128
952	8	1899	152

Table 5.4: Number of required iterations and corresponding lower bound of Algorithm-5.3.1 and 5.3.2

Algorithm-5.3.1 and 5.3.2 provide approximate solutions to the “maximum instantaneous capacity” problem. However, under ideal conditions it may be possible to achieve better lower bounds, and thus, show that under worst case analysis it is possible to exceed the results in [24]. Moreover, the solution is not sufficiently efficient. Selected links tend to be “re-activated” in numerous aggregate deferral sets, whereas, other links may be activated only once during the search for the solution. For the purpose of comparison in terms of efficiency and precision a random algorithm is again utilized. Table-5.5 shows the result. The table shows that the greedy algorithm achieves a tighter lower bound, however, random selection requires significantly less computation.

N	n_{avg}	rounds			bottlenecks		
		mean	std	ci (95%)	mean	std	ci (95%)
432	3	45	8.474065	1.729761	94	1.295897	0.264524
530	4	82	13.15728	2.685719	82	0.999094	0.203939
732	6	178	21.71956	4.433486	101	1.007220	0.205598
952	8	341	56.42641	11.51799	107	1.559798	0.318393
1312	12	785	79.15528	16.15750	109	0.931533	0.190148

Table 5.5: Number of required iterations and corresponding lower bound: random selection

5.3.3 Discussion

In light of the widely accepted limitations and their impact on the broader research community it is critical to examine above results with respect to [24] that studies the capacity of wireless networks. The main results from their analysis relevant to this work is summarized in what follows:

In [24], two models are used for a communication, “protocol model” and “physical model”, what we used in this work is similar to the “protocol model”. For network topology, [24] also

has an “arbitrary” network model and a “random” network model. The “random” network model consists of homogeneous nodes, fixed transmission range, independently and uniformly distributed location which is also the characteristics of the network model we are using in this work. For random network, protocol model, Gupta and Kumar has the following results[24]:

- Throughput is defined as the time average of the number of bits per second that can be transmitted by every node to its destination.
- The capacity can be expressed as:

$$\lambda(N) = \Theta\left(\frac{W}{\sqrt{N \log N}}\right)$$

where W is the channel capacity and N is the number of nodes in the network. Notice that here the capacity is the “virtual channel” capacity, or in other words, it is the “end to end” capacity regarding to the specific source- destination pair.

- Given ideal routing and scheduling their result is shown to improve to $\Theta\left(\frac{W}{\sqrt{N}}\right)$

The network configuration and parameters are the same in both analysis. However, the semantic with respect capacity differs, namely, the MIC analysis is a general bottleneck considering the entire network, whereas, in [24] an upper bound is determined on a per-node basis. This form of result can be misleading as any consumer will experience diminishing returns given a fixed network of resources. The two semantics for capacity in this paper are more useful as they reflect the aggregate scaling effect of the network versus an individual consumer. Furthermore, in [24] the asymptotic results are bounded from above and below. The results in this thesis reflect “worst case” analysis and are bounded only from below. Hence, it can be reasoned that the optimal results are even better.

In order to make a meaningful comparison of the results it is necessary to use information about the present analysis to (1) consider the worst case throughput for a single source destination pair, and, (2) look at asymptotic bounds. From Chapter-4 the average area covered by level-1 interference set is about $(\pi + 0.98)r^2$, thus the number of non-overlapping level-1

interference set in the network can be calculated by:

$$\begin{aligned}
 Num_{non-overlap} &= \frac{Area_{network}}{Area_1} \\
 &= \frac{\pi R^2}{(\pi + 0.98)r^2} \\
 &= \frac{\pi \frac{N}{n_{avg}+1} r^2}{(\pi + 0.98)r^2} \\
 &= \frac{\pi}{\pi + 0.98} \frac{N}{n_{avg} + 1}
 \end{aligned}$$

N	n_{avg}	$Num_{non-overlap}$	random selection	bottleneck of random selection
432	3	82	99	94
530	4	81	87	82
732	6	80	108	101
952	8	80	115	107
1312	12	77	118	109

Table 5.6: Comparison of number of concurrent links using different approaches

Table-5.6 listed the results from above estimation and the simulation result of random selection. Based on comparison of results from the above estimation and simulation using random link selection it can be shown that the number of non-overlapping level-1 interference sets is roughly equivalent to the number of maximum simultaneously active links. Corresponding asymptotic bounds can be expressed as follows:

$$O\left(\frac{N}{(n_{avg} + 1)}\right) = \Omega\left(\frac{N}{(n_{avg} + 1)}\right) > \Theta\left(\frac{N}{(n_{avg} + 1)}\right)$$

Considering only uni-cast communications there are at most $N/2$ source-destination pairs in the network. The average hop count is approximately $\sqrt{N/n_{avg}}$. Let C represents a constant that corrects for access capacity W be the channel bandwidth. The resulting capacity per-node is given by (when $C'=2C$)

$$\lambda(N) = \frac{C \cdot \frac{N}{n_{avg}+1} \cdot W}{\frac{N}{2} \cdot \sqrt{N/n_{avg}}} = \frac{C'W}{\sqrt{Nn_{avg}}} = O\left(\frac{W}{\sqrt{N}}\right)$$

5.4 Conclusion

In this chapter, another application example of deferral framework — the network capacity analysis of multi-hop wireless ad hoc network is presented. Two new metrics for the capacity of wireless ad hoc networks under ideal conditions: “network saturation capacity” and “maximum instantaneous capacity” are defined and compared. Special features regarding to the network

saturation capacity, the boundary condition is studied and its impact on the precision of estimation of NSC is evaluated. The instantaneous capacity problem reflects the true flow capacity of the network between any nodes — it is the bottleneck capacity, as such it reflects a lower bound on total throughput for all possible destinations. This property differentiates the metric from related work, for example, the asymptotic throughput analyzed in [24]. Determination of the bottleneck capacity is shown to be an NP-complete problem; two heuristic algorithms are presented for finding approximate solutions. Using the heuristic results and taking limiting values the results that reflect worst-case analysis when bounded from below are shown to agree with the results reported in [24]. The agreement mutually validates the two models, however, is also suggests that the previous work is pessimistic and does not provide insight regarding how to more efficiently leverage available network capacity.

Chapter 6

Routing Algorithm Design using deferral Set Framework — The Dynamic Codeword Routing (DCR)

Chapter-4 and 5 provide two applications of deferral set framework; the application of deferral framework is not limited to the area of analytical analysis, in this chapter a more practical application of deferral set framework: “dynamic codeword routing” — a adaptive routing algorithm using the concept of deferral set and equivalent competitor is presented.

6.1 Introduction

The rapid growth of wireless LAN and wireless ad hoc network is questioning traditional strict layering structure which has been proved work fairly in wired communication system. Cross-layer design idea has received a lot attention in the recent years and related work has proved that in wireless network, the “layers” are no longer independent from each other, on the contrary, in order to improve performance, information from other layer should be taken into account when the decisions are made at current layer. At the same time, it is desirable to maintain a high degree of architectural modularity for practical implementation and future network evolution. [10].

Examples of cross-layer design can be found in [11], [34], [12], [13], [38], [42], [46]. Among them, [12] focuses on joint routing and resource allocation based on different routing models, as well as [11] focuses on joint power control and scheduling and [34] on joint resource allocation and pricing, [13] on routing and pricing, [38] on medium access control and physical layer

diversity, [42] on routing and data compressing and [46] on resource allocation and scheduling. There are two major trends of cross-layer design, the first focuses on how to dynamically adjust protocol settings based on different type of service and the second adjusts system setting based on the physical condition. It turns out that the information from physical layer and application layer are among the most frequently used metrics for cross-layer design.

In the thesis, a cross-layer design concept “codeword routing” is discussed — different routes in the network are represented by different codewords, and the distance between different “codewords” reflects the potential interference between the routes. This provides another aspect of cross-layer design, the work presented here has fundamentally different approach and objective from the idea of integrating inter-flow interference into route selection. The originality and significance of this work differentiating it from related work [21], [26]: it starts from a theoretical basis seeking an inherent characteristics that can be leveraged to improve routing throughput, while [21], [26] presented application originated routing algorithm, tested what the throughput was based on random probe and made admission decision. Specifically, SWAN [21] is a real time protocol that uses explicit notification in order to support different services through admission control, while load balancing [26] is a source routing fashion routing protocol that make decisions based on information of node that are along the possible paths, no multi-hop interference that is important in wireless environment considered, while the codeword cross-layer routing idea quantify the effect of MAC layer behavior and module the network layer based on this information, thus, it distracted from a general “available bandwidth” solution. However, the “codeword routing” concept can be integrated with existing bandwidth aware/load balancing routing algorithms to improve performance.

Rather than propose a well-established routing protocol, the objective of this work is first to present an example of the practical application of the deferral set framework and the theoretical cross-layer design model which utilize the MAC and routing cross-layer information. Moreover, the dynamic codeword routing algorithm is presented as an example of practical implementation of the “codeword routing” design. It is not claimed to be an optimal solution, but it still can provide significant performance improvement. Since as stated in [10], cross layer designs usually improve performance at the expense of higher complexity in communication and computation, so it is important to reduce the complexity of the cross-layer design: dynamic codeword routing is a 100% reactive routing protocol that bases on modification of AODV with one more metric,

hence the increment in computation and communication complexity is really negligible.

6.2 Current Routing Algorithms

Prior to the discussion of the cross-layer codeword routing design, this section gives a brief review on the performance of current routing algorithms. Since the emergency of wireless networks, researchers have proposed different routing algorithms, for example, DSDV, AODV, DSR, ZRP, TORA, WRP etc [40]; as described in [40], those algorithms can be classified as either table driven (DSDV, WRP) or demand-driven (AODV, DSR, TORA); there exist other classifications, such as pro-active routing, reactive routing, topology based routing or geographically based routing, uniform/flat routing or cluster based/hierarchical routing; most of those algorithms fall into above one or several categories. Among those algorithms, AODV has gain great popularity and its performance is always selected when performance comparison is conducted.

Ad-hoc On-demand Distance Vector (AODV) is a well-known routing algorithm [8], the detail of the algorithm is not repeated here. In the rest of this section, the performance of AODV, as well as the possible improvement are illustrated. Given the network shown in Figure-6.1, communication pairs are described using the [source, destination] format, for example, in Figure-6.1, there are four communications pairs, respectively, [9,25], [25,9], [4,12] and [12,4]; in other words, node 9 and node 25 are communicating with each other at both directions and so does node 4 and node 12, etc.

Figure-6.1 shows the routes obtained by running AODV in the given network, IEEE 802.11 DCF with RTS/CTS [6] scheme is used in MAC layer:

node 9 to node 25, $9 \rightarrow 5 \rightarrow 13 \rightarrow 25$;
node 25 to 9, $25 \rightarrow 13 \rightarrow 11 \rightarrow 17 \rightarrow 9$;
node 4 to node 12, $4 \rightarrow 5 \rightarrow 13 \rightarrow 2 \rightarrow 5 \rightarrow 12$;
node 12 to node 4, $12 \rightarrow 3 \rightarrow 13 \rightarrow 5 \rightarrow 4$.

However, in wireless network, due to the broadcast nature of wireless communication, besides direct interference, there are hidden and exposed terminal problems, which implies that only one of every three consecutive links can be active for data exchange at a time, therefore above routing assignments in Figure-6.1 will cause interference between different routes and therefore the performance will be degraded. At the same time, the network resource (links) is not used

efficiently since a lot of links at the top and bottom part of the network have never been active.

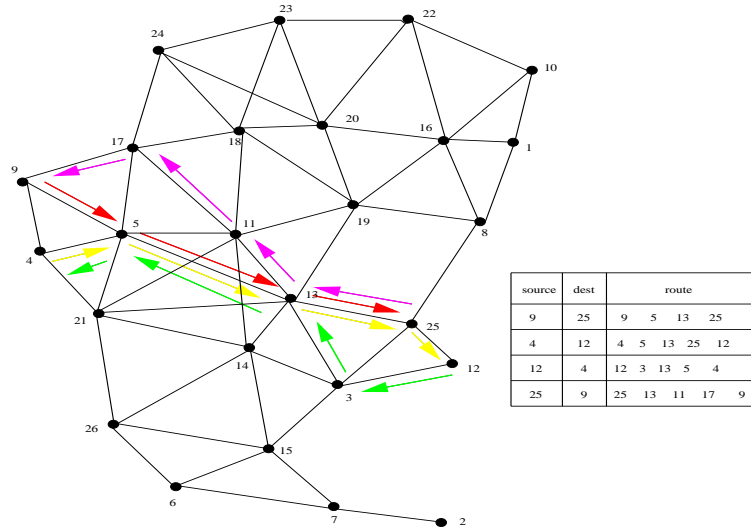


Figure 6.1: Routes obtained by AODV

Alternatively, for the same traffic, it is possible to pick more efficient routing assignments. Figure-6.2 shows one of the possible route assignments.

- node 9 to node 25, $9 \rightarrow 5 \rightarrow 13 \rightarrow 25$;
- node 25 to 9, $25 \rightarrow 8 \rightarrow 16 \rightarrow 20 \rightarrow 24 \rightarrow 17 \rightarrow 9$;
- node 4 to node 12, $4 \rightarrow 21 \rightarrow 26 \rightarrow 15 \rightarrow 3 \rightarrow 12$;
- node 12 to node 4, $12 \rightarrow 3 \rightarrow 14 \rightarrow 21 \rightarrow 4$.

In Figure-6.2, whenever possible, routes are set to be at least two hops away from each other, thus the potential interference is reduced and the performance will improve. The results of end-to-end throughput for the above communications using different routes are shown in Figure-6.3.

Figure-6.3 illustrates the end-to-end throughput of different route as the inter-arrival time of the CBR traffic increases. When the inter-arrival time is large enough, (to the right of x-axis), the traffic load is low, both routing assignments can provide 100% throughput, as inter-arrival time becomes smaller, traffic load increases, AODV reaches saturation first, while

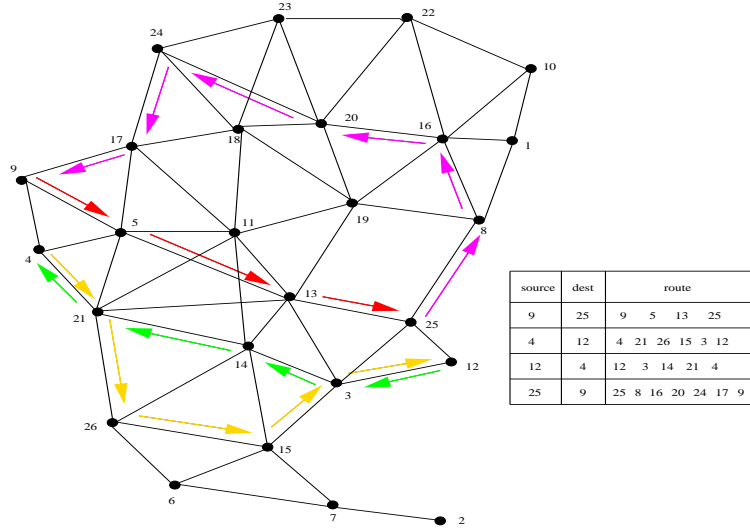


Figure 6.2: Alternative Routes for the Communications in Figure-6.1

the alternative routing assignment can provide higher throughput because data exchange along those routes will experience less interference from each other than AODV. It is clear that if the MAC interference is considered when the routing decisions are made, it is possible to improve the network performance. In next section this idea is presented as a cross-layer design model that utilizes the MAC layer interference information — the “codeword routing” model.

6.3 “Codeword Routing”— the Cross-layer Routing Design

Section-6.2 shows that the MAC layer interference should be considered when routing decisions are made in order to improve the network performance through a simple example. Based on this observation, the “codeword routing” cross-layer design idea is proposed. The idea of codeword routing design comes from the codeword selection in coding theory — the larger the distance between the constellation, the better SNR can be achieved, similarly, if the routes in the network are separated enough from each other, the effect cross-layer interference [18] can be remedied.

In this section, first the representation and notation used in the “codeword routing” are

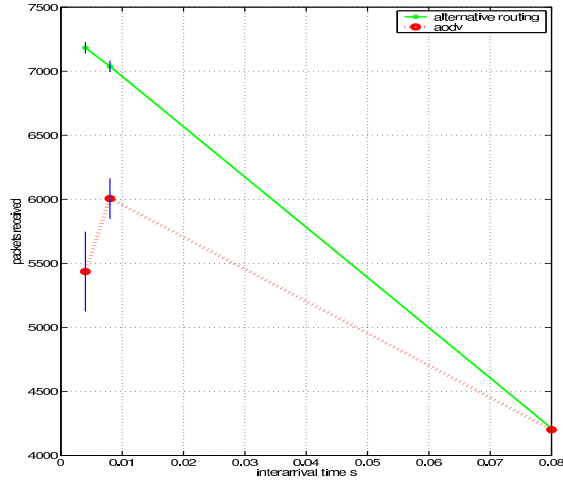


Figure 6.3: Performance comparison for different routing assignments

illustrated, then the criterion to calculate the potential interference among routes is presented. Finally, the “codeword routing” idea is discussed.

In “codeword routing” both the nodes and the routes in the network are represented by “codewords”: a vector of length N where N is the number of nodes in the network. Suppose there are N nodes in the network, each node will have a distinct identification from 1 to N ; at this time, for each node, it is sufficient to know all its direct neighbors, hence the “node codeword” is a $N \times 1$ vector where the i_{th} element represents the relationship between the current node with the i_{th} node in the network. For the i_{th} element in the “node codeword” e_i :

- “ $e_i = 2$ ”, iff it is the “node codeword” of node i ;
- “ $e_i = 1$ ”, iff the node i is the direct neighbor of the current node (not i);
- “ $e_i = 0$ ”, iff node i is not the neighbor of current node (not i)

For example, in Figure-6.4, the “node codeword” for node 2 will be expressed as [121000001110], indicates that node 1, 3, 9, 10, 11 are node 2’s neighbors.

Next, the route in the network then can be expressed by route indicator — a $N \times 1$ vector where i_{th} element corresponds to the i_{th} node in the network, the value of the i_{th} element r_i reflects the order of the node in the route:

- “ $r_i = 0$ ”, iff node i is not in the current route;

- “ $r_i = p \in Z, r_i \neq 0$ ”, iff node i is in the current route, and it is the p_{th} hop of the route.

For example, route $2 \rightarrow 11 \rightarrow 12 \rightarrow 6$ in Figure-6.4 will be expressed as [010004000023], indicates that this route is from node 2 to node 6 through node 11 and 12. Notice that the route indicator is different from the “codeword” of routes, in fact, the “route codeword” is derived from the route indicator and the “node codeword” of each involving node following the rules defined next.

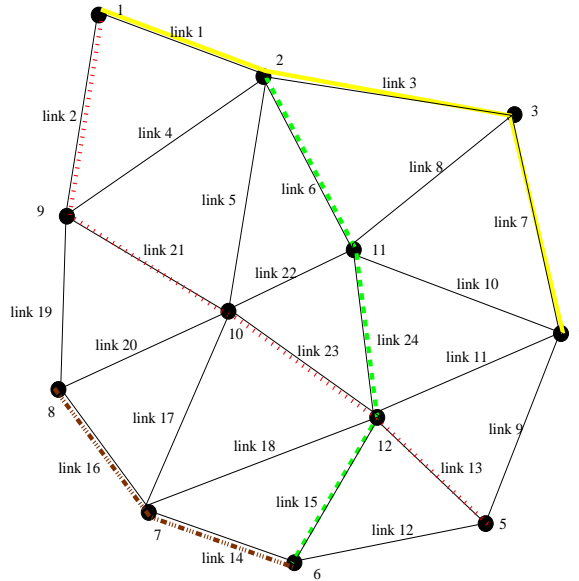


Figure 6.4: An example of wireless ad hoc network

Given the route indicator and the “node codeword”, the “route codeword” can be calculated. As in coding theory, in order to avoid the decoding error to the greatest extent, in the code space, the codewords are selected to be as far as possible away from each other, in other words, when a new codeword is picked from the available codewords, it is desirable that the newly added codeword is as far as possible away from all the existing codewords in the code space. Similarly, if the set of all the possible routes in the wireless network can be viewed as a code space, then in order to remedy the effect of interference due to the broadcast nature of wireless communication, the concurrent routes should be away from each other as much as possible. For example, it is clear that there will be less interference following the routes shown in Figure-6.2 than the routes in Figure-6.1, hence, it is similar to the case in coding theory, and if there is an appropriate mapping between the code space and the routing space, it might be possible to apply results from coding theory to improve the performance of wireless networks.

One of the possible mapping methods is provided here for “codeword routing”. Notice that the order in the route will not affect the interference between the routes, so in the final “route codeword” the information about the order of nodes in the route will be omitted. The “route code” space will still have three alphabets, 0, 1 and 2, and the “route codeword” will be the result of the “or” operation of the “node codeword” from every node in the route. The “or” operation is defined as follows:

$$\begin{array}{l}
 2 \parallel x = 2 \\
 1 \parallel 0 = 1 \\
 1 \parallel 1 = 1 \\
 0 \parallel 0 = 0
 \end{array}$$

hence, according to the above “or” operation, the final “route codeword” is still a $N \times 1$ vector, where the i_{th} R_i is:

- “ $R_i = 2$ ”, iff node i is in the route;
- “ $R_i = 1$ ”, iff node i is the direct neighbor of the route;
- “ $R_i = 0$ ”, iff node i is at least 2 hops away from the route.

For the previous example shown in Figure-6.4, the route $2 \rightarrow 11 \rightarrow 12 \rightarrow 6$ is represented by the route indicator [010004000023], and the “route codeword” for this route then can be calculated as:

		route codeword
node	2	121000001110
node	11	011100000121
node	12	000111100112
node	6	000012100001
route	2-11-12-6	121112101122

Table 6.1: An example of the calculation of “route codeword”

The final “route codeword” shows that nodes 2,6,11,12 belong to the route and nodes 1,3,4,5,9,11 are the neighbor of the route, similarly, the code for route $1 \rightarrow 9 \rightarrow 10 \rightarrow 12 \rightarrow 5$ is [210121112212], the potential interference between two different routes in the network is reflected by the so-called “code distance” between two “route codewords”, however, unlike in the coding theory, the bigger the distance is, the more potential interference there is between the two routes, therefore in a network with pre-existed routes, it is desirable to choose a new route that will generate the least sum of “code distance” to all the existing routes in the network.

The rules to determine the distance is open to applications, in this thesis, a simple yet effective example is shown, although it is a heuristic criterion, the improvement is significant and the effect of the more complicated distance assignments is promising. The simple “code distance” assignment scheme proposed is shown in the following table:

R_i in route code 1	R_i in route code 2	“distance”
0	X	0
1	1	0
2	1	3
2	2	4

Table 6.2: A “code distance” assignment for “codeword routing” algorithm

Table-6.2 illustrates a possible scheme to determine the “code distance” between two routes. If two routes share one same node, the degree of the interference will be the most serious, hence the “code distance” distance will increase by 4¹, while if the node from one route is the neighbor node of the other route, there will be interference still, however, the degree of interference will be less serious, so the “code distance” will increase by 3, otherwise the routes are at least two hops away from each other and will not affect the “code distance” at all. The increment of “code distance” of either case above can be set to include more metrics of interest, such as the remaining power, the channel quality, etc. The final “code distance” between two “route codewords” will be the sum of each digit from the “route codeword”. Following above rule in Table-6.2, the distance between route 2 → 11 → 12 → 16 and route 1 → 9 → 10 → 12 → 5 can be calculated as follows:

node id	1	2	3	4	5	6	7	8	9	10	11	12	sum
route 1	1	2	1	1	1	2	1	0	1	1	2	2	
route 2	2	1	0	1	2	1	1	1	2	2	1	2	
code distance	3	3	0	0	3	3	0	0	3	3	3	4	25

Similarly, assume there are only 2 routes in Figure-6.4, route 1 → 2 → 3 → 4 and route 8 → 7 → 6, the “code distance” between those routes will be:

node id	1	2	3	4	5	6	7	8	9	10	11	12	sum
route 1	2	2	2	2	1	0	0	0	1	1	1	1	
route 2	0	0	0	0	1	2	2	2	1	1	1	1	
code distance	0	0	0	0	0	0	0	0	0	0	0	0	0

The “code distance” between those two routes is 0, which implies these two routes can coexist in the network and will create no interference between each other! Based on the observation

¹The “code distance” are selected to reflect the MAC layer interference, currently it doesn’t reflect the actual traffic, in the future work this will be considered

that in a wireless network, whenever the channel reservation and floor acquisition is employed, (for example, the IEEE 802.11), among three consecutive links, only one of them can be active at a given time, it is clear that in the network route $1 \rightarrow 2 \rightarrow 3 \rightarrow 4$ and route $8 \rightarrow 7 \rightarrow 6$ are away from each other for at least 2 hops thus there is no interference between them, which agrees with the result from “codeword routing”.

From the above discussion, the objective of “codeword routing” is clear, that is, as in the coding theory, choose the codeword that will cause the least probability of error decoding, in the network, find the route between the specific source and destination from all the possible candidates which minimize the sum the “code distance” between the newly added route to all the existing routes in the network. The most straightforward but tedious way to do this is to build a centralized algorithm that find all the possible routes from the source to the destination and then choose the one minimize the “code distance”, a recursive algorithm is needed to complete such work; however, it is time-consuming and impractical to implement such algorithm, hence, in the thesis, the idea is implemented by a distributed fashion. In the next section the distributed algorithm — dynamic codeword routing (DCR) algorithm is discussed and the performance enhancement is showed afterwards.

6.4 Dynamic Codeword Routing Algorithm

Section-6.3 proposes the idea of the “cross-layer design routing” and the necessary concepts and methodologies for it. This section discusses one example of implementing the design idea — the dynamic codeword routing (DCR) algorithm.

Notice that the “code distance” is defined to be the sum of the distance between every corresponding node from different routes in the network, but in fact only the nodes involved in the route (nodes that are in the route or are the neighbors of the route) will affect the distance, hence it is quite similar to the distance vector algorithm if we assign appropriate link cost to each link in the network.

In Section-6.3, “code distance” is determined by the different roles by which the node plays at different route, for example, if in route 1, node i is an active node, $R(1)_i = 2$ and in route 2 node i is the neighbor, $R(2)_i = 1$, then the “code distance” will be increased by 3, from another aspect, the “codeword routing” idea can be interpreted as the follows: let the link cost reflect the potential interference among routes, for example, if one end node of a link belongs to

route # 1, ($R(1)_i = 2$), and the other end node is the neighbor of route # 2, ($R(2)_i = 1$), the interference will be greater than if the other end node is far away from route # 2 ($R(2)_i = 0$). While the link cost is related to the relative positions of nodes from different routes, in the thesis the link cost of link AB, represented by $C(AB)$, will be defined as the sum of the weight of both end nodes A and B, represented by $W(A)$ and $W(B)$, in other words, $C(AB) = W(A) + W(B)$. Based on above discussion, the following distributed version of “codeword routing” algorithm is proposed:

- step 1: At initialization, set the node weight $W(i)$ to be 0 for all nodes in the network.
- step 2: Assign node weight $W(i)$ according to the status of node i :
 - if node i is active or will be active, $W(i) = W(i) + 4$;
 - if node i is or will be the neighbor of an active node but not belongs to the route, if applicable, $W(i) = W(i) + 3$;
 - otherwise, $W(i)$ stays unchanged.
- step 3: Update the link cost in the network, $C(ij) = W(i) + W(j)$, thus the “code distance” between routes will be transformed to the different weights of each route;
- step 4: Run the traditional distance vector algorithm and obtain the routes that will generate the least possible interference.
- step 5: Periodically update the link status according to the route assignments.

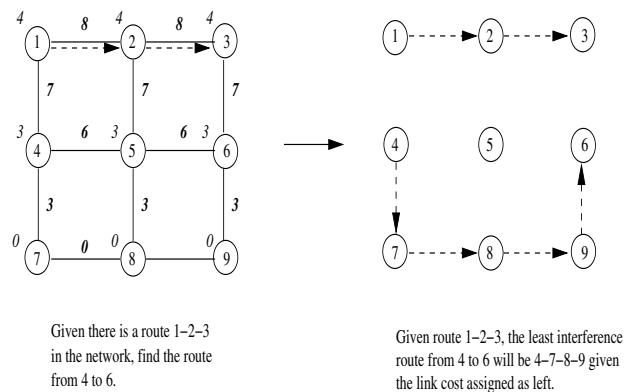


Figure 6.5: An example of link cost assignment and DCR algorithm implementation

The rest of this section provides several examples to illustrate how the algorithm works: In Figure-6.5, a route from node 4 to node 6 is under search given that route $1 \rightarrow 2 \rightarrow 3$ is already in the network. The weight of each node is shown at each node with italic font: node 1, 2 and 3 are in one and the only one active route, so their weights are set to 4, and 4,5 and 6 are neighbors of route $1 \rightarrow 2 \rightarrow 3$, so their weights are set to 3; and node 7,8,9 since they are two hops away from active route, their weights are 0. Hence the corresponding link cost can be easily obtained, as shown in bold font. The cost of link (1,2) is 8, and the cost of link (1,4) is 7 etc. When node 4 tries to communicate with node 6, first the weight of node 4 will increase by 4, $W(4)=W(4)+4$, at the same time, the next hop of node 4 will be determined as follows, node 4 has three neighbors, node 1, node 5 and node 7, with weights $W(1)=7$, $W(5)=3$, and $W(7)=0$ respectively, so if node 1 is the next hop, then $W(1)=W(1)+4=8$, and $C(4 \rightarrow 1)=8+7=15$; while if node 5 is the next hop, $C(4 \rightarrow 5)=14$ and $C(4 \rightarrow 7)=11$, hence the next hop will be 7. Similarly, the route from node 4 to node 6 given $1 \rightarrow 2 \rightarrow 3$ exists can be obtained, as shown in Figure-6.5, $4 \rightarrow 7 \rightarrow 8 \rightarrow 9 \rightarrow 6$.

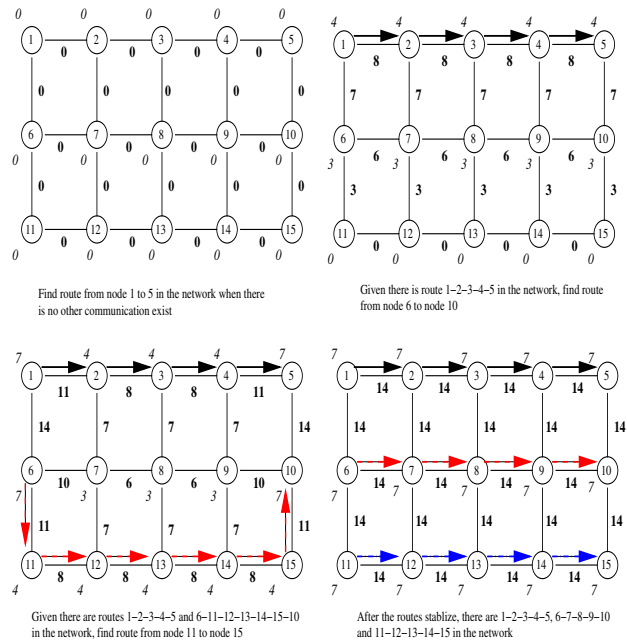


Figure 6.6: Another example of link cost assignment and DCR algorithm implementation

Next example shows how the proposed algorithm dynamically adjusts routes according to traffic. In the network shown in upper-left of Figure-6.6, first assume there is communication from node 1 to node 5, it is straightforward to obtain the route $1 \rightarrow 2 \rightarrow 3 \rightarrow 4 \rightarrow 5$ when

there is no other traffic in the network, as any traditional distance vector routing algorithm, the “codeword routing” algorithm will generate shortest path result, (the upper-right of Figure-6.6); then if there is one more communication between node 6 and node 10, similar to the first example, the route from node 6 to node 10 will be $6 \rightarrow 7 \rightarrow 8 \rightarrow 9 \rightarrow 10$ (the lower-left of Figure-6.6); finally, when one more flow from node 11 to node 15 is added, the weight of node 11 will increase to $W(11)=W(11)+4=8$, and correspondingly $C(11 \rightarrow 6) = 8+11=19$ and $C(11 \rightarrow 12) = 8+8 =16$, so the next hop for 11 to node 15 will be 12, following the same rule, the route from node 11 to node 15 will be $11 \rightarrow 12 \rightarrow 13 \rightarrow 14 \rightarrow 15$; while for communication from node 6 to 10, since node 11 has already been an active node for another route, the next hop to node 10 will then be node 7 ($C(6 \rightarrow 1)=7+8=15$, $C(6 \rightarrow 7)=7+7=14$, and $C(6 \rightarrow 11)=7+8=15$), hence the route will be $6 \rightarrow 7 \rightarrow 8 \rightarrow 9 \rightarrow 10$. The route assignment is shown as the lower right of Figure-6.6 after the routes become stable.

This section provides a distributed fashion implementation of the codeword routing idea, in next section the enhancement of this algorithm is illustrated through simulation results.

6.5 DCR Implementation and Performance Enhancement

Section-6.4 provides a distributed DCR routing algorithm as the implementation of “codeword routing”, in this section, first the implementation of DCR algorithm is briefly summarized then the performance enhancement compared to AODV is presented.

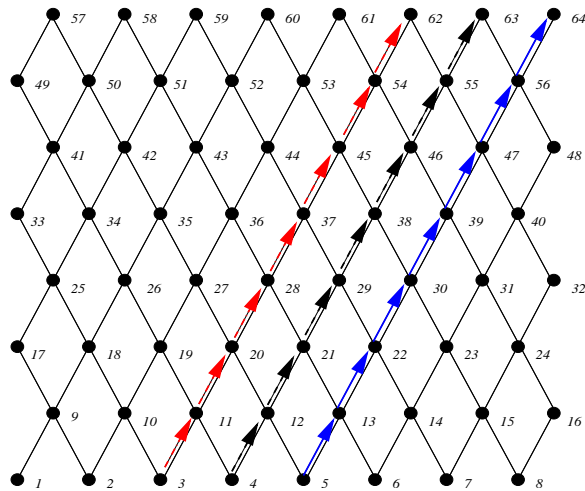


Figure 6.7: Routes selected by AODV, 3 parallel flows

The DCR algorithm is implemented in *ns2* simulator based on AODV. The status of each

node is broadcasted to its neighbors through *hello messages*. Upon the reception of hello message, the node will update its status according to neighbors' information and send out its own hello message, through the exchange of hello message, two hop way neighbors get to know MAC layer interaction and in turn set their status. Moreover, instead the hop counts used in AODV, the “codeword” is used as the routing metric. Hence like AODV, DCR is a reactive routing protocol without any periodical updates. Simulations are conducted under different scenarios, for each scenario, simulations are run for 15 times and the mean and confidence interval are recorded to compare with the results with the result obtained by running AODV algorithm for same scenario. Although in the scope of thesis AODV is selected, in fact the “codeword” routing just adds one more metric — the node status to any existing routing algorithm, so the same comparison can be made for any other routing schemes. Simulation results and the corresponding analysis are presented next.

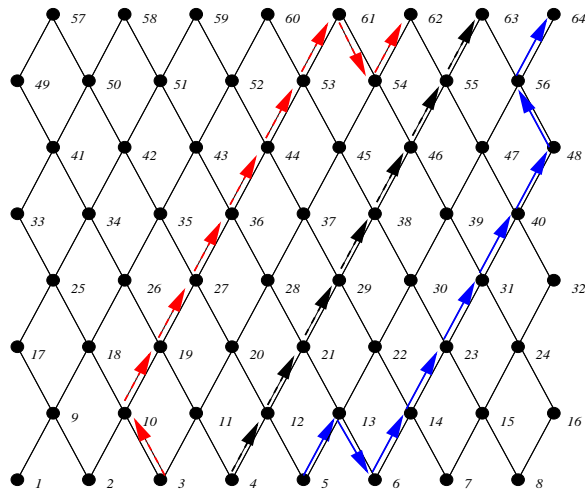


Figure 6.8: Routes selected by DCR, 3 parallel flows

The network of interest is a wireless ad hoc network with 64 nodes, each node will 4 neighbors (except the nodes at the boundary of the network), in the first scenario, there are 3 parallel flows in the network, which are from node 3 to node 62, node 4 to node 63 and node 5 to node 64.

Figure-6.7 shows routes obtained from AODV, and since the routes obtained by DCR are dynamic, Figure-6.8 shows the routes obtained by DCR at a specific instance. Notice that the order by which the traffic load are injected to the network will affect the result of DCR, the routes shown in Figure-6.8 are generated give the order of traffic injection is: first, node 4 to

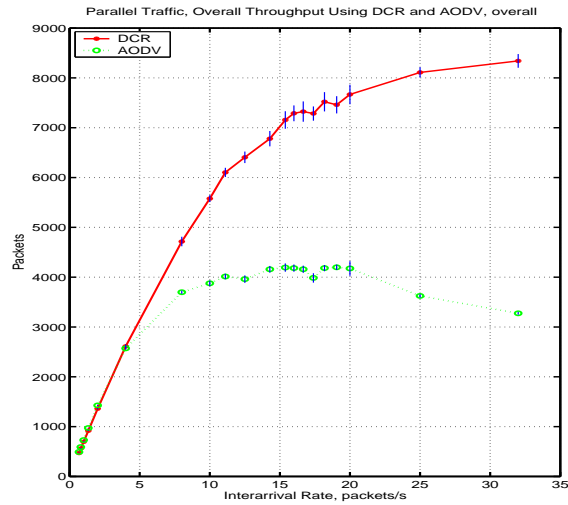


Figure 6.9: Comparison of overall throughput using AODV and DCR, 3 parallel flows

node 63, second, node 3 to node 62 and finally, node 5 to node 64.

Figure-6.8 shows that when DCR is employed, the routes are more spread out through the network than AODV, although the length of the routes may be longer, but the end-to-end throughput is in fact increasing because packets following the routes generated by DCR experiences less interference than AODV, in other words, the overall link cost through the addition of hops is still less than the cost caused by the interference of a shorter path. This implies a tradeoff between route length and end-to-end throughput.

Figure-6.9 illustrates the overall 3 end-to-end communication throughput obtained from DCR and AODV, when the load is low, both AODV and DCR are capable to route 100% packet to the destination, as the traffic load increases, AODV reaches the saturation stage first, while DCR can accommodate more load for a wide range of traffic load than AODV, as shown in Figure-6.9, DCR can provide twice as much the throughput of AODV when the traffic load increases. From those figures it shows that when the traffic are parallel, DCR will improve the end-to-end throughput significantly, this case is similar to the scenario that in sensor networks, sensors send information to the destination node, the data flow will somehow “parallel” to each other.

Figure-6.10 and Figure-6.11 depict the end-to-end throughput of each individual flow in the network of AODV and DCR respectively. It is shown that when AODV is used, each flow get

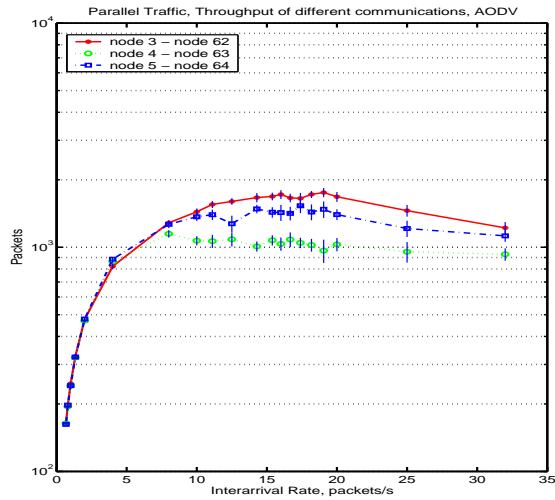


Figure 6.10: Throughput of each of the 3 flows when using AODV, 3 parallel flows

a equal share of the end-to-end throughput, while for DCR, the route in the “middle” has the least end-to-end throughput, which is still comparable to as the corresponding AODV result. The reason for this un-equilibrium is that the flow in the middle will face interference from both side, while the other two flows only have one competition each. From Figure6.10 and Figure-6.11 it is shown that the enhancement of the throughput by DCR is not homogeneously, the degree of enhancement is related to the position of the flow, however, even the worst case the performance is still as good as AODV.

The next scenario under simulation is for the same network, but with 3 flows which cross each other, more specifically, node 3 to node 62, node 4 to node 63 and node 7 to node 59. The routes obtained from AODV and DCR are shown in Figure-6.12 and Figure-6.13 respectively, again Figure-6.13 shows just the routes at a specific instance due to the dynamic nature of DCR. Similar to the first scenario, the traffic from node 4 to node 63 is injected first followed by traffic from node 3 to node 62 and node 7 to node 59 when DCR is employed. DCR still spread out the traffic to some extent, however, for cross traffic, the space for improvement will not be as good as parallel scenario, since it is impossible to avoid the cross point of routes in the network.

Figure-6.14 illustrates the overall end-to-end communication throughput obtained from AODV and DCR, as stated previously, since the traffic flows crossed at some point, it is difficult

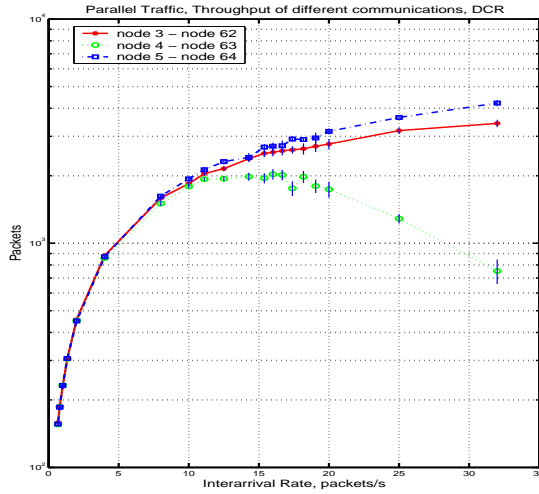


Figure 6.11: Throughput of each of the 3 flows when using DCR, 3 parallel flows

to spread the routes since there will always be two cross points, therefore there is not as much improvement as in the parallel scenario. However, from the simulation result, there is still some improvement which implies that even sometimes in sensor network when there is some problems in present and the routes are crossed, the DCR can still outperform AODV.

Figure-6.15 and Figure-6.16 depict the end-to-end throughput of each individual flow in the network using AODV and DCR respectively. The end-to-end throughput of the same communication pair is less than the end-to-end throughput obtained in parallel flow scenario since higher degree of interference is faced in the cross flow scenario. As in the parallel flow case, the end-to-end throughput of each flow using AODV are close to each other, while in DCR there is no big difference about the performance of each individual flow because of each flow will have the same amount of interference from other flows.

Above simulation show that DCR will enhance the performance of wireless ad hoc network under some scenarios, more specifically, when there is few routes cross each other and the traffic is moderate, moreover, the performance of DCR still outperform AODV, under the worst case, e.g. very high traffic load and/or a lot of cross traffic in the network. Since DCR is proposed as an application example of joint MAC and routing cross-layer design and as stated before, can be viewed as the extension of current routing algorithm with one more metric — potential interference between routes which reflected by the node status (active, neighbor of active node,

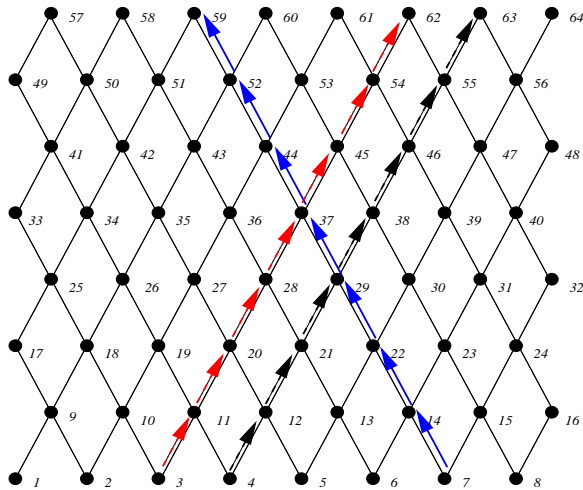


Figure 6.12: Routes selected by AODV, 3 cross flows

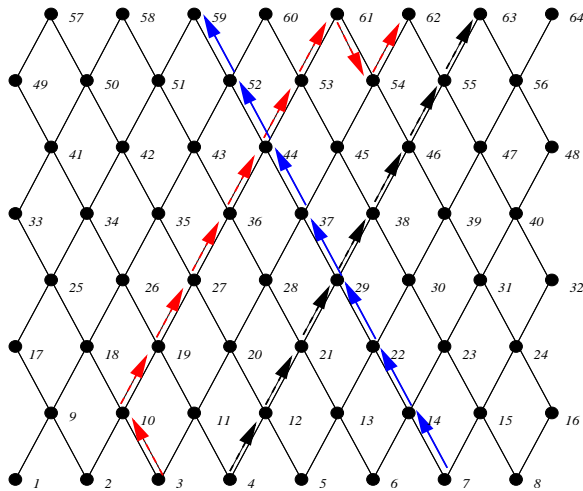


Figure 6.13: Routes selected by DCR, 3 cross flows

or non-active), hence issues regarding to routing such as the stability, robustness of routes, the error-tolerance and route repair etc, are similar to those algorithm and will not be discussed here. However, in order to be a complete and applicable routing algorithm, above problems should be considered and that will be the next step of the research.

6.6 Conclusion

The cross-layer design idea — codeword routing is presented as the theoretical model for improving the performance of wireless ad hoc network. As a distributed implementation of such design idea “dynamic codeword routing” algorithm is proposed. It is shown that the proposed

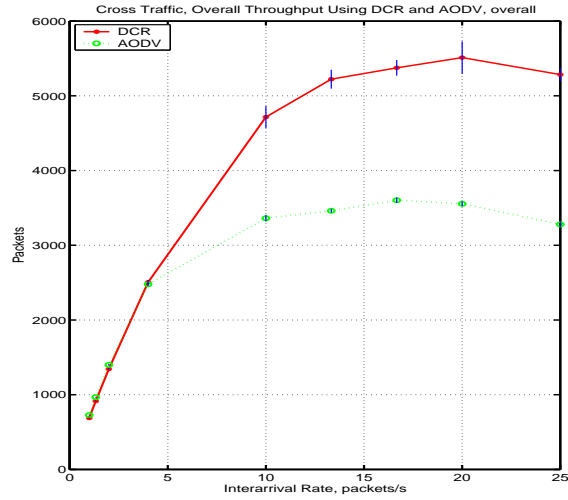


Figure 6.14: Comparison of overall throughput using AODV and DCR, 3 cross flows

DCR algorithm have the overall performance comparable with AODV and will enhance the network performance significantly under specific scenarios.

In the scope of the thesis, homogeneous traffic is considered, the next step will be consider non-homogeneous traffic, a more adaptive algorithm which can reacts to the real-time traffic is under study. Future work also includes finding more appropriate node and link assignment for both the routing model and its implementation, for example, the weight of node that is just neighbor of one active route should be different from the weight of the node which is neighbor of more than one active routes; more parameters can be considered in the routing algorithm besides the potential interference, such as, the remained power, etc. Another direction is to study the adaptive algorithm which can change dynamically based on the traffic, (percentage of the throughput, in other words), we shall also investigate the problem of stability when considering the existing routes can be re-arranged according to newly added communications.

Moreover, the authors are also interested in integrating the cross-layer design idea with the current bandwidth aware or load balancing routing algorithms [21] [26]. The cross-layer design idea can work on top of the current algorithms provide promising space of performance improvement.

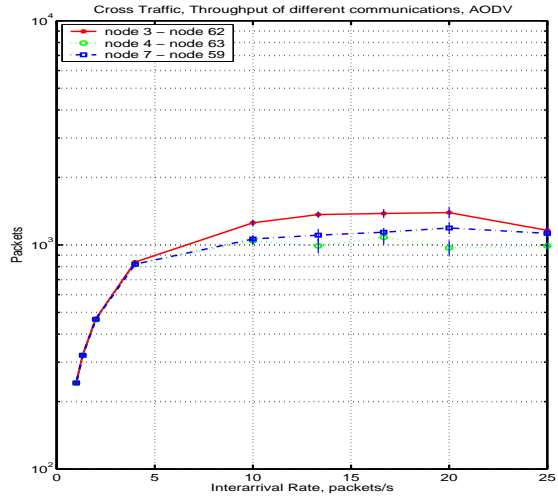


Figure 6.15: Throughput of each of the 3 flows when using AODV, 3 cross flows

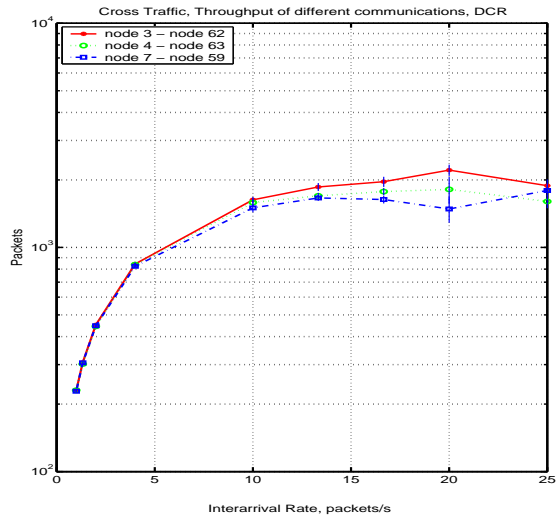


Figure 6.16: Throughput of each of the 3 flows when using DCR, 3 cross flows

Chapter 7

Conclusion and Future Work

7.1 Review of the Thesis

7.2 Future Work

Bibliography

- [1] Nikhil Bansal and Zhen Liu, *Capacity delay and mobility in wireless ad-hoc networks*, Proceedings of IEEE INFOCOM'03, vol. 2, 30 March - 3 April 2003, pp. 1553–1563.
- [2] Lichun Bao and J.J. Garcia-Luna-Aceves, *Pama: A novel link-activation channel access scheduling in ad hoc network*, MobiCom (Rome,Italy), 2001, pp. 210–221.
- [3] Stefano Basagni, *Distributed clustering for ad hoc networks*, Proceedings of the 1999 International Symposium of Parallel Architectures, Algorithms and Networks (ISPAN '99), 1999, p. 310.
- [4] Dimitri Bertsekas and Robert Gallager, *Data networks*, 2nd ed., Prentice Hall, 1992.
- [5] G. Bianchi, *Performance analysis of the ieee 802.11 distributed coordination function*, IEEE Journal on Selected Areas in Communications **18** (2000), no. 3, 535–547.
- [6] IEEE Standards Board, *Ieee standard 802.11 - wireless lan medium access control (mac) and physical layer (phy) specifications*, The Institute of Electrical and Electronics Engineers, Inc, 345 East 47th Street, New York, NY 10017-2394, USA, June 1997.
- [7] Jeong Geun Kim Brain P. Crow, Indra Widjaja and Prescott T. Sakai, *Ieee 802.11 wireless local area networks*, IEEE Communications Magazine (1997), 116–126.
- [8] Elizabeth M. Royer Charles E. Perkins and Ian Chakeres, *Ad hoc on-demand distance vector routing*, Proceedings of the 2nd IEEE Workshop on Mobile Computing Systems and Applications (New Orleans, LA), Februray 1999, pp. 90–100.
- [9] Harshal S. Chaya and Sanjay Gupta, *Performance modeling of asynchronous data transfer methods of ieee 802.11 mac protocol*, Wireless Networks **3** (1997), 217–234.
- [10] Mung Chiang, *To layer or not to layer: Balancing transport and physical layers in wireless multihop networks*, Proceedings of IEEE InfoCom 2004, 2004.

- [11] R. Cruz and A. Santhanam, *Hierarchical link scheduling and power control in multihop wireless networks*, Proceedings of Allerton Conference, October 2002.
- [12] J. A. Morrison D. Mitra and K. G. Ramakrishnan, *Virtual private networks: Joint resource allocation and routing design*, Proceedings of InfoCom 1999, April 1999.
- [13] K. G. Ramakrishnan D. Mitra and Q. Wang, *Combined economic modeling and traffic engineering: Joint optimization of pricing and routing in multi-service networks*, Proceedings of 17th International Teletraffic Congress., 2001.
- [14] J. Deng and Z. Haas, *Dual busy tone multiple access (dbtma): A new medium access control for packet radio networks*, Proceedings of IEEE ICUPC'98 (Florence, Italy), October 1998.
- [15] Sung-Ju Lee Elizabeth M. Royer and Charles E. Perkins, *The effects of mac protocols on ad hoc network communication*, Proceedings of the IEEE Wireless Communications and Networking Conference (2000), 543–548.
- [16] Farshad Eshghi and Ahmed K. Elhakeem, *Performance analysis of ad hoc wireless lans for real-time traffic*, IEEE Journal on Selected Areas in Communications **21** (2003), no. 2, 204–215.
- [17] Mario Gerla Fabrizio Talucci and Luigi Fratta, *Maca-bi (maca by invitation) a receiver oriented access protocol for wireless multihop networks*, In Waves of the Year 2000+ PIMRC '97. The 8th IEEE International Symposium on Personal, Indoor and Mobile Radio Communications. Technical Program, Proceedings (Cat. No.97TH8271)., vol. 2, 1997, pp. 435–439.
- [18] Yue Fang and A.Bruce Mcdonald, *Cross-layer performance effects of path coupling in wireless ad hoc networks: Power and throughput implications of ieee 802.11 mac*, Proceedings of 21st IEEE International Performance, Computing, and Communications Conference (IPCCC 2002) (Phoenix, Arizona), April 3-5 2002, pp. 281–290.
- [19] Marco Conti Federico Cali and Enrico Gregori, *Dynamic tuning of the ieee 802.11 protocol to achieve a theoretical throughput limit*, IEEE/ACM Transactions on Networking **8** (2000), no. 6, 785–799.

- [20] C.L Fullmer and J.J. Garcia-Luna-Aceves, *Floor acquisition multiple access (fama) for packet-radio networks*, Proceedings of the Conference on Applications, Technologies, Architectures and Protocols for Computer Communication (SIGCOMM), 1995, pp. 262–273.
- [21] Andras Veres Gahng-Seop Ahn, Andrew T. Campbell and Li-Hsiang Sun, *Swan: Service differentiation in stateless wireless ad hoc networks*, Proc. IEEE INFOCOM'2002 (New York, New York), 2002.
- [22] Nitin Vaidya Gavin Holland and Paramvir Bahl, *A rate-adaptive mac protocol for wireless network*, Technical Report TR00-019, Texas A&M University, August 2000.
- [23] Matthias Grossglauser and David N. C. Tse, *Mobility increases the capacity of ad-hoc wireless networks*, INFOCOM, 2001, pp. 1360–1369.
- [24] P. Gupta and P.R. Kumar, *The capacity of wireless networks*, IEEE Transactions on Information Theory **46** (2000), no. 2, 388–404.
- [25] Shiduan Cheng Haitao Wu and Jian Ma, *Performance of reliable transport protocol over iee 802.11 wireless lan: Analysis and enhancement*, Proceedings of the IEEE INFOCOM'02 (New York, NY), vol. 2, June 23-27 2002, pp. 599–607.
- [26] Audrey Zhou Hossam Hassanein, *Routing with load balancing in wireless ad hoc networks*, Proc. of the 4th ACM international workshop on Modeling, analysis and simulation of wireless and mobile systems (Rome, Italy), 2001, pp. 89–96.
- [27] Panos Paradalos James Abello, Sergiy Butenko and Mauricio G.C Resende, *Finding independent sets in a graph using continuous multivariable polynomial formulations*, Journal of Global Optimization (2001), no. 21, 111–137.
- [28] Pushkin Peddabachagari Jangeun Jun and Miail Sichitiu, *Theoretical maximum throughput of iee 802.11 and its applications*, Proceedings of the 2nd IEEE international Symposium on Network Computing and Applications (NCA'03) (Cambridge, MA), April 16-18 2003, pp. 249–256.
- [29] Tang Jian, *An $o(2^{0.304n})$ algorithm for solving maximum independent set problem*, IEEE Transactions on Computers **C-35** (1986), no. 9, 847–851.

- [30] P. Karn, *Maca-a new channel access protocol for packet radio*, Proceedings of ARRL/CRRL Amateur Radio Ninth Computer Networking Conference, 1990, pp. 234–140.
- [31] L. Kleinrock and F. A. Tobagi., *Packet switching in radio channels: Part 1-carrier sense multiple-access modes and their throughput-delay characteristics*, IEEE Transactions on Communications **23** (1975), no. 12, 1400–1416.
- [32] ———, *Packet switching in radio channels: Part 2-the hidden terminal problem in carrier sense multiple-access and the busy-tone solution*, IEEE Transactions on Communications **23** (1975), no. 12, 1417–1433.
- [33] Jinyang Li, Charles Blake, Douglas S. J. De Couto, Hu Imm Lee, and Robert Morris, *Capacity of ad hoc wireless networks*, Mobile Computing and Networking, 2001, pp. 61–69.
- [34] P. Marbach and R. Berry, *Downlink resource allocation and pricing for wireless networks*, Proceedings of IEEE InfoCom 2002, June 2002.
- [35] Riku Mettala, *Bluetooth protocol architecture verion 1.0*, white paper, Bluetooth Special Interest Group (SIG), Aug 1999.
- [36] Eugene Perevalov and Rick Blum, *Delay limited capacity of ad hoc networks: Asymptotically optimal transmission and relaying strategy*, Proceedings of IEEE INFOCOM'03, vol. 2, 30 March - 3 April 2003, pp. 1575–1582.
- [37] C.E Perkins and E.M Royer, *Performance comparison of two on-demand routing protocols for ad hoc networks*, IEEE Personal Communication Magazine **8** (2001), no. 1, 16–28.
- [38] X. Qin and R. Berry, *Exploiting multiuser diversity for medium access control in wireless networks*, Proceedings of InfoCom 2003, April 2003.
- [39] J.M Robson, *Algorithms for maximum independent sets*, Journal of Algorithms **7** (1986), 425–440.
- [40] E. M Royer and Chai-Keong Toh, *A review of current routing protocols for ad hoc mobile wireless networks*, IEEE Personal Communications (1999), 46–55.
- [41] R. Rozovsky and P. Kumar, *Seedex: A mac protocol for ad hoc networks*, Proceedings of the ACM Symposium on Mobile Ad Hoc Networking and Computing, MobiHoc2001, 2001, pp. 67–75.

- [42] A. Scaglione and S. Servetto, *On the interdependence of routing and data compression in multihop sensor networks*, Proceedings of ACM MobiCom 2002, September 2002.
- [43] Robert Endre Tarjan and Anthony E Trojanowski, *Finding a maximum independent set*, SIAM Journal of Computing **6** (1977), no. 3, 537–546.
- [44] Y.C Tay and K.C Chua, *A capacity analysis for the ieee 802.11 mac protocol*, ACM/Baltes Wireless Networks **7** (2001), no. 2, 159–171.
- [45] S. Xu and T. Saadawi, *Does the ieee 802.11 mac protocol work well in multihop wireless ad hoc networks?*, IEEE Communication Magazine **39** (2001), no. 6, 130–137.
- [46] J. Zhang, *Bursty traffic meets fading: A cross-layer design perspective*, Proceedings of Allerton Conference, October 2002.